ALTERNATIVE SPLICING AND mRNA STABILITY:
Control of SERCA2 Expression

BY

CHRISTINE M. MISQUITTA, B.Sc.

A Thesis
Submitted to the School of Graduate Studies
in Partial Fulfillment of the Requirements
for the Degree
Doctor of Philosophy
Biology

McMaster University

ALTERNATIVE SPLICING
AND
mRNA STABILITY:

CONTROL OF SERCA2 EXPRESSION

Doctor of Philosophy (2003)
(Biology)

McMaster University
Hamilton, Ontario

TITLE: Alternative Splicing and mRNA Stability: Control of SERCA2 Expression

AUTHOR: Christine M. Misquitta, B.Sc. (McMaster University)

SUPERVISOR: Dr. A. K. Grover

NUMBER OF PAGES: xv, 166

ABSTRACT

The overall hypothesis is that sequences in the 3'-region and tissue-specific protein factors contribute to the stability of the sarco/endoplasmic reticulum (SERCA) pump mRNA. Calcium pumps, which sequester calcium ions into the sarcoplasmic reticulum in left ventricular myocytes (LVM) or stomach smooth muscle cells (SSM), are encoded by the SERCA2 gene. SERCA2 transcripts are alternatively spliced at base 3495, giving mRNA which differ mainly in the 3'-UTR and also encode two proteins (SERCA2a in LVM and SERCA2b in SSM) with small differences in their C-termini. The rate of SERCA2 transcription in LVM and SSM is similar, yet there is 20 to 30-fold more SERCA2 mRNA and 100-fold more SERCA2 protein in LVM than in SSM. This thesis relates the differences in the SERCA2 expression level in the two tissues to their 3'-domains via sequences affecting mRNA stability.

Using primary cell cultures of LVM and SSM, transcription was inhibited and the half life of SERCA2 mRNA was determined. The half-life of SERCA2 mRNA in LVM was 27 ± 3 h while in SSM it was 13 ± 0.5 h. Thus, SERCA2 mRNA is more stable in LVM than in SSM.

The abundance of SERCA2 and control RNA in isolated nuclear and cytoplasmic fractions was compared to determine whether the difference in the SERCA2 mRNA

abundance originates in the nucleus or the cytoplasm. SERCA2a is already 20-fold more abundant than SERCA2b in the nucleus suggesting a nuclear mechanism of decay or differences in export rates.

Since SERCA2a and 2b mRNA differ in their 3'-regions, the decay rates of the 3'-region mRNA (starting from 3446) from SERCA2a and 2b was examined in nuclear and cytoplasmic extracts of both tissues. In all extracts, except SSM cytoplasm, the 3'-region mRNA of SERCA2a was significantly more stable than that of SERCA2b with the biggest difference being observed in LVM nuclear extracts. *In vitro* decay experiments using poly A^+ RNA isolated from the two tissues also showed that, in the presence of LVM nuclear protein extracts, the SERCA2a mRNA was more stable than the SERCA2b. Thus, *cis*-acting elements (RNA sequences) in the 3'-region may play a role in SERCA2 mRNA stability.

To identify possible *cis*-acting elements of SERCA2a and 2b, individual decay rates of large overlapping fragments that spanned the length of their 3'-regions were examined. In SERCA2a, this fragment represents the last 108 bases of the mRNA sequence (2A6). In SERCA2b, several unstable regions were identified but the most unstable fragment is within the first 300 bases after the splice site (2B1). Experiments using hybrid fragments with 2A6 and 2B1, however, showed that the effects of these sequences on RNA decay may be context dependent.

The *cis*-acting elements function by binding to *trans*-acting factors (RNA-binding proteins). The ability of the large overlapping 3'-region fragments from SERCA2a and 2b to bind proteins was determined using electrophoretic mobility shift assays. Only one

fragment within SERCA2a did not bind to at least one protein while all the SERCA2b fragments were able to bind proteins. The least stable fragment in SERCA2a (2A6) was able to bind more than one protein. Using small RNA oligonucleotides to compete for protein binding with 2A6, we showed that hairpin loops in this region may be involved in protein binding. In contrast, the GC-rich coding region sequence from 3521-3555 appears to contain the key *cis*-acting element in SERCA2b (2B1). As several fragments downstream of 2B1 were also unstable, this *cis*-acting element may act in conjunction with other downstream sequences.

In summary, the 3'-region plays a role in the predominantly nuclear decay of SERCA2a and 2b in LVM and SSM via specific *cis*-acting elements and *trans*-acting factors. This decay may be important in development and disease.

List of Publications as result of the present study:

C.M. Misquitta, J. Mwanjewe, L. Nie, and A.K. Grover. Sarcoplasmic reticulum Ca^{2+} pump mRNA stability in cardiac and stomach smooth muscle: role of the 3'-untranslated region. American Journal of Physiology 283:C560-C568 (2002).

C.M. Misquitta, V.R. Iyer, E.S. Werstiuk, and A.K. Grover. The role of 3'-untranslated region (3'-UTR) mediated mRNA stability in cardiovascular pathophysiology. Molecular and Cellular Biochemistry 224:53-67 (2001).

C.M. Misquitta, D. P. Mack, and A.K. Grover. Sarco/endoplasmic reticulum Ca^{2+} (SERCA)-pumps: Link to heart beats and calcium waves. Cell Calcium 25(4):277-90 (1999).

List of Publications related to the present study:

C.M. Misquitta, A. Sing, and A.K. Grover. Control of sarco/endoplasmic reticulum Ca^{2+} pump expression in cardiac and smooth muscle. Biochemical Journal 338:167-74 (1999).

ACKNOWLEDGMENTS

There are many people that have contributed to the completion of this work. Above anyone I must thank Dr. Grover, and yet words can hardly express my gratitude. Thank you for the opportunities you have given me, the knowledge you have shared with me, and for your confidence in my abilities. You will never know how much you have taught me–about molecular biology and also about myself.

I would like to thank Dr. Harnish and Dr. Andrews for their time and expertise. James and Lin–you have both added so much to this project, thank you for the late nights and all your help. I also want to thank Dr. Eva Werstiuk and Sue Samson, not only for their assistance and insight within the lab, but also for their friendship outside of it.

A special thank you to my family. Errol and Chris–you have been wonderful through all of this. Thank you for everything, especially my two angels, Jacob and Zachary, who help to put everything in perspective. Frances–thank you for always listening and for making me feel as ordinary or as exceptional as the situation required. Des–thank you for your never-ending PATIENCE. Your love and support means everything to me.

Finally, this thesis is for my parents. Thank you both so much for all your love, support, encouragement, and understanding. I have the best parents in the world and I hope you are half as proud of me as I am of you. I love you both.

TABLE OF CONTENTS

LIST OF FIGURES

LIST OF TABLES

LIST OF ABBREVIATIONS

ARE	AU-rich elements
AUBP	ARE binding protein
BSA	bovine serum albumin
Ca^{2+}	calcium ions
$[Ca^{2+}]_i$	intracellular Ca^{2+} concentration
CaM	calmodulin
CaM kinase II	Ca^{2+}-CaM dependent protein kinase II
CBP	cap binding protein
CRD	coding region determinant
DHFR	dihydrofolate reductase
DMEM	dulbecco's modified eagle's medium
DRB	5,6-dichloro-1-B-D-ribofuranosyl-benzimidazole
DTT	1-4-dithiothreitol
EDTA	(ethylenedinitrilo)-tetraacetic acid ethylene glycol
eIF	eukaryotic initiation factor
FBS	fetal bovine serum
G3PDH	glyceraldehyde 3-phosphate dehydrogenase
GM-CSF	granulocyte macrophage-colony stimulating factor
HEPES	4-(2-hydroxyethyl-1-piperazine ethane sulfonate)
hnRNA	heteronuclear RNA
hnRNP	heterogeneous ribonucleoprotein
IP_3	1,4,5-inositol trisphosphate
IP_3R	1,4,5-inositol trisphosphate receptor
LHR	leutinizing hormone receptor

LVM	left ventricular muscle
MIC	microsome
MOPS	3-[N-Morpholino] propanesulfonic acid
NPC	nuclear pore complex
PABP	poly A^+ binding protein
PAGE	polyacrylamide gel electrophoresis
PBS	phosphate buffered saline
PCR	polymerase chain reaction
PKC	protein kinase C
PLN	phospholamban
PMCA	plasma membrane Ca^{2+} ATPase
PMSF	phenylmethylsulphonyl fluoride
PNS	post-nuclear supernatant
poly A^+	polyadenylated
ROCCs	receptor operated Ca^{2+} channels
RRM	RNA recognition motif
SERCA	sarco/endoplasmic reticulum Ca^{2+} ATPase
SDS	sodium dodecyl sulfate
SLN	sarcolipin
SOCCs	store operated Ca^{2+} channels
SOF	State of Filling
SR/ER	sarcoplasmic reticulum / endoplasmic reticulum
SSM	stomach smooth muscle
TCA	trichloroacetic acid
TM	transmembrane domain
Tris	tris (hydroxymethyl) aminomethane
UTR	untranslated region
VOCCs	voltage operated Ca^{2+} channels

CHAPTER ONE

INTRODUCTION

Calcium ions (Ca^{2+}) act as a common intracellular second messenger and, as such, regulation of Ca^{2+} within the cell is essential to many cellular processes (5;26;87). One means by which intracellular Ca^{2+} concentration ($[Ca^{2+}]_i$) is controlled is via sequestration into the sarcoplasmic reticulum (SR/ER) via the Ca^{2+} ATPases found on its membrane (SERCA pumps) (34;87;108). The various SERCA isoforms are regulated in their expression by both developmental stage and tissue type. The two SERCA2 protein isoforms, SERCA2a and 2b, show large differences in their expression in cardiac and stomach smooth muscle, respectively. Based on our previous results, it is proposed that mRNA stability is the key mechanism by which SERCA2 expression is regulated (76). The following introduction will elaborate on Ca^{2+} regulation in the cell with a specific focus on SERCA pumps, their structure, expression, and regulation. It will then discuss levels of gene expression, with special emphasis on the role of the 3'-untranslated region (3'-UTR) of mRNA in its stability. Evidence for sequences found within various mRNA species and some of the known RNA-binding proteins which bind to these motifs will be reviewed. The elements that control gene expression will then be related to SERCA2 based on the results obtained in our lab before, or by others, during the completion of this thesis. Finally, our current hypothesis will be outlined and the experiments used to test them in this thesis will be described.

1.1 Ca^{2+} and its Regulation

1.1.1 Overview: The role of Ca^{2+} in heart and smooth muscle contraction

Ca^{2+} is a vital second messenger within mammalian cells. Changes in $[Ca^{2+}]_i$ provide the signal for many intracellular functions including cell motility, neurotransmitter release, cell growth and proliferation, apoptosis, and muscle contraction (4;5;26;34;35;72;77;87). This introduction focuses on the role of Ca^{2+} in contraction of heart and smooth muscle.

The levels of Ca^{2+} inside and outside of the cell differ to a great extent. A resting cell has a $[Ca^{2+}]_i$ of approximately 0.1 μM and is surrounded by fluid containing a Ca^{2+} concentration of 1 mM (115). This difference in Ca^{2+} levels is finely regulated so that changes are easily detected by the cell. One such process that is triggered by the increase in $[Ca^{2+}]_i$ is muscle contraction as $[Ca^{2+}]_i$ is a major determinant in actomyosin activity (116). The basic contractile process is the same in both cardiac and smooth muscle although the exact mechanism of regulation differs between the tissues. Another difference is the rate at which contraction and relaxation occurs within these two tissues, with these events being faster in cardiac muscle. Factors influencing the rate at which Ca^{2+} enters the intracellular space control the rate of contraction while those that restore intracellular Ca^{2+} to its resting levels regulate the rate of relaxation. Below, the various pumps, channels, and receptors that regulate intracellular Ca^{2+} homeostasis and mobilization are discussed.

1.1.2 Ca^{2+} removal from the cytosol

Increases in $[Ca^{2+}]_i$ are essential to various cellular functions but continued levels of high $[Ca^{2+}]_i$ can be toxic to the cell, can signal apoptosis, or would prevent the cell from

recovering from a contractile phase (4;77). Thus, mechanisms exist to reduce the $[Ca^{2+}]_i$ (77;115). These include **sarcoplasmic/endoplasmic reticulum Ca^{2+} ATPase (SERCA)** which returns Ca^{2+} to the SR and the **plasma membrane Ca^{2+} ATPase (PMCA)**and **the Na^+/Ca^{2+} exchanger** which both remove Ca^{2+} to outside the cell.

1.1.2 1 Refilling of Ca^{2+} stores: Sarcoplasmic reticulum (SR) Ca^{2+} pumps

In addition to removal of Ca^{2+} to the outside of the cell, the $[Ca^{2+}]_i$ can be restored to resting levels by sequestration of Ca^{2+} in the SR. This is an active process performed by Ca^{2+} pumps in the SR membrane. The ATP-driven pumps which sequester Ca^{2+} into the sarco/endoplasmic reticulum (SR/ER) **(SERCA)**, are encoded by three genes: SERCA1, 2, and 3 (33;34). The basic function of SERCA proteins is common although some structural and regulatory differences exist between the isoforms. The stoichiometry of Ca^{2+} transport has been examined in SERCA1. SERCA1 pumps transport two cytosolic Ca^{2+} into the lumen of the SR/ER through the hydrolysis of one ATP molecule in the presence of Ca^{2+} and Mg^{2+} (136). SERCA pumps, therefore, play a large role in the maintenance of Ca^{2+} levels within the cell, impacting on relaxation, and many other cellular processes.

The general pump structure of SERCA is that of 10 membrane spanning domains (TMs) with both amino and carboxyl termini on the cytoplasmic side of the membrane. The domains responsible for Ca^{2+} binding in SERCA are in TM4, TM5, TM6, and TM8 (113;131). The Ca^{2+} transport function of the SERCA pump can best be described as a sequence of conformational changes between at least two forms that differ in their affinity for Ca^{2+}. Initially, the pump (E) is in its high-affinity state (E1). In this conformation, 2 Ca^{2+}

can be bound (Ca2-E1) in an ordered manner on the cytoplasmic side of the SR membrane and transferred into an occluded state. Upon phosphorylation by ATP the pump is activated for transport (Ca2-E1P). The enzyme then changes conformation to the low-affinity (Ca2-E2P) state and consecutively expels the 2 Ca^{2+} to the lumen of the SR (E2P). As the phosphoryl group dissociates during hydrolysis, the high-affinity (E1) state of the enzyme is regenerated (2;34).

1.1.2.1.1 SERCA structure and expression

The SERCA proteins can be divided into three main segments: 1) the stalk domain (S), 2) the transmembrane region (TM), and 3) the hinge domain (H). These domains each play a critical role in the function of the ATPase. In particular, the stalk domain contains two cytoplasmic loops. The smaller of these loops, which extends into the cytoplasm between the S2 and S3, contains the domain responsible for transduction. The larger of the loops, from S4 to S5, contains sequences vital for phosphorylation (Asp 351) and ATP binding. The hydrophobic transmembrane region is comprised of 10 segments (or 11 in the case of SERCA2b) and is joined to the cytoplasmic domain by the hinge region. It is within TM4, TM5, and TM6 that the two Ca^{2+} binding sites of the SERCA pump are located. Other sites common to all isoforms include those for inhibition by thapsigargin and cyclopiazonic acid, which are both found in the third transmembrane domain (2;34;38).

1.1.4.1.2 SERCA Isoforms

The SERCA proteins are encoded by three separate genes: SERCA1, 2 and 3 or ATP2A1, 2, and 3, respectively. Here, the structure and regulation of the SERCA pump

isoforms will be described with emphasis on the SERCA2 isoforms.

Although the general structure and the key sites of function are the same in all SERCA isoforms, there are also some key differences between these proteins. Specifically, their size and gene sequence, their tissue expression, and their affinity for Ca^{2+} differ not only between SERCA1, 2 and 3 but also between the alternate splices of each isoform. Some of the differences between isoforms are summarized in **Table I** and described in detail, below.

TABLE I: COMPARISON OF SERCA ISOFORMS

ISOFORM	CHROMOSOME LOCATION (human)	EXONS	PROTEIN SIZE (amino acids)	AFFINITY for Ca^{2+} (Kd in μM)	TISSUE DISTRIBUTION	REGULATION
SERCA 1	**16p12.1**					sarcolipin phospholamban (*in vitro*)
SERCA1a		1-23	994	0.4	adult fast-twitch skeletal muscle	
SERCA1b		1-21,23	1001	0.4	neonatal fast-twitch skeletal muscle	
SERCA2	**12q23-24.1**					phospholamban CaM kinase II
SERCA2a		1-21,25	997	0.4	Slow-twitch skeletal, cardiac, and smooth muscles	
SERCA2b		1-22	1042	0.27	Smooth and non-muscles	
SERCA3	**17p13.3**					none known
SERCA3a		1-20,22	999	2	platelets, lymphoid, endothelial and mast cells, neurons	
SERCA3b		1-20,22, partial 21	1043	>2	kidney and pancreatic cells	
SERCA3c		1-22	1029	>2	kidney and pancreatic cells	

The human **SERCA2** gene is estimated to be 45-50 kb at locus 12q23-24.1. It is made up of 25 exons of which the four terminal exons are alternatively spliced to produce 4 classes of mRNA which encode two distinct proteins: SERCA2a and SERCA2b (see schematic in Figure 1). These are expressed in a tissue specific manner: SERCA2a protein is abundant in cardiac and slow-twitch skeletal muscle, and SERCA2b protein is in most other tissues including smooth muscle. Class 1 mRNA is muscle specific in its expression and includes exons 1-21, and 25. It is 4.4 kb in length, encodes 997 amino acids, and gives a protein of 110 kDa. It is generated by splicing of an optional intron in the 3' end of the mRNA(67;71;117). This mRNA is translated to the SERCA2a isoform. Class 2 mRNA is expressed in non-muscle cells and includes exons 1-22 and is also 4.4 kb. The mRNA of class 2 is polyadenylated at a site that lies in the muscle-specific intron. Class 3 mRNA, which is 8 kb, has been detected in both muscle and non-muscle cells and includes exons 1-25. Class 4 mRNA is expressed specifically in brain, includes exons 1-23, and 25, and is 5.6 kb. Classes 2 - 4 share a termination codon in exon 22 and all translate to the SERCA2b isoform which has 1042 amino acids and a molecular weight of 115 kDa (130;131). Two of these splices, class 3 and 4, are rare and will not be discussed further. The two abundant proteins are SERCA2a and SERCA2b given by class 1 and class 2 mRNAs, respectively, and these will be the only SERCA2 isoforms referred to in this thesis. The difference between these two classes lies in the choice between muscle-type splicing and non-muscle polyadenylation indicating that the processes that generate these two classes of mRNA are mutually exclusive (71;117).

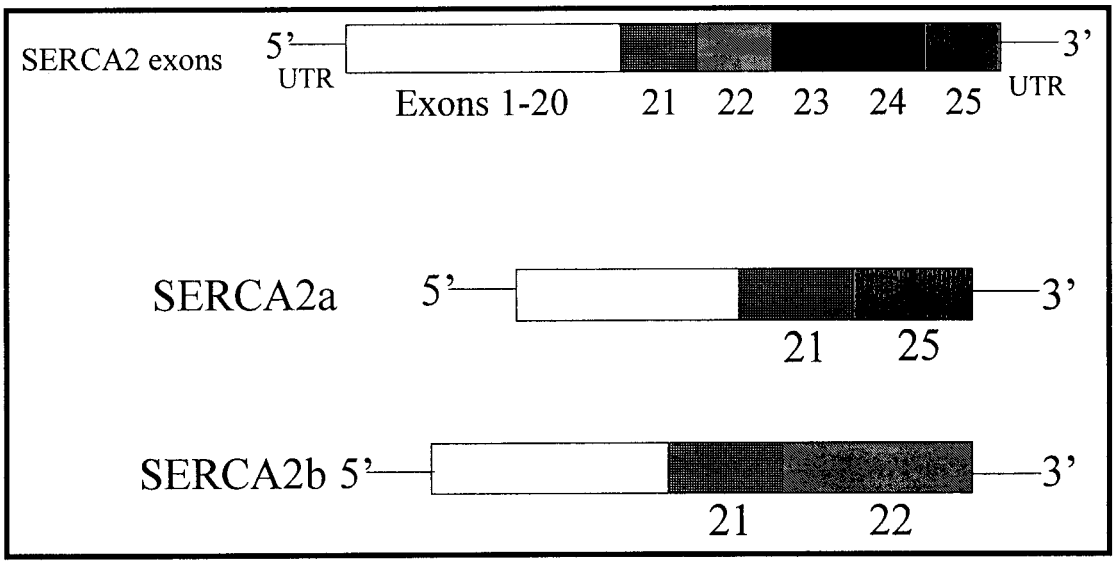

Figure 1. Alternative splicing of the SERCA2 gene. As described in the text, the SERCA2 pre-mRNA can be alternatively spliced to give either SERCA2a mRNA or SERCA2b mRNA. These mRNA species differ primarily in their 3'-UTR and in the sizes and location of the proteins they produce. See Fig.2 for codon locations. NOTE: the minor isoforms containing the exons 21,22,23,25 or 21 to 25 are not shown.

The protein isoform selectively expressed in cardiac and slow-twitch skeletal muscle is 2a, while most tissues express 2b. This difference in isoform expression may be a function of selective needs of the tissue. For instance, the cardiac muscle requires a pump that can be regulated to finely control contraction and relaxation (possible through regulation of SERCA2a by phospholamban) while non-muscle or smooth muscle cells may be able to utilize a pump that has a slower transport rate but is more effective at lower Ca^{2+} concentrations (SERCA2b) (34). As described above, these isoforms are homologous up to and including exon 21. SERCA2a is then spliced to exon 25 while in SERCA2b it is followed by exon 22. This results in mRNAs which have common 5'-untranslated regions

(5'-UTRs) and partial coding regions but which differ in translated amino acid number (997 in 2a vs. 1042 in 2b), transmembrane domains of the complete protein (10 in 2a vs. 11 in 2b), and 3'-UTRs. The Ca^{2+} affinity differs between the two isoforms, being about 2-fold higher for SERCA2b than for SERCA2a while the turnover rate of SERCA2b is approximately 2-fold lower than SERCA2a (34;74). Reports indicate that the last 12 amino acids in SERCA2b are critical for eliciting some of the functional differences from SERCA2a including Ca^{2+} affinity, Ca^{2+} turnover rate, and ATP hydrolysis (71;120). The specific cDNA sequences of SERCA2a and 2b are compared in Figure 2.

SERCA2, specifically SERCA2a because of its expression in cardiac tissue, has been widely studied in many animal models of heart failure. Low levels of SERCA2 pump activity are associated with heart failure in humans and animal models (59;90;91). Also, overexpression of the SERCA2 protein can increase the strength of cardiac contractions and can counteract experimentally-induced heart failure (34). Thus, the regulation of SERCA2 expression is of importance in many cardiovascular diseases.

The **SERCA1** gene is 26 kb and is found at the human locus 16p12.1. The SERCA1 protein is expressed predominantly in fast-twitch skeletal muscle. The pre-mRNA transcript contains exons1-23 but is alternatively spliced into SERCA1a and 1b. The expression of these two splices is developmentally regulated - 1a is expressed in adults and 1b in neonates. The change in sequence causes a minor change in coding sequence between the two isoforms but does not produce differences in function or apparent affinity for Ca^{2+} (136).

The **SERCA3** protein is the most recently studied and has been found in a number

of secretory tissues including pancreas, kidney, and vascular endothelium. The transcripts are spliced into three known isoforms: 3a, 3b, and 3c. The alternative splicing produces proteins that are unique in size, function, and tissue expression (33).

```
1     GCGACGCGCGCCTCCTGCTCCGCCGCAGTTTCCTCCGCCGCTGCCGGGGGGTGCGGACGTG
61    AGGGACCCGGGCGAGCGCGCGCGTGCCCCGCCGGCTCGCCGCCTTCGCTCCGCTGCGCCC
121   TCAGGGGTGGGCCGGGCGCCCCCTCCTCCGGCCCGGCCGGGGCCCGAGCCGCCGCAGGAC
181   AGCGGGGAGGGGGCCGGGGGCCGGCCTGCGCTCCCTGCGGGCGGTTGAGGGCGAAGGAGG
241   CCCTGGGTTCTGACGAGGGAAGGGGAGGGTCGGGAGCCCCCCGCCCGCCCTGCGGAGCCC
301   GGGCGCCCGAGGGCGGTTGTCTGGGGGAGGGGGTGCGGGGTGATTCACCGCCCGGCGAGG
361   CGGAAGCGGCCGGAGCGGCAGCGGCGGCAGCGGGAGGAGGGCGAGCGGCCAGTCGGCGCC
421   GGGGCGCCCGCGGTGGCACGAGCCCGCGGCCCGAGTGCGAGGCGGAGGCGACGAGGCCGC
481   GGGGACGGGGGGCGAACGGCCGGGCCCCCGCAGCCATGGAGAACGCGCACACAAAGACGG
541   TGGAGGAGGTGCTGGGCCACTTCGGCGTCAACGAGAGCACGGGGCTGAGCCTGGAGCAGG
601   TCAAGAAGCTCAAGGAGAGATGGGGCTCCAACGAGTTACCGGCTGAAGAAGGAAAAACCT
661   TGCTGGAACTTGTGATTGAGCAATTTGAAGATTTACTAGTTAGAATTTTATTGCTGGCAG
721   CATGTATATCTTTTGTTTTGGCTTGGTTTGAAGAAGGTGAAGAAACCATTACAGCCTTTG
781   TAGAACCTTTTGTAATTCTGCTTATATTGGTAGCCAATGCCATCGTGGGTGTATGGCAGG
841   AAAGGAATGCTGAAAATGCAATTGAAGCCCTTAAGGAGTATGAGCCTGAAATGGGCAAAG
901   TGTATCGGCAGGACAGAAAGAGTGTACAGCGCATTAAAGCTAAAGACATCGTTCCTGGTG
961   ATATTGTAGAAATCGCAGTTGGTGACAAAGTTCCTGCCGACATAAGATTGACTTCTATCA
1021  AGTCTACAACTCTAAGAGTTGACCAGTCAATTCTCACAGGTGAATCTGTCTCTGTCATCA
1081  AGCACACTGACCCTGTCCCAGACCCGCGGGCTGTCAACCAGGATAAGAAGAACATGCTTT
1141  TTTCTGGCACAAACATTGCTGCAGGGAAAGCCATGGGAGTGGTGGTGGCAACTGGAGTCA
1201  ACACTGAGATTGGCAAGATTCGGGATGAGATGGTGGCGACAGAACAGGAGAGGACGCCTC
1261  TTCAGCAGAAACTAGATGAATTCGGAGAACAGCTTTCCAAAGTCATCTCCCTTATTTGCA
1321  TTGCAGTCTGGATCATAAACATTGGGCATTTCAATGACCCAGTTCATGGAGGCTCCTGGA
1381  TTAGAGGTGCTATTTACTACTTTAAGATTGCAGTGGCCCTGGCGGTAGCAGCTATTCCTG
1441  AAGGTCTGCCTGCCGTCATCACCACCTGCCTGGCTCTTGGAACTCGCAGGATGGCAAAGA
1501  AAAACGCCATCGTCCGAAGCCTGCCTTCTGTGGAAACCCTCGGCTGCACTTCTGTGATCT
1561  GCTCTGACAAGACTGGCACACTCACAACAAACCAGATGTCAGTCTGCAGGATGTTCATCC
1621  TGGACAAGGTTGATGGTGATACTTGTTCCCTTAATGAGTTCACCATAACTGGATCAACGT
1681  ACGCACCTATTGGAGAAGTGCATAAAGATGATAAACCAGTGAAGTGTCATCAGTATGATG
1741  GTCTTGTAGAATTAGCAACAATTTGTGCTCTTTGTAATGACTCTGCTTTGGATTACAATG
1801  AGGCCAAAGGTGTGTATGAAAAGGTTGGAGAAGCTACAGAGACTGCCCTGACGTGCCTGG
1861  TGGAGAAGATGAACGTGTTTGACACTGAATTGAAGGGTCTCTCTAAAATAGAGCGCGCGA
1921  ATGCCTGCAACTCGGTCATTAAGCAGCTGATGAAAAAGGAATTCACTCTAGAATTTTCAC
1981  GTGATAGAAAATCAATGTCAGTGTATTGTACGCCAAACAAACCAAGCCGGACGTCCATGA
2041  GCAAGATGTTTGTGAAGGGTGCTCCTGAGGGTGTCATCGACAGGTGCACCCACATTCGGG
2101  TTGGAAGTACCAAGGTCCCCATGACAGCTGGAGTCAAGCAGAAGATCATGTCTGTCATTC
2161  GGGAATGGGGTAGTGGCAGCGACACACTGCGGTGCCTGGCCCTGGCCACTCACGACAACC
2221  CACTGAGAAGAGAAGAAATGCACCTGAAGGACTCTGCCAACTTTATTAAGTATGAGACCA
2281  ACCTGACTTTTGTTGGCTGCGTGGGCATGCTGGATCCTCCCAGGATTGAGGTGGCCTCCT
2341  CCGTGAAGCTGTGCCGGCAAGCAGGCATCCGGGTCATCATGATCACCGGGGACAACAAGG
2401  GTACTGCCGTAGCCATCTGTCGCCGCATTGGCATCTTTGGTCAGGAGGAGGATGTGACGG
2461  CCAAGGCTTTCACAGGCCGGGAGTTTGACGAACTCAACCCCTCAGCCCAGCGAGATGCTT
2521  GCCTAAATGCCCGGTGCTTTGCTCGAGTTGAACCTTCCCACAAGTCCAAGATCGTAGAAT
2581  TTCTTCAGTCCTTTGATGAGATCACAGCTATGACTGGCGACGGTGTGAATGATGCCCCTG
2641  CTCTGAAGAAAGCGGAGATTGGCATTGCCATGGGCTCTGGCACCGCGGTGGCTAAAACTG
2701  CCTCTGAGATGGTCCTGGCTGATGACAACTTCTCCACCATTGTGGCTGCTGTGGAGGAGG
2761  GGCGGGCCATCTACAACAACATGAAGCAGTTCATCCGCTACCTCATCTCCTCCAACGTGG
2821  GGGAGGTTGTCTGCATTTTCCTGACGGCAGCCCTTGGGTTTCCTGAGGCCCTGATTCCCG
2881  TGCAGCTGCTCTGGGTCAATCTGGTGACAGATGGCCTGCCTGCCACCGCGCTGGGCTTCA
2941  ACCCTCCGGATCTGGACATCATGAATAAACCGCCTCGGAACCCAAAGGAACCACTGATCA
3001  GCGGGTGGCTCTTTTTCCGTTACCTGGCTATTGGCTGTTACGTTGGCGCCGCGACAGTGG
3061  GTGCTGCTGCGTGGTGGTTCATTGCTGCCGATGGTGGTCCAAGAGTGTCCTTCTACCAGC
3121  TGAGTCACTTCCTGCAGTGTAAAGAGGACAACCCGGACTTCGAGGGCGTGGATTGTGCAA
3181  TCTTTGAGTCTCCATATCCCATGACAATGGCACTGTCTGTTCTGGTCACCATAGAGATGT
3241  GCAACGCCCTCAACAGCCTGTCTGAAAACCAGTCCTTGCTGCGGATGCCGCCCTGGGAGA
3301  ACATCTGGCTGGTGGGCTCCATCTGCCTGTCCATGTCACTGCACTTCCTCATCCTCTACG
3361  TCGAGCCCCTGCCGCTTATCTTCCAGATCACACCGCTGAATGTGACCCAGTGGCTGATGG
3421  GCTTGAAAATCTCCTTACCTGTGATTCTCATGGACGAGACTCTCAAGTTCGTGGCCCGCA

                                *
3481  ACTACCTGGAACCTGCAATACTGGAGTAACCGCTTCCTAAACATTTTGCAGAAGTGTAAG
3481  --------------GTAAAGAGTGTGTGCAGCCTGCCCCCCAGTCCTGCTCGTTGTGGG

3541  GGTGTTCCGTTGCGTGCATGTGCGTTTTTAGCAACACACCTGCCAGCCCTCTGCATGATT
3541  CGTGCACCGAGGGGGTCTCCTGGCCGTTTGTGCTGCTCATAGTGCCCCTGGTGATGTGGG
```

```
3601 GATGTTGGGGTTCCCAGCTCCTTGTGTGTAGTGTGGAGGAAATGTGTGTTACCATTGGGG
3601 TCTACAGCACCGACACTAACTTCAGTGATCTGCTCTGGTCCTGACTGACAGCTCCCTAAG
                                                  *
3661 TTTCTGACTTTTCAAAATAATTACAAATGTACAACTAGAAAGCCTCTCCAGAGAAGTTTG
3661 AAGATGTGTAACTTAACCCATTAATTTTTTATTGTTTAAAGCAAGTGTCTTTCTGCTGAA

3721 GTTTCTTTGCTGCAAGAACAATGAGGTTCTGAAACCTCCCAAGAGTTTGGATACCGTCGG
3721 TTTTCACATGAACATACTGGCTGGTGAGGAGGTTTCCTACTCTAGATTGTGTTTTGCTTT

3781 CCAAGTCTCCACATTTCTCTGTGCTGTCAGCTTATCCAGATGTGCACTGTTGAGTTGTAA
3781 TTCTGACTCCAGTGGGGCAAGATTTTCCTTTTTTTATACACATAATTAAAGTGTCCATTG

3841 TGCATGCCTTCAGCTCAAGTAGCCAGCGTTTCCCTGCAGTGACCTTGAAACCTGCTACTT
3841 ACATGTACAGAGAACTAACACTATTTTATGCAAATATTTTTTTGTAGATGAAAAAGCATG

3901 TTTAATCGGCCCTGTACAGTTTGCTTATTTATAAATTCATGGAAACACTACAGGTATTGA
3901 TACAGTGTTCTGTTTAATACTCATCCTTGTACAAAAAAAACCAGTTGAGCCAGCAGACAT

3961 ATGGTTAAAATGTAGGCCTCCAGTTCATAACTTCAGTTATTCTGAGTGTGCAGACAGCTA
3961 TGTCAGCAGATTAATTGGTAGCAGATTTTAGGAAACGAATGTGTGTGGTTTTTTCTGAAA

4021 TTTTGCACTGTATTAAATGTAACTTATTTAATGAAATCAGAAGTAGACAGATGTTGGTGC
4021 CTAAATAGCATGTATTGTGTCTTTTGCATGATTATCTGGATTTAATTTGATATCACAGTC

4081 AATACAAACATTGTGATGCATTTATCTTAATAAAATGCTAAACGTCAGTTTATCACAACG
4081 TAATTTTTATTCATAAGCCAATTTTTCTGCACTGAGCAGAGTCCTGCTACCTCAGTCAGT

4141 CATGTCTGACTGTAGACTGTAAATAGCGATCGGTTTGTTTCTGTGCTGGTACCAAGCGTC
4141 GTTCTTGGTTTGCACCCCTCACCCTCCTGGCCTCCACTCACTCGCTGCCCTCCCCCCCGG

4201 GCACAGAACTGATTTCAGGTAAATAAATCTATATTCTACAATA.................
4201 CCCACTCAGCTTCCTCTGTAGGATTTGGATGGTTCTGTTGACATCAGTCGTCACGAGGTA

     .....................................................................
4261 TGCCTGTTCTGCCTTGTGCAGAAAATATTGTTCCAGATTCAATTGACTGGGTTTATGTCC

     .....................................................................
4321 CTTCACATAGTTTTTAAGGTTATTTAGTTAAATGTCTAATGTATTTTATTGTAACAGACA

     .....................................................................
4381 TTGTTTTGCCAACATTGCCTATTTCAGTGGCACTTCACAATCTAGTTGAAAAAGAAAAAT

     ..................................
4441 AAAACATTTTAAATGGAAAAAAAAAAAACCG
```

Figure 2. Comparison of full-length SERCA2a and 2b sequences. The sequences from the conserved region is listed for both together followed by the SERCA2a specific sequence above SERCA2b. Both sequences are numbered with the first base of the coding region designated as 517. Alternative splicing begins at 3496. The coding regions of SERCA2a and SERCA2b end at 3507 and 3642, respectively (depicted by * above or below the base). The numbers designated in this figure are used throughout the text. The regions of SERCA2a and 2b used in this thesis for analysis of the 3'-end are shown in bold.

1.1.2.1.3 Regulation of SERCA pump activity

The regulation of SERCA pumps is specific to each isoform. SERCA1 undergoes cellular regulation by sarcolipin, a protein which acts to both stimulate the rate of Ca^{2+} uptake and decrease the Ca^{2+} affinity of the pump (84). *In vitro*, SERCA1 and SERCA2 proteins are both regulated by phospholamban, which inhibits Ca^{2+} uptake into the SR by decreasing the affinity of the pump for Ca^{2+}. To date, SERCA3 has no known regulating protein.

1.1.2.1.3.1 Regulation by Phospholamban (PLN)

As described, the SR Ca^{2+}-ATPase is known to exist in equilibrium between two states, E1 and E2, of which E1 binds Ca^{2+} with high affinity. **Phospholamban (PLN)** interaction with the SERCA pump is thought to shift the E1/E2 equilibrium toward the E2 state by binding preferentially to this second conformation at specific residues within TM6 (52). In this way, PLN regulates Ca^{2+} affinity of the pump but has no effect on the rate of Ca^{2+} transport.

The PLN gene is highly conserved and consists of two exons separated by an intron. A region in the second exon codes for a protein having two distinct domains: I) a cytoplasmic/hydrophilic motif, and II) a transmembrane/hydrophobic motif (54;59). The cytoplasmic domain can be subdivided into Ia) having a helical structure and sites of phosphorylation, and Ib) an unstructured, highly polar region, important in stabilizing the formation of pentamers (54;59). PLN can be phosphorylated and, in this state, cannot inhibit the SERCA pump (113). Domain Ia contains the three specific targets of phosphorylation: Ser^{10} by Protein Kinase C (PKC), Ser^{16} by cAMP- or cGMP-dependent protein kinase, and

Thr^{17} by Ca^{2+}-calmodulin protein kinase II (CaM kinase). Phosphorylation at any one of these sites relieves inhibition by PLN and effectively increases Ca^{2+} affinity of the pump (54;59;60;108). In addition to these kinases which can modify PLN control of SERCA, a "State of Filling" (SOF) kinase has also been proposed to phosphorylate PLN at Ser^{10}. It is thought the SOF kinase may be sensitive to the Ca^{2+} concentration within the SR and that, upon store depletion, is activated to inhibit PLN to allow SR refilling (94). Phosphorylation of PLN is a reversible reaction and there exists a membrane bound phosphatase to re-establish pump inhibition (59;60). In addition to phosphorylation, there are other ways that the interaction between PLN and SERCA2 can be reversed (54;84).

PLN exists in an equilibrium between monomeric and pentameric forms of which the monomers have been found to be more effective at inhibiting the Ca^{2+}-ATPase (54). The monomer, according to Stokes' model, interacts with the pump at two sites: one within the cytoplasm and one within the membrane (108). Phosphorylation, as described above, disrupts the cytoplasmic interaction with the SERCA pump. Thus, it has been proposed that phosphorylation, which reverses inhibition, also shifts the structural equilibrium to the pentameric form (54). The main function of domain II in PLN is to stabilize the pentamer structure. It is thought that cysteine amino acids in the transmembrane domain of PLN contribute to pentamer stabilization (59).

1.1.2.1.3.2 Regulation by Calmodulin-dependent Protein Kinase II

The SERCA2 pump is also phosphorylated directly by **Ca^{2+}/calmodulin (CaM)-dependent protein kinase II (CaM kinase II)**. Although three serine residues are potential

targets, only Ser^{38} stimulation by CaM kinase II produces increases in rates of Ca^{2+} transport and ATP hydrolysis (34). A potential CaM kinase II site of phosphorylation exists in SERCA1 at Ser^{167}, but this was not found to be an actual target, as there was no effect on the rate of Ca^{2+} transport. Thus, phosphorylation of the SERCA2 isoform by CaM kinase II is unique (112).

In SERCA2, the Ser^{38} residue is believed to be a part of a loop structure between a cytoplasmic α-helix near the NH_2 terminus of the molecule and a long α-helix which makes up the predicted stalk sector 1 and transmembrane sector 1 α-helices (112). Phosphorylation of Ser^{38} is suggested to regulate SERCA pump function in one of the following two ways: a) since this serine is within the same area as the site of interaction between PLN and SERCA, CaM kinase II can regulate the apparent Ca^{2+} affinity of SERCA2, or b) through long range interactions between the NTP binding/phosphorylation domain and the sites of Ca^{2+} binding and translocation. *In vivo*, the significance is that PLN and CaM kinase II may act synergistically to stimulate cardiac function (112).

1.1.4.1.3.3 Regulation by Sarcolipin

Sarcolipin (SLN) is a 6 kDa regulatory protein of SERCA1 encoded by 31 amino acids. It is primarily found in fast twitch skeletal muscle but in addition, is found less often in slow twitch skeletal muscle (85). The two main functions of sarcolipin are decreasing apparent affinity for Ca^{2+} and stimulating maximum Ca^{2+} uptake rates. Although SLN and PLN are structurally and functionally similar, it is this second effect on SERCA function which makes it different from PLN. The dual action of SLN is regulated by the Ca^{2+}

concentration. For example, at low [Ca^{2+}] SLN lowers apparent affinity for Ca^{2+}, thereby lowering Ca^{2+} uptake rates. At saturating concentrations of Ca^{2+}, however, the rate of transport is stimulated (84;85). SLN also differs from PLN as it is not regulated by CaM kinase II or PKC phosphorylation.

1.1.2.2 Plasma membrane Ca^{2+} pumps

Plasma membrane Ca^{2+} pumps (PMCA) actively remove Ca^{2+} from the cytoplasm of the cell to the extracellular space through the hydrolysis of ATP and are the major means of Ca^{2+} removal in all eukaryotic cells. PMCA are low-capacity, high-affinity pumps (86). There are four different PMCA isoforms (1,2,3, and 4) which are each subject to alternative splicing in their 3' region, giving rise to a wide variety of PMCA proteins. These share a similar structure and function but differ in their distribution and Ca^{2+} affinity (109). The individual PMCA isoforms are well conserved between species but within a species the variation between isoforms is much larger. This suggests that each of the isoforms is unique, explaining the maintenance of all 4 isoforms within a single organism. Some key differences among splice variants include tissue expression, interactions with scaffolding proteins, binding to and regulation by CaM, and regulation by kinases (109).

1.1.2.3 The Na^+/Ca^{2+} exchanger

The Na^+/Ca^{2+} exchanger is a large-capacity, low-affinity carrier that exchanges Ca^{2+} to the extracellular space for sodium ions (Na^+) coming into the cell (15;16). Since its exchange of these ions is unequal in charge, the Na^+/Ca^{2+} exchanger also contributes to changes in the cell membrane potential that may influence voltage operated Ca^{2+} channels

(VOCC) opening in excitable cells (72;115).

1.1.3 Ca^{2+} entry into the cell

The extracellular fluid contains a high concentration of Ca^{2+}, thus, it is one of the most important sources for cellular processes that depend on elevated $[Ca^{2+}]_i$. Located in the plasma membrane are **voltage-operated Ca^{2+} channels (VOCCs)** and **receptor-operated Ca^{2+} channels (ROCCs)** that allow Ca^{2+} to enter the cell. Influx of Ca^{2+} through VOCCs is caused by changes in the membrane potential of the cell while ROCCs allow entry of Ca^{2+} in response to ligand stimulation.

Voltage-operated Ca^{2+} channels (VOCCs) are opened by changes in the membrane potential of the cell, usually depolarization caused by an influx of K^+ ions. VOCCs are generally more selective for Ca^{2+} than ROCCs and various subtypes of these channels exist. The primary differences between VOCC subtypes are their conductance, agonist and antagonist sensitivity, and tissue expression (72;115).

Receptor-operated Ca^{2+} channels (ROCCs) can be directly or indirectly linked to plasma membrane channel opening. Directly, an agonist can induce a conformational change in the receptor to expose an ion-conducting pore while indirectly, G-protein-coupled-receptor stimulation of phospholipase C (PLC) may open an associated channel (115). The precise mechanism by which non-selective channels influence Ca^{2+} entry is not well understood but has been the subject of recent reviews. Receptor stimulation may also result in the opening of **store-operated Ca^{2+} channels (SOCCs)**. SOCCs may be a type of ROCC that is directly coupled to the SR (115). Transient receptor potential proteins have been suggested to be the

main link between intracellular stores and extracellular Ca^{2+} entry for ROCCs and SOCCs (4;93).

1.1.4 Ca^{2+} release from intracellular stores

Another large source of Ca^{2+} is within the cell itself. The SR contains approximately 1000X the amount of Ca^{2+} stored in other cellular organelles (56). The mitochondria are another potential storage site for Ca^{2+} but they do not take up significant quantities unless the $[Ca^{2+}]_i$ is >5 μM, and their role in signal transduction has been questioned (115). The nucleus also contains Ca^{2+} but this thesis will focus only on the contribution of SR Ca^{2+} to cells.

The large amounts of SR Ca^{2+} can be released in response to either **1,4,5-inositol trisphosphate (IP_3)** or drugs such as **caffeine**. IP_3 receptor (IP_3R) activation results from stimulation of plasma membrane receptors coupled to G-proteins. Stimulatory G-proteins activate adenylyl cyclase, which then stimulates phospholipase C to cleave phosphotidylinositol-4,5-bisphosphate into IP_3 and diacylglycerol (DAG). DAG activates PKC which is thought to increase the sensitivity of myofilaments of the contractile apparatus to Ca^{2+} while IP_3 binds to its receptors found on the SR membrane (115;116). The activation of an IP_3R causes Ca^{2+} to be released from the SR and increases $[Ca^{2+}]_i$. The release of Ca^{2+} by IP_3 occurs only from one of two postulated pools in the SR. IP_3 may release Ca^{2+} only from the "superficial" SR because it is metabolized by a specific phosphatase before it can reach the "deep" SR (115;116). Control of the IP_3R is also mediated by cAMP and the local $[Ca^{2+}]$ in the vicinity of the IP_3R (77). The other means by which Ca^{2+} is released from the

SR is by Ca^{2+}-induced Ca^{2+}-release channels. These channels may also be opened by ryanodine or caffeine.

1.1.5 Ca^{2+} binding proteins

Several proteins within the cell bind Ca^{2+} but their resulting functions differ widely. **Calmodulin (CaM)** has been mentioned already for its role in contraction and in regulation of SERCA pumps (82). **Calreticulin** is another important Ca^{2+} binding protein which will be described along with its smooth muscle counterpart, **calsequestrin**. Others include calcineurin, calnexin, calmegin, and calbindin (43;53;61). CaM is from a family of proteins that can function either as Ca^{2+} buffers or transporters without any conformational change or as Ca^{2+} sensors that undergo a Ca^{2+}-induced conformational change. Calmodulin usually functions while bound to Ca^{2+} in the Ca^{2+}-CaM complex. CaM, as a sensor, has many effectors. One of its roles is in the contractile apparatus and in regulation of the SERCA2 pump (24). Calreticulin is a Ca^{2+} binding protein found in the SR/ER (61). Calsequestrin is another ER protein responsible for buffering Ca^{2+} within the lumen and effectively increases the Ca^{2+} storage capacity of the ER. It is a high capacity, low affinity binding protein that can release Ca^{2+} upon stimulation of the Ca^{2+} channels in the ER (5;115).

1.2 The Role of the 3'-UTR in Control of Gene expression

1.2.1 Levels of regulation of expression

The level of expression of any gene can be modulated at several steps. Generally, a gene is transcribed into heteronuclear RNA (hnRNA) which is then spliced, capped with

methyl guanosine at its 5' end, and polyadenylated at its 3' end to produce messenger RNA (mRNA). The mRNA is then exported out of the nucleus where it binds to ribosomes before translation is initiated. The translated protein may then require processing to achieve its functional form. Each step within the pathway from DNA to functional protein provides a means by which the cell can regulate expression. Some examples are: binding of transcription factors and the presence or absence of promoter sequences are some elements which affect the rate of transcription in the cell; the strength of splice sites, specific sequences of the splice sites, and tissue-specific expression of splicing factors may inhibit or decrease the expression of certain splice forms; precise binding and functioning of initiation, elongation, and termination factors control the correct translation of a protein; translation and the ribosome may be essential for nonsense-mediated or non-stop mRNA decay to control levels of aberrant mRNA species in higher eukaryotes (7;42;68;118).

Degradation of normal mRNA and proteins are also carefully controlled events. **Here, the focus will be on the decay of mRNA.** There appear to be a number of regulatory elements for this step including specific sequences within the RNA itself (*cis*-acting factors) and proteins which bind the RNA (*trans*-acting factors) (97;98;102). Some families of RNA-binding proteins have been well characterized as have their consensus RNA binding sequences, while other proteins are still under investigation. The general kinetics of mRNA decay have been determined such that it is known to proceed in a step-wise fashion but numerous possible pathways have been suggested (17;30;49;97-99). The cellular location of mRNA decay is also an area of exploration. Some of the proteins which mediate decay

have been found in the nucleus and others in the cytoplasm, while still others appear to shuttle between the two compartments (36;37;125;135). The next section will discuss the various elements controlling mRNA decay.

1.2.2 mRNA decay: Directionality and kinetics

Sequences throughout the mRNA and proteins which bind them are vital determinants of the rate of mRNA degradation. In most cases, the first step in mRNA decay is the removal of the poly A^+ tail before decay of the body of the mRNA (101. The kinetics of mRNA decay have been shown to proceed by one of two mechanisms: decay of all poly A^+ tails before decay of any mRNA bodies (synchronous or distributive) or decay of each poly A^+ tail and mRNA body in sequence (asynchronous or processive). Following deadenylation, decay of the mRNA proceeds in one of many ways (17;30;50;97;100). One pathway is initiated with deadenylation, followed by 3'→5' exonuclease digestion and decapping (64). This is the most supported pathway for mRNA decay in mammals, however, evidence exists from many organisms to suggest other possible patterns. Alternatives include 5'→3' or 3'→5' exonucleolytic decay after deadenylation, or 5'→3' degradation following decapping, independent of deadenylation. Another possible event initiating decay, endonucleolytic cleavage, may allow mRNAs to undergo degradation initiated at any site within the mRNA body before or without deadenylation.

The two main features used to distinguish mRNA species into 3 specific classes are the decay kinetics described above and sequences found in their 3'-UTR. The 3'-UTR of mRNA in class I and class II both have AU-rich elements (AREs) that contain various copies

of the AUUUA motif. Class I AREs (ie. c-*fos*) contain one to three copies of AUUUA motif which are dispersed between U-rich sequences and undergo a biphasic decay pattern. In the first phase, all the mRNA molecules are deadenylated with little degradation of the mRNA body. Following this synchronous poly(A) shortening, the mRNAs are then quickly degraded. Class II AREs (ie. GM-CSF) in contrast, contain clustered AUUUA motifs that often combine to form the nonamer sequence, UUAUUUA(U/A)(U/A), and undergo asynchronous decay (132). While the rapid decay of class I mRNA can be specifically impeded by pretreatment of cells with these inhibitors, the decay of class II mRNA is less affected because they are targets of two distinct decay pathways (21). Finally, class III AREs (ie. c-*jun*) do not contain the AUUUA motif and, like class I, are deadenylated by synchronous kinetics (132). These mRNA classes also differ in their sensitivities to the transcription inhibitors, actinomycin D and 5,6-dichloro-1-B-D-ribofuranosyl-benzimidazole (DRB) (20;89b).

1.2.3 RNA stability: cis-acting elements

Sequences within the mRNA species itself that may affect its degradation are referred to as *cis*-acting elements. Specific sequences have been identified throughout the bodies of many different mRNA transcripts, and consensus sequences influencing stability or instability have been determined. These may act a) alone as endonuclease sites, b) only after binding sequence-specific *trans*-acting factors (or proteins), or c) in conjunction with other *cis*-acting elements.

1.2.3.1 The 3'-untranslated region

The 3'-untranslated region (3'-UTR) is probably the most important region of RNA regulating its stability. It carries several *cis*-acting elements that can affect the rate of RNA turnover. These include the poly A^+ tail, secondary structures, or AREs. These regions play important roles not only as isolated sequences but also by providing targets for proteins which may bind in this area. The following sections will focus on the *cis*-elements themselves and a later section will describe their effects with respect to RNA-binding proteins.

1.2.3.1.1 The poly A^+ Tail

One possible role for the eukaryotic mRNA poly A^+ tail in decay is protection at the 3' end from 3'→5' exonucleases (30). Since the first step in mRNA decay may be deadenylation (either processively or distributively), this tail may prevent or delay degradation of the mRNA body. In theory, those mRNA molecules with longer poly A^+ tails should take longer to deadenylate and should, thus, appear more stable than mRNA with shorter tails. The relative stabilities of some mRNA species have been correlated with the lengths of their poly A^+ tails and show this relationship to exist (83). In the same study, the stability of dihydrofolate reductase (DHFR) mRNA varied with the polyadenylation site used. Here, stronger polyadenylation sites correlated with more stable mRNA. The poly A^+ tail not only plays a role in message stability but also in translational efficiency in the cytoplasm (48). This, then, implies a secondary effect of deadenylation: that an mRNA that undergoes rapid removal of its poly A^+ tail will also be limited in amount for specific translation (134).

Another important influence of the poly A^+ tail may be due to the specific *trans*-acting proteins it binds. At least one characterized protein, poly A^+ binding protein (PABP), is known to bind this sequence of adenosine repeats. PABP may play an important role in mRNA stabilization through prevention of exonuclease digestion of the poly A^+ tail and will be discussed in detail in *1.2.4.3*.

1.2.3.1.2 AU-rich elements

Many mammalian RNAs contain AREs within the 3'-UTR (1;104). AREs may consist of one or more repeats of the consensus sequence, AUUUA. As the sequences in this region contain many adenosine residues, AREs may compete with the poly A^+ tail for non-specific PABP binding (1). If the primary role of PABP is to slow down the rate of deadenylation by binding to the poly A^+ tail, displacement of the PABP to the ARE through competition may increase the rate of mRNA turnover. However, if PABP can protect mRNA from degradation independently of the poly A^+ tail, non-specific binding of PABP to the ARE may provide the same protective effect (27).

In addition to possible competition with the poly A^+ tail for PABP binding, AREs are known to bind specific *trans*-acting AUBPs (ARE binding proteins) either in the nucleus or in the cytoplasm (36;98;135). Evidence suggests that binding of AUBPs to AREs may either induce or prevent destabilisation depending on the specific sequences and proteins involved. Some AUBPs may produce the stabilization by protecting mRNAs with the AUUUA motif from nucleolytic attack. For example, GM-CSF is normally unstable due to the AUUUA sequences in the 3'-UTR. However, binding of an AUBP to these instability elements has

been found to lengthen the half-life of the transcript (96). This has since been found to be due to binding of an RNA-stabilizing factor, AUBF, to the AUUUA consensus sequence. In this way, AUBPs may act similarly to PABP and any indirect removal would accelerate decay. During translation these protective RNA-binding proteins may be displaced by the moving ribosomes, making the RNA susceptible to degradation (1).

Other evidence shows direct destabilisation by AUBPs. It is proposed that after binding AREs, a specific AUBP, AUF1, is ubiquinated and targets the associated RNA for degradation in a proteasome (62). In bacteria, specific 3' exonucleases have been identified which target the exposed 3' ends of several mRNA. An endonuclease function associated with an RNA-binding protein that binds AREs may be responsible for this exposure by cutting internally at these sequences (9). During the process of translation these destabilizing AUBPs may be removed by changes in RNA structure, thereby protecting the RNA (1). Thus, although the AREs are thought to destabilize RNA, their role depends on the specific RNA-binding proteins with which they interact.

1.2.3.1.3 Secondary Structure

Secondary structures in the 3'-UTR have also been identified as influencing mRNA decay. In the same way that AREs may promote or deter degradation, secondary structures may also play alternative roles in the decay process. For example, the presence of a stem-loop at the 3' end of histone H3 mRNA is required for decay (10). This is most likely explained by the binding of a specific protein or endonuclease to this site of internal cleavage. In contrast, a GA-rich sequence in chicken elastin mRNA forms a secondary structure that

may be essential for stability (45). Binding of cytosolic proteins to this region increases the stability of mRNA at different stages during development (44). Thus, hairpin loops or other secondary structures within the 3'-UTR may have a role similar to the poly A^+ tail, that is to attract binding proteins that affect mRNA stability to this region of the mRNA.

1.2.3.2 The 5'-untranslated region and the coding region

Several features within the 5'-UTR can also influence RNA stability including: 1) the methyl guanosine cap, 2) binding sites for the ribosome and other translation initiation factors, and 3) specific *cis*-acting elements. Most mRNAs are capped at their 5' end by a 7-methyl guanosine which protects the chain from 5'→3' exonucleases as well as stimulating efficient translation (30;39). Early work showed that exonucleases processively cleave unmethylated/ uncapped RNAs in a 5' → 3' direction, yielding 5' mononucleotides (39). Thus, the cap appears to deter the degradation process that may begin at the 5' end of mRNA. In addition, there exist several different types of cap binding proteins (CBPs) that can form a complex with the cap at the 5' end of the transcript. While the formation of such a complex would be expected to hinder exonuclease digestion originating at this end, the role of these associated CBPs during mRNA turnover has not been confirmed.

Understanding the 5'-UTR has become increasingly more important as the role of translation in mRNA stability is further delineated since it is the binding site of the ribosome and other eukaryotic translation initiation factors (eIFs). Evidence includes the following observations: a) inhibition of translation results in stabilization of mRNA; b) some unstable mRNAs must be in the process of translation for degradation to occur; and c) PABP, AUF1,

hsp70 (heat shock protein), and eIF4G are found together in a complex on rapidly degraded mRNA (1;62). Thus, the 5'-UTR may be involved in maintaining RNA stability based on the role of translation and the factors required for this process.

Other *cis*-acting elements within the 5'-UTR may also affect 5' → 3' mRNA decay. Specific sequences, such as the leader sequence of the c-*myc* transcript, act to destabilize mRNA upon interactions with other sequences in the RNA (9). Also, secondary structures in this region that function primarily to inhibit or enhance translation may also indirectly act to deter exonuclease activity (31;97). Finally, sequences of the 5'-UTR may provide binding sites for *trans*-acting factors to stabilise the RNA. The role of such regulatory proteins in stability may be indirect, as their effects may be due to inhibition of ribosome translocation in this position (30;39).

In addition to stability sequences in the 3'- or 5'-UTR, several mRNAs also contain *cis*-acting elements within their coding regions that may affect turnover (30). For example, the last 249 nucleotides of the c-*myc* mRNA coding region contain an instability element known as the Coding Region Determinant (CRD) (10). An RNA-binding protein, CRD-BP, prevents endonucleolytic attack when bound at or near this element (98). It is not known how ribosomes interact with the protective RNA-binding proteins of internal coding sequences in translation: they may ignore the proteins and simply continue processing the RNA or may first have to displace the factor before translation can proceed (98). In other mRNA species, including c-*fos*, the coding region sequences act only in conjunction with instability elements in the 3'- or 5'-UTR and have no effect on their own (18).

1.2.4 RNA stability: trans-acting factors

In addition to *cis*-acting elements within the mRNA, proteins (or *trans*-acting factors) which bind these sequences also function in RNA stability. One of the protective factors for a specific region, the PABP, has already been described above. In addition, there are several known AUBPs that provide both stabilization and destabilization of mRNA by binding sequences within the 3'-UTR. Interestingly, because these are AUBPs, the consensus binding sequences for proteins with opposite functions are often the same or very similar. A large number of AUBPs have been reported but poorly characterized. Here, two of the key RNA-binding proteins, HuR and AUF1, will be discussed in terms of their general effects on RNA. These proteins have been studied in more detail than others. While these proteins are described as stabilizing or destabilizing, anomalies in their effects will also be discussed to show that these roles may vary.

1.2.4.1 Stabilizing RNA-binding proteins

Several RNA-binding proteins have been shown to have a stabilizing effect on one or more transcripts. Many of these proteins, however, have yet to be characterized. Some of the stabilizing factors that have been well characterized belong to the family of Hu proteins. The Hu proteins belong to the *elav* (embryonic lethal, abnormal vision) gene class which was originally identified as playing an essential role in neuronal development in *Drosophila* (89a). All Hu proteins share a common structure which includes a hinge region and three RNA recognition motifs (RRMs) that are essential for efficient RNA binding and stabilizing activity. The family includes at least four genes, HuA (HuR), HuB (Hel-N1), HuC

(Ple-21), and HuD, of which HuR will be described in detail.

The HuR protein is expressed ubiquitously and binds to the AURE of many mRNAs including vascular endothelial growth factor, endothelial nitric oxide synthase, and some cell cycle regulators (37;89a). Its specific consensus binding sequence is repeats of AUUUA but overexpression of HuR increases the stability of both class I and class II mRNA (37). HuR is expressed in a variety of mammalian cell lines and, although HuR can shuttle between nucleus and cytoplasm, under normal conditions it primarily appears in the nucleus with nucleolar exclusion (36;37). While this suggests HuR may bind and sequester mRNA species in the nucleus, away from the degradation machinery, this possibility has been eliminated by studies showing enhanced translation of ARE-containing mRNA in HuR overexpressing cells (37). In fact, HuR may bind to mRNA molecules in the nucleus and translocate with them to the cytoplasm, exhibiting a protective effect throughout the cell. Once HuR returns to the nucleus, however, decay of the RNA body may occur. Another plausible mechanism for the protective effect of HuR binding is through possible association with the poly A^+ tail even though it has little effect on deadenylation (37;89a).

One interesting study has identified HuR as the dominant binding protein in the regulation of human and hamster β-adrenergic receptor mRNA (6). Rather than stabilizing β-adrenergic receptor mRNA, HuR destabilizes this RNA. The authors explain this discrepancy by suggesting that HuR may be multifunctional and its effect on mRNA stability may vary with the cell type, cytosolic or nuclear localization, specific mRNA substrate, specific mRNA binding site, or state of phosphorylation (6). Thus, while HuR and members

of the Hu family are known primarily for their stabilizing effects on mRNA, these proteins may have different roles in mRNA stability.

1.2.4.2 Destabilizing RNA-binding proteins

The heterogeneous nuclear ribonucleoprotein (hnRNP) family of proteins has been shown to bind several different RNAs. One member of this family, AUF1 (hnRNP D), is a well characterized destabilizing protein (55;135). The single copy AUF1 gene is alternatively spliced into 4 isoforms which encode the proteins p37, p40, p42, and p45. These proteins are differentially expressed depending on cell type, developmental stage, and response to cellular stimuli (14). All the isoforms have the same overall structure, sharing a conserved 5'-UTR and amino terminal with an alanine-rich region. This alanine-rich region is required for ARE binding possibly by allowing dimerization of AUF1 proteins. Because this is a general feature of all 4 of the isoforms it is possible that different isoforms could form hetero-oligomeric complexes on AU-rich RNA via this common protein-protein interaction domain (32;121). AUF1 forms dimers with high affinity in solution and after dimer binding of AREs, the formation of trimers and tetramers is also evident, most likely as a result of sequential dimer binding. The isoforms also share 2 RRMs and a short glutamine-rich region in the carboxyl terminal which are necessary but not sufficient for ARE binding (32). Although the RRMs and glutamine region are shared between isoforms, these are subject to post-translational modifications including methylation, phosphorylation and glycosylation which may affect isoform affinity, specificity, cellular location, and protein association (65).

The isoforms are derived from 10 exons, with alternative splicing of these exons affecting both binding affinity and sequence specificity as previously reviewed (121). An amino terminal insert found in exon 2 of isoforms p37 and p42, gives these isoforms higher affinity for AU-rich regions than those without the insert (p40 and p45) (32;65). It has been suggested that this amino terminal insert may interfere with the alanine-rich region required for ARE binding. In addition, an insert found in exon 7 decreases binding if the exon 2 insert is absent but increases binding in the presence of it. Thus, the p37 isoform is the most potent destabilizing AUF1 and its affinity for a sequence reflects the destabilizing potential of that ARE (see schematic in Figure 3).

AUF1 has been shown to affect the decay of many mRNAs including c-*myc*, c-*fos*, β-adrenergic receptor, leutinizing hormone receptor (LHR), interleukin-1β, GM-CSF, and H4 histone (14;65;88;100). While its target genes are well known, the sequences and mechanism of AUF1 decay still have to be clarified. AUF1 recognizes both AU-rich and U-rich elements included within class I, II, and III mRNAs. Generally, as the number of tandem repeats of AUUUA increases, the AUF1 binding affinity and instability of the mRNA also increase while insertions of G and C residues into AREs stabilize the RNA (32). Others have shown that the AUUUA motif need not be an integral part of ARE for destabilisation to occur, as with LHR mRNA, and that AUF1 recognizes U-rich stretches of RNA without the AUUUA repeats. Its binding affinity for a sequence of U32, however, was at least 20-fold lower than binding to (AUUU)5 (32;121;126). The binding affinity of AUF for most destabilizing AREs is in nM range, which is similar to binding affinities of other RNA-

binding proteins that recognize specific sequences. This would suggest that AUF isoforms bind specific sequences rather than any combinations of A and U residues. The sequences recognized by the different isoforms appear to be relatively constant as AREs but the p40 isoform, which contains exon 7 but not exon 2, binds a different consensus sequence with higher affinity and can also bind DNA (121).

The exact means by which AUF1 leads to degradation of unstable mRNAs is not clear. AUBPs can be nuclear, cytoplasmic, or shuttle between the two compartments. AUF1-related proteins in different species appear to bind pre-mRNA in the nucleus and accompany mRNAs through nuclear pores so that decay is generally cytoplasmic but involves a nuclear step. The p42 and p45 isoforms, which contain exon 7, were shown to remain in the nucleus due to interactions with the nuclear scaffolding protein, SAF-B (3). Isoforms p37 and p40 appear to shuttle between the nucleus and the cytoplasm where one of its functions may be to exert a cytoplasmic destabilisation activity in contrast to its nuclear counterparts (3;121). More complexity is given to AUF1 function with some evidence that those isoforms that shuttle between the nucleus and the cytoplasm have an inhibitory effect on mRNA decay while mutants that are confined exclusively in the cytoplasm lose their ability to block mRNA turnover (19).

Different evidence has linked degradation of mRNA in the cytoplasm by AUF1 with polyribosomes and translation or a proteasome complex (65). Some of the data supporting this role for translation include the following: the ability of translation inhibitors to increase stability of unstable RNAs, co-precipitation of AUF1 and eIF4G, and studies that show ARE

decay is blocked by preventing ribosome binding and ongoing translation (14). Another proposal is that AUF1 is only one protein in a larger degradation complex. Some studies have shown that a >20S proteasome complex is formed on short-lived mRNA and this might be delivered through association with the ribosome (104). Others have shown that the 20S proteasomes are able to destabilize and cleave AUUUA-containing mRNA (52b). AUF1 was found to interact with hsp70, hscp70, PABP, eIF4G, and other proteins that may recognize ubiquitinated lysine residues as a proteasome complex (62). Thus, a more complex structure of the RNA than suggested by the translation model alone is envisaged as there are not only interactions between AUF1 and PABP within the 3'-UTR but also with 5'-UTR initiation factors.

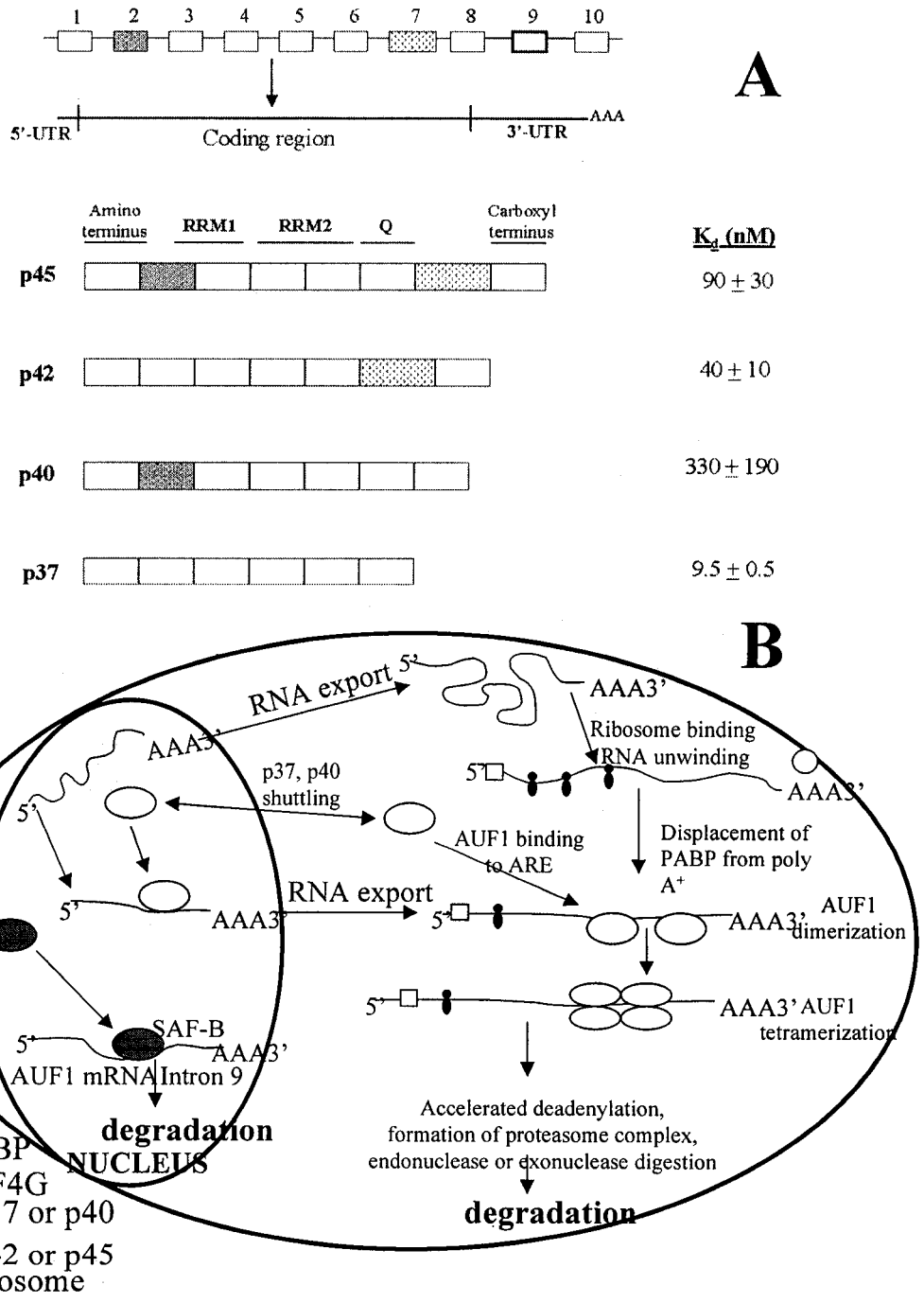

Figure 3. AUF1. A. AUF1 isoforms. Comparison of AUF1 isoform RNA structure and binding affinity. **B. Roles in mRNA decay.** See text for details. Reprinted with permission from Kluwer Academic Publishers (73).

One of the key differences between stabilizing or destabilizing effects by AUF1 may be its regulation by splicing, phosphorylation, or association with other proteins. Phosphorylation, in particular, occurs for each of the isoforms but is not required for RNA-binding (135). Since phosphorylation is not a requirement for the role of AUF1 in RNA stability, it is possible that this modification is involved instead in the regulation of AUF1, itself. This is supported by the reduction in AUF1 protein in response to phosphorylation by β-agonists (88). AUF1 activity may also be regulated via sequestration by other proteins. AUF1 has been coimmunoprecipitated with other cellular proteins in several instances. One example is the proteasome complex, mentioned above, that is formed during degradation of RNA (62). Another example is a poly C protein complex, termed αCP, formed on α-globin mRNA with a poly C element in its 3'-UTR. Not only does the binding of αCP increase the stability of α-globin mRNA, but it initiates the assembly of interacting proteins. These may include both AUF1 and PABP that are otherwise bound to alternate sites within the 3'-UTR (25). By removing these proteins from their normal binding sites, the αCP complex at a 3'-UTR may further promote or prevent mRNA decay. While all the AUF1 isoforms can bind αCP1 *in vitro*, it is the p40 isoform that may provide the *in vivo* interaction, possibly through its glycine-rich domain in its carboxyl terminus (122). Other unidentified proteins are involved in the complex but it is not known whether these are all involved at the same time. Most of the proteins within this complex do not bind the poly C element individually but they do so within the context of the complex. More interesting is the existence of αCP proteins both within the nucleus and the cytoplasm, sharing the cellular locations of AUF1 and

suggesting that this stabilizing α-complex may also affect both nuclear and cytoplasmic stability (122). The finding of AUF1 within an RNA stabilizing complex suggests that either AUF1 can not exert a destabilizing effect when sequestered in specific protein complexes or that, like HuR, AUF1 is multifunctional and may be involved in the stabilization of certain RNAs.

1.2.4.3 Poly A^+ Binding Protein

Another key protein which may have a role in mRNA decay is the cytoplasmic poly A^+ binding protein (PABP). Although it does not specifically bind to *cis*-elements in the 3'-UTR, it does bind the poly A^+ tail located at the 3' end of most mRNAs. Several different functions have been suggested for PABP. Its basic role was thought to be to protect mRNAs from deadenylation, thereby indirectly deterring subsequent degradation of the mRNA body (98). Its presence at the end of the mRNA suggests a function in protection of the mRNA from 3' → 5' degradation by exonucleases. It has since been deemed necessary for initial shortening of the poly A^+ tail before complete deadenylation and eviction of the final PABP molecule from the last 10-12 residues of the poly A^+ tail triggers turnover (27). In this study, the domains of PABP required for mRNA stabilization are distinct from those required for poly A^+ binding. Thus, the primary role of the poly A^+ tail may simply be to attract PABP to the mRNA where it can then act as a protective RNA-binding protein. Thus, ARE in the 3'-UTR may have additional effects on decay by competing with poly A^+ sequence for PABP binding. That is, if the PABP binds the ARE instead of the the poly A^+ tail, protection from exonucleases may be lost. Alternatively, the ARE sequences may simply attract PABP as a

stabilizing protein, acting independent of its effects at the poly A^+ tail. A role for PABP in both translation of mRNA and mRNA decay is suggested by its co-precipitation with eIFG4 and AUF1 on rapidly degraded RNAs but its presence in this complex does not support the theory that its displacement is the cause of instability (62). Thus, the role of PABP in the decay process may be more complex.

Some of the complexity of PABP may be explained by the discovery of PABII and *i*PABP, two distinct but related proteins. These differ from PABP in their sequences and molecular mass, their cellular localization and, possibly, their role within the cell. For example, PABII is a nuclear protein that regulates the length of the poly A^+ tail: first, by stimulating its elongation by poly (A) polymerase and second, by limiting the overall length of the poly A^+ tail to 200-250 residues (41). In comparison, *i*PABP appears to be expressed in the cytoplasm of most tissues and upon cellular activation, can be rapidly induced. Although it has similar binding specificity to PABP, it is expressed at much higher basal levels than PABP in tissues including cardiac and skeletal muscle (133). The precise function of *i*PABP is not known. At least two additional proteins, PABP-interacting proteins, have also been characterized. Unlike PABPII and iPABP, these interact with PABP but resemble portions of the eukaryotic translation initiation factors, further adding to the possibility of protein complexes involving PABP in mRNA translation and decay.

1.2.4.4 The role of the ribosome and translation in decay

The need for RNA binding to ribosomes and translation in mRNA decay is controversial. While some studies have provided evidence to show translation to be

necessary for turnover, others have shown that degradation can proceed after the mRNA has been uncoupled from translation by ribosomes (1;21;27;62;97;104). In histone mRNA the 3' stem-loop and the site reached by moving ribosomes must be less than 300 bases apart for decay to occur and translation through at least part of the coding region is required for the decay of tubulin mRNA (10). Another way to explain the coordination of decay with translation is through association of exonucleases with ribosomes (104). Alternatively, protective proteins which bind mRNA may be removed by ribosomes during translation. Opposing arguments have suggested that preventing translation allows ribosomes to accumulate along the RNA or may prevent a labile degradation factor from being synthesized, thus preventing degradation(9;97).

1.2.5 mRNA decay: Nuclear or cytoplasmic localization

Many RNAs undergo co-translational decay, suggesting that the cytoplasm is the main site of mRNA degradation. However, evidence given of the RNA-binding protein, HuR, in the nucleus suggests that mRNA decay may have a nuclear component. Further still, some AUF1 protein isoforms, which can shuttle back and forth from the nucleus to the cytoplasm, imply that decay may occur in either or both cellular compartments.

Having established that mRNA decay may be either nuclear or cytoplasmic, another important cellular process to consider in gene regulation is nuclear export. Both the efficiency of export of different mRNAs and the presence of specific protein factors may influence its stability. Some theories propose simple diffusion of RNA through the nuclear membrane to the cytosol (29). Given the vast complexity of the nuclear pore complex

(NPC), it is much more likely that this complex regulates RNA transport in the same way that transport of proteins is controlled. Furthermore, the NPC and its machinery can discriminate between processed and nonprocessed RNA so that immature species do not get into the cytoplasm (80). Size may be another limitation to simple diffusion out of the nucleus which was tested using linear, double stranded DNA. Only DNA less than 200 bp was found to move freely through nuclei of living cells without energy (66). Also, with regard to processed RNA, the cap structure may be important in transport as it binds the cap binding complex and other proteins of the NPC to mediate transport of small nuclear RNA. In fact, both the poly A^+ tail and the cap stimulate mRNA export but neither is required (80;81). Another means of controlling RNA transport may lie within the RNA molecules themselves. For example, splicing of mRNA is important as those molecules transcribed from cDNAs with introns intact are not exported until splicing occurs (47). Some transport may also be linked to the function of RNA polymerase II. Cells treated with RNA polymerase II inhibitors may show redistribution of many abundant RNA-binding proteins to the cytoplasm where they prevent further transport of RNAs. Finally, all RNA exhibit selective saturability. That is, when present in excess in the cytoplasm, the RNA will block export of its own RNA but not others. This suggests yet another mechanism of control of export which may or may not lie in the NPC (51).

The key proteins involved in the transport of mRNA may either be retained in the nucleus due to nuclear localization sequences or may travel through the NPC with the RNA because they contain nuclear export sequences. The signals which determine localization are

recognized by a family of proteins (termed importins, exportins, or karyopherins) that all have a RanGTP-binding domain, C-terminal cargo-binding domain, and ability to bind components of the NPC. Additional proteins bound to specific mRNAs during transport are becoming more characterized. The affinity of these proteins for their cargo is dependent on mRNA sequence, and protein phosphorylation or methylation state (80;81).

1.3 Control of SERCA2 Gene Expression

In the previous section, the various means of controlling gene expression in the cell were outlined with special emphasis on mRNA decay. The following section will discuss the control of SERCA2 gene expression in cardiac and stomach smooth muscle tissue.

1.3.1 Previous data

A previous study in our lab examined the abundance of SERCA2a and 2b in adult rabbit cardiac and stomach smooth muscle tissue (57;58;76). Briefly, SERCA2a protein in cardiac tissue was 60-80 times more abundant than SERCA2b in stomach smooth muscle. The poly A^+ RNA also differed between the two tissues, with SERCA2a levels being 6-8 times higher than SERCA2b in their respective tissues. The next step was to determine the mRNA half-lives of the two transcripts in cultured cells but this procedure was better accomplished using neonatal cardiac tissue for the cell isolation. As such, the analysis of SERCA2 protein and mRNA levels was repeated in neonatal tissues before proceeding with further examination of SERCA2 gene expression. The data obtained using neonatal rabbit cardiac and stomach smooth muscle is summarized below.

1.3.1.1 SERCA2 Protein abundance

The abundance of SERCA2 protein was examined in both post-nuclear supernatant (PNS) and microsome (MIC) fractions from cardiac and stomach smooth muscle using Western Blots. The monoclonal antibody used, IID8, reacts with both SERCA2 isoforms. The results in neonates are similar to the data obtained using adult rabbits, with SERCA2 in cardiac muscle being 100-200 times more abundant than in stomach smooth muscle.

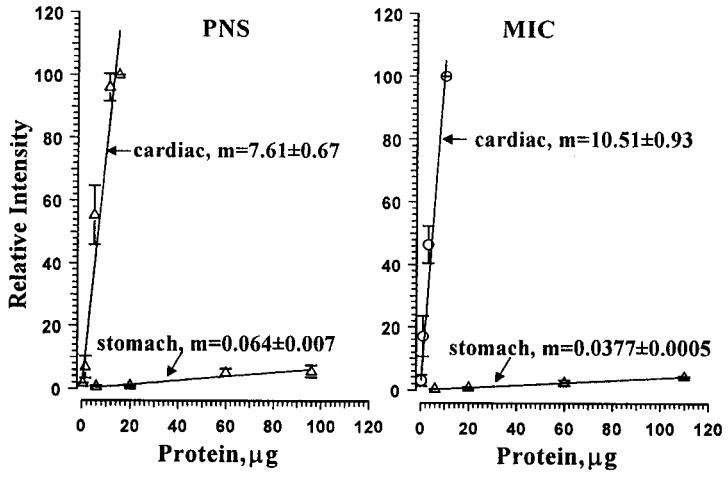

Figure 4. Protein Abundance of SERCA2 in cardiac and stomach smooth muscle tissue. Western Blots showed SERCA2 to be 119 ± 10 times or 250 ± 22 times greater in cardiac than stomach smooth muscle (using PNS or MIC, respectively). Reproduced with permission from (76) © the Biochemical Society.

1.3.1.2 SERCA2 mRNA abundance

Having established that the protein levels of SERCA2 differed in neonatal tissue, the SERCA2 mRNA levels in the two tissues was determined using Northern Blots. The riboprobe used was from a conserved region found in both SERCA2 isoforms (bases 514 to

1282). The results are similar to the data obtained using adult rabbits, with SERCA2 in cardiac muscle being 20-30 times more abundant than in stomach smooth muscle.

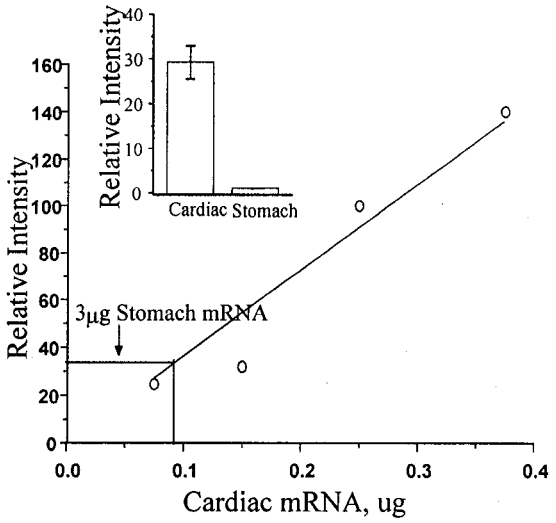

Figure 5. mRNA Abundance of SERCA2 in cardiac and stomach smooth muscle tissue. Analysis of Northern Blots showed SERCA2 in poly A^+ RNA to be 29 ± 4 times greater than SERCA2 in stomach smooth muscle. Using total RNA, SERCA2 mRNA in cardiac muscle was 20 to 30-fold greater than in stomach smooth muscle (not shown). Reproduced with permission from (76) © the Biochemical Society.

1.3.1.3 SERCA2 Transcription Rates

In proceeding with the examination of SERCA2 gene expression, the rates of transcription in the two tissues were compared using nuclear run-on experiments. Nuclei were isolated from both tissues and incubated with radioactivity (α-^{32}P-CTP) in order to label

any RNA transcripts already initiated. Using either single stranded DNA or synthetic RNA as a probe to hybridize the labelled transcripts, these was no significant difference between the SERCA2 transcription rate in cardiac tissue and that in stomach smooth muscle. As a control for non-specific binding, plasmid DNA was used as a probe but did not bind a detectable amount of radiolabelled transcripts from either tissue (not shown).

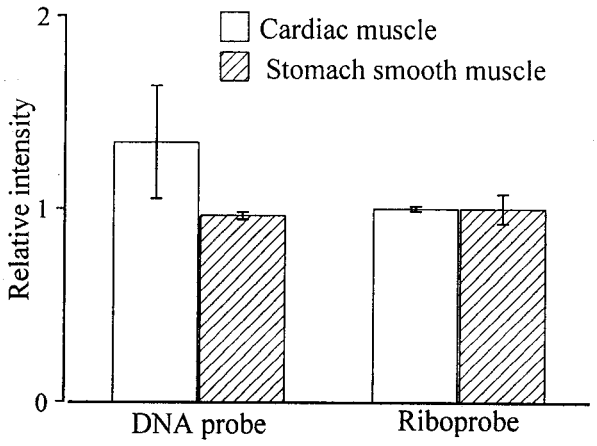

Figure 6. Comparison of SERCA2 Transcription Rates in cardiac and stomach smooth muscle tissue. Analysis with either DNA or RNA probes showed no significant difference between the rate of transcription in cardiac and stomach smooth muscle. Reproduced with permission from (76) © the Biochemical Society.

1.3.1.4 SERCA2 Translation Rates

The efficiency of ribosome binding in cardiac and stomach smooth muscle was also compared as an indication of the relative translation rates (not shown) (76). The amounts of

SERCA2, poly A^+, or 18S ribosomal RNA in either the polysomal pellet or subpolysomal supernatant fractions did not differ significantly between the two tissues. In sucrose gradient density experiments, the distribution of SERCA2 mRNA and ribosomal RNA in polysomal fractions did not differ between the two tissues suggesting that the translation of SERCA2 is similar.

1.3.1.5 Comparison of SERCA2 3'-untranslated region

As previously mentioned, SERCA2a and 2b have identical 5'-UTR sequences and the first 993 amino acids of their coding regions are also conserved. Thus, the major difference in the sequences of SERCA2a and 2b lies within the 3'-UTR. This region has been shown to be of significant importance in control of mRNA due to the AU-content, sequence motifs, secondary structure, and protein binding potential of several other mRNAs. A brief analysis of features in this region is given, below.

1.3.1.5.1 The poly A^+ tail

Several genes have been shown to produce multiple transcripts that differ in the length of their 3'-UTR, suggesting that multiple polyadenylation sites within a gene occur quite commonly (106). The stability of different DHFR mRNA species was shown to vary with the polyadenylation site used within their 3'-UTR (83). Only one of four DHFR transcripts contained the consensus polyadenylation signal, AAUAAA, found 15-20 nucleotides upstream of the polyadenylation site (106). A comparison of SERCA2a and 2b sequences show that the transcripts use different polyadenylation sites and that the site used in SERCA2b is weaker than that in SERCA2a (71). Thus, from the polyadenylation

sequences of SERCA2a and SERCA2b, the hypothesis is that SERCA2a may be more stable than SERCA2b.

1.3.1.5.2 AU-rich elements

Both SERCA2a and 2b have 3'-UTR which are AU-rich and contain some of the known consensus motifs. This means that they could both be stable or unstable mRNA species depending on the proteins that interact with them. A summary of the known ARE features of SERCA2a and 2b is given in TABLE II.

Table II. Comparison of known AU-rich features of SERCA2a and 2b 3'-UTR.

	percentage of AU in 3'-UTR	AU motif	sequence location (bp)
SERCA2a	57.5	UUAUUUA(U/A)(U/A) AUUUA GUUUG	3925, 4044 4100 3716, 3765, 3919, 4173
SERCA2b	60.5	AUUUA GUUUG	4060, 4342 4188

The known ARE motif is given with the corresponding base number in SERCA2a or 2b mRNA. These numbers correspond to the sequences in Figure 2.

This analysis of the 3'-UTR of SERCA2a and 2b suggests possible interactions with known binding proteins, such as AUF1 or HuR, which use AUUUA as a binding motif. Another point of interest is that SERCA2a has more of the known consensus sequences,

indicating that stabilizing proteins may play a larger role than destabilizing proteins in control of SERCA2 mRNA stability. Specific proteins that bind to GUUUG have not yet been identified, but this motif is present in both 2a and 2b. This highlights another important possibility–that SERCA2a or 2b may bind to novel *trans*-acting factors via these motifs or unique sequences.

1.3.1.6 Comparison of SERCA2 5'-untranslated region and the coding region

With respect to SERCA2a and 2b, the 5'-UTR is conserved between the two isoforms. Thus, any possible effect of this sequence on mRNA decay will play a role for both species. However, this assumes that any proteins that bind this region may be found in both cardiac and stomach smooth muscle. In fact, differences in mRNA stability may occur due to tissue-specific RNA-binding proteins found in either tissue.

Specific coding region determinants may also exist in the SERCA2 mRNA splices. Although SERCA2a and 2b share 993 translated amino acids, they differ in their C-terminal amino acids due to alternative splicing. In SERCA2a, this means 4 amino acids follow the 993 while in SERCA2b these are replaced by 49 different amino acids. It has already been noted that the last 12 amino acids of SERCA2b play an important role in determining functional differences between the two isoforms, thus, the few differences that do occur in the coding region may also be important for additional protein binding and stability influences.

1.3.2 Hypothesis and experiments

Previously, we compared the expression of SERCA2a in hearts and SERCA2b in

stomach smooth muscle of neonatal rabbit (76). The transcription rates in the two tissues were measured by nuclear run-on assays and showed no significant difference. The level of mRNA, however, was 30-fold greater in the heart when measured by Northern Blot analysis. In addition, the size of ribosomes to which SERCA2 RNA was associated also appeared to be similar, but the differences in protein abundance in Western Blot analysis were 100-fold (see Table III for summary).

Table III. Comparison of SERCA2 gene expression.

	CARDIAC MUSCLE	STOMACH SMOOTH MUSCLE
Transcription Rate	1	1
mRNA Abundance	20-30	1
Translation Rate	1	1
Protein Abundance	100-200	1

Comparisons of gene expression for SERCA2 levels in cardiac and stomach smooth muscle were calculated relative to the amount in stomach smooth muscle, taking this amount as 1.

Thus, a 30-fold difference in SERCA2 expression is already apparent at the mRNA level. The differential expression of SERCA2 proteins in cardiac and stomach smooth muscle is, therefore, most likely controlled at a step that is post-transcriptional but pre-translational.

Analysis of SERCA2a and 2b sequences shows that both transcripts are AU-rich in their 3'-UTR with relative AU percentages of 57.5% and 60.5%, respectively. In addition, further analysis shows that both SERCA2a and 2b contain random occurrences of the

consensus *cis*-acting AREs, both the pentamer or the nonamer in some cases (Table II). Since these motifs are not clustered or overlapping, both of the SERCA mRNA species may belong to class I mRNA rather than class II type mRNA.

Steady-state levels of mRNA depend on two independent processes: the synthesis of mRNA and the decay of mRNA. In the previous experiments, we have already shown the rates of SERCA2 mRNA transcription initiation to be the same (76). The degradation rates, in comparison, have not been studied. ***The overall hypothesis is that mRNA decay, mediated by the 3'-UTR, is the key step in controlling the level of SERCA2 expression. The differential SERCA2 expression is regulated in an isoform and tissue specific manner.*** Towards testing this hypothesis, the following experiments are presented in this study: 1) determination of the *in vivo* half-lives of SERCA2 mRNA in primary cultures of left ventricular myocytes (LVM) and stomach smooth muscle (SSM), 2) determination of the relative nuclear to cytoplasmic ratios of SERCA2 in LVM and SSM in order to identify nuclear or cytoplasmic decay mechanisms, 3) experiments using synthetic 3'-region RNA and native RNA to determine the roles of the 3'-UTR and protein factors in mRNA decay, 4) *in vitro* decay experiments with transcribed 3'-region fragments of SERCA2a and 2b to identify *cis*-acting elements which regulate stability, 5) mobility shift experiments with the same 3'-region fragments of SERCA2a and 2b to identify potential regions of binding for trans-acting factors, and 6) identification of a minimal binding sequence from the most unstable fragment from both 2a and 2b.

CHAPTER TWO

METHODS

2.1 Cell isolation, culture conditions and transcription inhibition

Neonatal rabbits (2 days old) were obtained from Reiman Fur Farms and anaesthetized with methoyflurane (Metofane; Jannsen Pharmaceuticals). All animal experiments were performed according to guidelines of the Canadian Council on Animal Care. Cells from left ventricular muscle (LVM) and stomach smooth muscle (SSM) were isolated by collagenase digestion as previously described (76) and briefly, below.

For LVM cell isolation, whole hearts were removed and placed in Joklik's media (S-MEM, Joklik modified; Invitrogen, Burlington, CANADA). Isolation of the left ventricle, removal of blood vessels, and mincing of the tissue was performed in the same media. LVM pieces were then incubated at 37°C and oxygenated (95 % O_2 / 5 % CO_2) in Joklik for 3 min after which the media was discarded and replaced with Joklik digestion buffer [3 mg/ml collagenase (>400 units/mg; Sigma Aldrich, Mississauga, CANADA), 1 mg/ml trypsin inhibitor (Sigma Aldrich), 1 mg/ml Bovine Serum Albumin (BSA, Sigma Aldrich), 3 mg total volume DNase I (Roche, Laval, CANADA), 0.2 mM $CaCl_2$] for 5 min. After the 5 min digestion, Joklik rinse media [1 mg/ml BSA, 0.2 mM $CaCl_2$] was introduced for 5 min, the tissue was triturated and removed. This rinse step was then repeated for an additional 5 min with fresh Joklik rinse media. The cells obtained from the digestion step were kept on ice

and pooled with those cells obtained from both of the following rinses. Single cells for plating were obtained after centrifugation at 50 g for 10 min.

For isolation of SSM cells, stomachs were removed, opened, and placed directly in Dulbecco's modified Eagles media (DMEM, Invitrogen) supplemented with 1 mg/ml BSA and 0.1 mg/ml trypsin inhibitor. After rinsing in fresh supplemented media, SSM was isolated by gently removing the mucosal layers from the stomachs. All SSM samples were pooled and minced into small pieces for digestion. SSM pieces were incubated at 31°C for 50 min in DMEM digestion media [1 mg/ml collagenase, 1 mg/ml BSA, 1 mg/ml trypsin inhibitor, 3 mg total DNase]. The media was discarded and the remaining tissue was incubated with fresh DMEM digestion media for another 50 min. Following the second digest, the media was replaced with DMEM containing 1 mg/ml BSA and 0.1 mg/ml trypsin inhibitor and incubated for 30 min. Following this rinse step, the tissue was triturated before passing through the Cellector (Mandel, Guelph, CANADA). The cells obtained from the second digestion step were kept on ice and pooled with those cells obtained from the following rinse.

LVM cells were then plated in DMEM with 20 % Fetal Bovine Serum (FBS, CanSera, Rexdale, CANADA), 50 mg/L gentamicin (Invitrogen), and 0.125 mg/L amphotericin B (Invitrogen) at a density of 1 x 10^7 cells/ 10 cm dish. After 24 hours, cells were rinsed with PBS, and either harvested by trypsinization or treated with 70 μM of the transcription inhibitor, 5,6-dichloro-1-B-D-ribofuranosylbenzimidazole (DRB, Sigma Aldrich) in fresh DMEM with 10% FBS. DRB was dissolved in dimethylsulphoxide

(DMSO, BDH Chemicals, Toronto, CANADA) at a stock concentration of 70 mM before each experiment. DRB treatment was stopped at various times by rinsing with PBS and cells were harvested by trypsinization. Transcription was inhibited in cultured SSM cells as described for the LVM cultures with the only modification being the plating of the cells at a density of 1 x 10^6 cells/ 10 cm plate for 7 days before treatment with DRB.

2.2 Isolation of Nuclear and Cytosolic Fractions

Cytoplasmic and nuclear fractions were isolated essentially by using a previously reported protocol (8). Fresh LVM or SSM tissue was dissected in sterile PBS and homogenized in ice cold buffer MA [250 mM sucrose, 10 mM Tris-HCl (pH 7.4), 10 mM $MgCl_2$, 2 mM dithiothreitol (DTT, Invitrogen), 1 mM phenylmethylsulphonyl fluoride (PMSF, Sigma Aldrich) and 10 units/ml RNAsin (Promega, Madison, USA)] using a Polytron PT20 (setting 4.5, Brinkman, Mississauga, CANADA) for 12 sec. The homogenate was centrifuged at 1,000 g for 10 min and the supernatant taken as the cytoplasmic fraction. The pellet was resuspended in Buffer MA using 6 strokes of a motorized teflon homogenizer, filtered through a nylon mesh (350 μM, Small Parts Inc, Miami, USA) and the filtrate centrifuged at 1,000 g for 10 min at 4°C. The resulting pellet was termed the nuclear fraction.

2.3 Protein Isolation and Quantification

Nuclear extracts were obtained after dissection and disruption by polytron of LVM

tissue in Lysis buffer [in mM: 10 HEPES (BioShop, Burlington, CANADA) (pH 7.6), 40 KCl, 3 $MgCl_2$] with 2 mM DTT, 0.5 mM PMSF, and 8 µg/ml each pepstatin and leupeptin (Sigma Aldrich). The non-ionic detergent, Nonidet P-40 (Sigma Aldrich), was added to a final concentration of 0.5 % and left on ice for 15 min with occasional inversion before centrifugation at 3000 g for 10 min. The crude nuclear pellet was resuspended in Wash buffer [in mM: 10 HEPES (pH 7.6), 10 KCl, 1.5 $MgCl_2$] with 1 mM DTT and 0.5 mM PMSF, before centrifugation at 3000 g for 10 min. The resulting pellet was suspended in Extraction buffer [in mM: 20 HEPES (pH 7.6), 420 NaCl, 1.5 $MgCl_2$, 0.2 EDTA, 20% glycerol] with 1 mM DTT and 0.5 mM PMSF and allowed to stir on ice for 30 min. The suspension was then centrifuged at 3000 g for 10 min and the supernatant was removed for dialysis against Dialysis buffer [in mM: 20 Hepes (pH 7.6), 100 KCl, 1.5 $MgCl_2$, 0.2 EDTA, 25% glycerol] with 1 mM DTT and 0.5 mM PMSF for 4-5 hours at 4°C. Insoluble particles were removed by centrifugation at 420,000 g for 15 min at 4°C and the soluble material was retained as the nuclear fraction.

Protein amounts were estimated from all fractions in comparison with a standard curve of BSA protein using the Bradford reagent (BioRad) and reading absorbance at a wavelength of 595 nm. Protein extracts were then aliquotted and stored at -80°C until use.

2.4 RNA isolation and Quantification

Unless otherwise noted, total RNA was isolated from all samples using Trizol reagent (Invitrogen) according to the manufacturer's instructions and the RNA concentration was

estimated routinely as the absorbance at 260 nm (A_{260}) using a Beckman DU640 spectrophotometer. At A_{260}, an absorbance reading of 1 corresponds to approximately 40 µg/ml (103).

For harvested LVM or SSM cells, the cell pellets were resuspended directly in Trizol (Invitrogen) for isolation of total RNA. Since the amount of RNA available from cultured cells was small and tRNA was included as a carrier, the total cellular RNA in this instance was determined by dot blot analysis using an 18S ribosomal RNA probe as described previously (76). Briefly, total RNA was estimated by dot blot analysis after prehybridization at 45°C for 1 hour with a biotinylated anti-sense probe corresponding to the rabbit 18S ribosomal RNA sequence (5'-CGT CTT CGA ACC TCC GAC TT-3') in Hybridization Buffer [0.25 M Na_2PO_4, pH 7.2, 7 % Sodium dodecyl sulfate (SDS, BioShop) (w/v) and 1 mM EDTA]. Membranes were hybridized overnight in the same buffer with 1 nM probe and washed at room temperature for 5 min in 2X SSC [20X SSC contains in M: 3 NaCl, 0.3 Na citrate (pH 7)], followed by a wash at 37°C for 30 min in 0.5X SSC + 0.1% SDS, and another wash at room temperature for 5 min in 2X SSC. The biotin probe was then detected using the Southern Light detection system (Tropix).

To isolate RNA from the nuclear and cytosolic fractions, Trizol was added to the final nuclear resuspension at a ratio of 2:1 and to the cytoplasmic supernatant at a ratio of 3:1. RNA was suspended in formamide for use. Total RNA concentration for these samples was estimated as A_{260} using solutions containing equivalent formamide as blanks and 18S rRNA was quantified by dot blot using the method described above. Poly A^+ RNA was similarly

estimated by dot blot analysis using a biotinylated oligo-dT_{20} probe (76). The conditions for poly A^+ RNA estimation were: prehybridization at 35°C for 30 min followed by hybridization for 1 h with 1 nM probe in Hybridization buffer. Blots were washed at room temperature for 20 min at room temperature in 2X SSC before detection with the Southern Light detection kit.

A standard curve consisting of known amounts of total RNA was spotted on the same membrane as total RNA samples to be quantified. Total RNA samples used in the standard curve were from rabbit SSM previously isolated, quantified by OD reading, and checked for purity. Similarly, a standard curve of poly A^+ RNA (Roche) dissolved to a known concentration and serially diluted, was spotted on membranes with test RNA samples. The intensity of each dot (both test and standard) was determined by image analysis using the software, MCID (Brock University, St. Catherines, CANADA). Non-linear standard curves were constructed using Fig. P. software ($y = Max/ (1 + (x/x_{50})^{-1})$ and used for interpolation of values of RNA in the samples.

2.5 Template Construction

DNA templates for all *in vitro* transcription reactions were constructed by PCR with the appropriate primers from a plasmid containing the required sequence. SP6 RNA polymerase sites were included in each template using extended primers during a second round of PCR to allow transcription of the antisense RNA (probes) or sense RNA (synthetic) by SP6 RNA polymerase. The transcribed RNA were synthesized using the SP6 MaxiScript

in vitro transcription kit (Ambion, Austin, USA). *The primers and SERCA2 locations for all fragments are given in Tables IV through VIII located at the end of the Methods section. The locations given in these tables correspond to the sequence given in Figure 2.*

For probes used in both RNase Protection Assays and Northern Blotting, antisense RNA was transcribed. The probe used to detect SERCA2 mRNA corresponded to a conserved domain and did not distinguish between SERCA2a and 2b. This probe corresponded to 3064 to 3370 bp of rabbit SERCA2 cDNA. The probe for G3PDH was designed from 241 to 389 bp of the rabbit G3PDH DNA sequence (GeneBank accession number gi/406106/gb/ L23961.1/rabgly3pho). The expected size of the protected fragment is 147 b.

For *in vitro* decay experiments and electrophoresis mobility shift assays, sense RNA was transcribed to mimic *in vivo* decay and protein binding. The 3'-end of both SERCA2a and 2b were each divided into 6 overlapping fragments for further analysis. This included 52 bases common to both isoforms (3444 to 3495), the isoform-specific sequences in the end of the coding region (3496 to 3507 in SERCA2a and 3496 to 3642 in SERCA2b), and the isoform-specific 3'-UTR. All the fragments for SERCA2a were between 100 and 250 bp in length, while those for SERCA2b are between 250 and 500 bp long. For the *in vitro* decay assays, an upstream SP6 polymerase site and a downstream 40 bp dT tail were added to each fragment in a second PCR reaction using extended primers. In the mobility shift assays, these fragments were extended only with an upstream SP6 RNA polymerase site before purification and quantification. The cap analogue and poly A^+ tail were excluded to prevent

binding of cap binding proteins (CBPs) or poly A^+ binding proteins (PABPs). All PCR products were gel purified using the Concert Gel Extraction kit (Invitrogen) or the QIAquick Gel Extraction Kit (QIAgen, Mississaga, CANADA) and quantified by electrophoresis with a DNA ladder (MBI Fermentas, Burlington, CANADA). The same region of G3PDH used for the antisense probe (241 to 389 bp) was used to synthesize sense G3PDH RNA used in the *in vitro* decay experiments.

For SERCA2 hybrid constructs, a 100 b region of SERCA2, just upstream of both 2A1 and 2B1 start sites (conserved in both isoforms) was ligated to the most unstable fragments and the most stable fragments from each isoform. In addition, a non-related control sequence was used in the construction of hybrids. This sequence was the same 147 b fragment from G3PDH previously used. First, the stability of both the 100 b SERCA RNA and the 147 b G3PDH RNA was determined in *in vitro* decay assays. To then obtain stable and unstable hybrid constructs, each of these SERCA fragments with a 40 b poly A^+ tail but without an SP6 polymerase site was amplified by PCR with the primers used previously and Vent DNA Polymerase (New England Biolabs, Mississauga, CANADA). Each product was gel purified (QIAgen) and quantified. They were each treated with Polynucleotide Kinase (New England Biolabs) to phosphorylate the 5' ends and spun through an Ultrafree DA column to remove any residual buffer. In parallel, the 100 b region of SERCA and the 147 b region of G3PDH were also amplified by PCR with Vent DNA Polymerase and extended with the appropriate primer to include the upstream SP6 polymerase site. These PCR products were also gel purified (QIAgen) and quantified.

Subsequently, each purified, phosphorylated SERCA2 fragment was ligated to the SERCA or G3PDH fragments at 16°C overnight using Fast-Link DNA ligase (EpiCentre, Madison, USA). Ligation mixtures were used in large scale PCR reactions using the SP6-SR3344 or SP6-G3P upstream primer and the sequence-specific downstream primer with the poly T extension. Although multiple bands were produced from each ligation, the correct size band was gel purified and amplified for further use. The sequence of each hybrid was then confirmed by sequencing (MOBIX, McMaster University, Hamilton).

2.6 *In vitro* transcription

As all the templates for either antisense probes or sense RNA were extended by an upstream SP6 RNA polymerase site, all transcription reactions were performed using the SP6 MaxiScript Transcription kit (Ambion) using 50 ng template per 40 μl reaction. Transcription reactions for probes and hot, sense RNA was set up according to Ambion instructions with ^{33}P-α-UTP (2500 Ci/mmol, Amersham Pharmacia, Baie d'Urfe, CANADA). Cold, sense RNA (self) used for competition in the mobility shift assays were synthesized as above using ^{3}H-CTP (20 Ci/mmol, Amersham Pharmacia). For those fragments and the hybrid constructs used in the *in vitro* decay assays, a m^{7}G(5')ppp(5')Gm cap analogue (Amersham Pharmacia) was included in the reaction and the amount of cold GTP in the reaction was reduced to 1/10.

During this process it was noticed that, for fragments 2A6 and 2B6, synthesis with a cap and poly A^{+} tail did not yield products that were visible when analysed by gel

electrophoresis. For these 2 fragments, templates without the 40 base pair dT tail were used for *in vitro* transcription with the mMessage mMachine transcription kit (Ambion) which adds a cap analogue to the 5'-end. Subsequent to the synthesis of capped ^{33}P-labelled RNA, the poly A^+ tail was added using the Poly A^+ Tailing kit (Ambion) with slight modification. While manufacturer's protocol calls for 8 U/rxn of Poly A^+ Polymerase at 37°C for 1 h to produce > 150 b tail, diluted Poly A^+ Polymerase can be used to shorten the length of the tail. Preliminary tests were performed to determine the effect of changing the temperature and time of the reaction on tail length. Subsequently, fragment 2A6 was extended with a 40-50 b poly A^+ tail by incubating the capped RNA with 8 U/rxn of Poly A^+ Polymerase at 37°C for 2 min. To obtain the same length of tail for fragment 2B6, 8 U/rxn Poly A^+ Polymerase was used at 25°C for 5 min. The tailing reaction was stopped by addition of EDTA to a final concentration of 10 mM. To remove any components in the reaction mixture that may interfere with the subsequent decay experiments, products were run through an Ultrafree-DA column (Millipore, Bedford, USA) and heated to 65°C for 5 min to inactivate any remaining Poly A^+ Polymerase enzyme.

The sizes of all the fragments synthesized by *in vitro* transcription were confirmed with an RNA marker (Novagen, Madison, USA). RNA concentrations were determined by both direct counting and trichloroacetic acid (TCA) precipitation. Briefly, each labelled RNA sample was diluted 100-fold. The radioactivity (DPM) in 100 µl was determined by direct counting in scintillation cocktail. In addition, 100 µl was placed on ice with 2 ml of 10 % TCA. After at least 10 minutes, samples were vacuum filtered through glass fibre filters, and

the tubes used for precipitation were washed 2X with 1 ml of 10 % TCA, and finally with 2-3ml of 95 % EtOH. The radioactivity (DPM) retained on the filters was also determined by counting in scintillation cocktail. The counts retained on the filter were used to determine the amount of radiolabelled NTP incorporated into the transcribed RNA. This number was then converted to moles of radiolabelled NTP based on the percentage of that base and the length of the RNA fragment. Finally, this was converted to a concentration of RNA (ng/μl).

2.7 Assays of Specific Proteins

2.7.1 Western Blotting

As controls for the purity of the cytoplasmic and nuclear cell fractions, 20 and 80 μg of each protein extract from both tissues were boiled in a reducing SDS sample buffer for 2 min and analyzed by 12% SDS/PAGE. This was followed by Western blotting with an anti-α-tubulin primary antibody (Sigma Aldrich) and an anti-mouse secondary antibody (Amersham Pharmacia). Detection was then performed using enhanced chemiluminescence (ECL) detection reagents (Amersham Pharmacia) and exposure to X-ray film.

2.7.2 Enzyme Linked Immunosorbant Assay (ELISA)

In addition, samples were used in an ELISA with an anti-histone H1 primary antibody, AE-4 (Santa Cruz Biotechnology, Santa Cruz, USA) and an anti-mouse IgG conjugated to alkaline phosphatase secondary antibody (Sigma Aldrich). Linearity of the assays was determined in initial experiments by using several concentrations of the nuclear extracts. The histone contents were then compared by using 1 and 2 μg protein for LVM and

SSM samples, respectively.

2.8 Assays of Specific RNA

2.8.1 RNase Protection Assays

RNase Protection Assays were performed using the RPAIII kit (Ambion). For each reaction, total RNA was co-precipitated with the appropriate probe and 10 μg of yeast tRNA. The precipitate was resuspended in 10 μl of Hybridization Buffer III and incubated at 42°C overnight. The RNA was then digested at 37°C for 30 min with a 1/100 dilution of RNase A/T1 mix. Samples were analysed by electrophoresis through a 6 % polyacrylamide /urea gel (Invitrogen) in 1X TBE buffer [10X TBE contains in M: 0.9 Tris, 0.9 Boric Acid, 0.02 EDTA]. Gels were dried under vacuum and exposed to a PhosphorImager (Molecular Dynamics, Amersham Pharmacia) overnight for image analysis.

Initial reactions were performed in order to determine the concentrations of samples and the amount of probe (determined as DPM) required to produce results within a linear range of intensity. Protection assay reactions required 5-6 μg of LVM or 50-60 μg of SSM total RNA and 50,000 DPM per reaction to detect SERCA2 mRNA. For G3PDH detection, protection assays were performed with 30,000 DPM G3PDH probe per reaction with either 500 ng of LVM or 1 μg of SSM total RNA. All RNase protection assays were determined to be linear over the range of RNA amounts used.

2.7.2 Northern Blotting

Northern blots were performed as previously described (76). Briefly, RNA samples

were electrophoresed through a 1% agarose/formaldehyde gel in 1X 3-[N-Morpholino] propanesulfonic acid (MOPS, Sigma Aldrich) buffer [10X MOPS contains in M: 0.2 MOPS-NaOH (pH 7), 3 Na Acetate, 0.5 EDTA]. All RNA samples (to a maximum of 5 μl) were heated in the presence of a denaturation buffer at 55°C for 15 min then quick chilled on ice before adding dye and loading directly. 18S ribosomal RNA was measured by Northern Blotting with the biotinylated 18S rRNA probe described above.

2.9 *In vitro* decay experiments

For decay of 3'-end fragments, only LVM nuclear extracts were used based on results obtained with the full-length 3'-UTR and native RNA (75). *In vitro* decay assays were conducted as described previously for the full-length 3'-UTR with slight modifications (11). For decay of 3'-end RNA fragments or SERCA2 hybrids, 5 ng of ^{33}P-labelled RNA was incubated with 25 μg of LVM nuclear protein extracts (described above) for between 0-30 min at 37°C in MOPS Reaction buffer [in mM: 10 MOPS-NaOH (pH 7.2) 200 NaCl, 2.5 Mg Acetate] containing 1 mM ATP, 0.1 mM spermine, 2 mM DTT, and 1 U/μl RNAguard (Amersham Pharmacia). Yeast tRNA (5 μg) was added as a carrier and the RNA was extracted by phenol-chloroform followed by EtOH precipitation. Precipitated samples were then analysed by denaturing urea/PAGE using the appropriate percentage of Gel Mix (Invitrogen). Gels were then dried and exposed overnight to a PhosphorImager for quantification.

Intensity of the bands was determined using the ImageQuant software. Each time

point for each RNA was repeated in duplicate on each gel and the average intensity of these two bands was calculated. Relative RNA remaining over the time course was determined by assuming the RNA intensity at time t=0 to be 100 % and expressing the intensities of each band average relative to this. Decay rates were then calculated for each experiment using the Fig. P. software and the equation for monoexponential (first order) decay kinetics (A * exp [-k * x] + R) assuming A=100 and no residual. The average rates from 3-7 experiments for each fragment were then compared using a student's t-test to determine significant ($p<0.05$) differences in decay rates. Statistical significance was also determined using oneway ANOVA analysis.

2.10 Electrophoresis Mobility Shift Assays

Electrophoresis mobility shift assays were performed as previously described with minor revisions (127). Briefly, for concentration curves, 0-25 μg protein was pre-incubated with Binding buffer [in mM: 10 HEPES (pH 7.6), 40 KCl, 3 $MgCl_2$, 2 DTT, 50% glycerol, 0.5% NP40] with 13 U total RNasin (Promega), 6.5 U total SUPERasin (Ambion), and 9 U total RNAguard (Amersham Pharmacia) on ice for 30 min. Yeast tRNA (750 ng / 20 μl reaction) was added as a competitor and the incubation was continued on ice for another 15 min. Finally, 5 ng / 20 μl reaction of hot, sense RNA was then added and incubated for an additional 15 min on ice. Samples were then mixed with glycerol loading buffer [60% glycerol, 0.1% bromophenol blue] and loaded immediately onto 4% or 6% non-denaturing acrylamide gels for electrophoresis in 0.4X TBE at 4°C. A protein size marker was run in

parallel (BenchMark Prestained Protein Ladder, Invitrogen) and approximate sizes of proteins involved in binding were determined by calculating the difference between the size of the RNA alone and the RNA+ protein extract.

2.10.1 Competitive Mobility Shift Assays

Competitive mobility shift assays were performed with each fragment that showed initial binding to at least one protein in the concentration curves. Experiments were performed as above with the competitor tRNA being replaced by various concentrations of: a) unlabelled fragments of the same RNA (cold sense RNA, b) unlabelled polycytidylic acid (poly C RNA), c) unlabelled polyuridylic acid (poly U RNA), and d) unlabelled polyadenylic acid (poly A RNA) (all from Amersham Pharmacia). Competitive shift assays were also performed with small RNA oligonucleotides (10 - 35 bases) that were synthesized by Dharmacon Research Inc. (Lafayette, USA) and deprotected according to the manufacturer's instructions and dissolved in 100 µl RNAse-free H_2O. Concentrations of the oligonucleotides were determined by A_{260} readings as described for all other RNA.

name	**TABLE IV. SERCA2a primers for large fragments 1-6**
SR2aN3444up	5'-ATT CTC ATG GAC GAG AC-3'
SR2aN3558dn	5'-TG CAC GCA ACG GAA CAC-3'
Sp6N3444up	5'-ATT TAG GTG ACA CTA TAG ATT CTC ATG GAC GAG AC-3'
polyA3558dn	5'-TTT TTT TTT TTT TTT TTT TTT TTT TTT TTT TTT TTT TTT TTT TTG CAC GCA ACG GAA CAC-3'
SR2aN3546up	5'-TCC GTT GCG TGC ATG TG-3'
SR2aN3783dn	5'-TGG CCG ACG GTA TCC A-3'
Sp6N3546up	5'-ATT TAG GTG ACA CTA TAG TCC GTT GCG TGC ATG TG-3'
polyA3783dn	5'-TTT TTT TTT TTT TTT TTT TTT TTT TTT TTT TTT TTT TTT TTT T TGG CCG ACG GTA TCC A-3'
SR2aN3701up	5'-AGC CTC TCC AGA GAA GT-3'
SR2aN3870dn	5'-AA CGC TGG CTA CTT GAG-3'
Sp6N3701up	5'-ATT TAG GTG ACA CTA TAG AGC CTC TCC AGA GAA GT-3'
polyA3870dn	5'-TTT TTT TTT TTT TTT TTT TTT TTT TTT TTT TTT TTT TTT TTT TAA CGC TGG CTA CTT GAG-3'
SR2aN3845up	5'-TGC CTT CAG CTC AAG TA-3'
SR2aN4082dn	5'-TT GCA CCA ACA TCT GTC-3'
Sp6N3845up	5'-ATT TAG GTG ACA CTA TAG TGC CTT CAG CTC AAG TA-3'
polyA4082dn	5'-TTT TTT TTT TTT TTT TTT TTT TTT TTT TTT TTT TTT TTT TTT TTT GCA CCA ACA TCT GTC-3'
SR2aN4065up	5'-AGA TGT TGG TGC AAT A-3'
SR2aN4207dn	5'-TC TGT GCG ACG CTT GGT-3'
Sp6N4065up	5'-ATT TAG GTG ACA CTA TAG AGA TGT TGG TGC AAT A-3'
polyA4207dn	5'-TTT TTT TTT TTT TTT TTT TTT TTT TTT TTT TTT TTT TTT TTT TTC TGT GCG ACG CTT GGT-3'
SR2aN4135up	5'-ACA ACG CAT GTC TGA CT-3'
SR2aN4253dn	5'-TAT TGT AGA ATA TAG ATT TAT TTA CC-3'
Sp6N4135up	5'-ATT TAG GTG ACA CTA TAG ACA ACG CAT GTC TGA CT-3'
polyA4253dn	5'-TTT TTT TTT TTT TTT TTT TTT TTT TTT TTT TTT TTT TTT TTT T TAT TGT AGA ATA TAG ATT TAT TTA CC-3'

location	name	**TABLE V. SERCA2A6 oligonucleotides**
4135	2A6-one	ACA ACG CAU GUC UGA CUG UAG ACU G
4139	2A6-two	CGC AUG UCU GAC UGU AGA CUG UAA AUA GCG
4154	2A6-three	AGA CUG UAA AUA GCG AUC GGU UUG U
4169	2A6-four	AUC GGU UUG UUU CUG UGC UGG UAC C
4179	2A6-five	UUC UGU GCU GGU ACC AAG CGU CGC ACA GAA
4194	2A6-six	AAG CGU CGC ACA GAA CUG **CAC AGA ACU**
4211	2A6-seven	**CUG CAC AGA ACU** GAU UUC AGG
4211	2A6-eight	GAU UUC AGG UAA AUA AAU CUA UAU U
4220	2A6-nine	UAA AUA AAU CUA UAU UCU ACA AUA
4199	2A6-6neg	UCG CAC AGA ACU CUG CAC AGA ACU
4230	2A6-9neg	UAU AUU CUA CAA UA
3842	2A4neg	GCA UGC CUU CAG CUC AAG UAG
4152	2A6-mini	G UAG ACU GUA

Fragments 2A6-six and 2A6-seven contain a additional linker sequence highlighted in bold. This linker was added in order to maintain the size of fragments while keeping predicted hairpin loops separated.

name	**TABLE VI. SERCA2b primers for large fragments**
3446up	5'-TCT CAT GGA CGA CGA GAC TCT CAA G-3'
3753dn	5'-ACC TCC TCA CCA GCC AGT ATG-3'
Sp63446up	5'-ATT TAG GTG ACA CTA TAGTCTCAT GGA CGA CGA GAC TCT CAA G-3'
polyA3753dn	5'- TTT TTT TTT TTT TTT TTT TTT TTT TTT TTT TTT TTT TTT T ACC TCC TCA CCA GCC AGT ATG-3'
3601up	5'-TCT ACA GCA CCG ACA CTA AC-3'
3973dn	5'-TAA TCT GCT GAC AAT GTC TGC T-3'
Sp63601up	5'-ATT TAG GTG ACA CTA TAG TCT ACA GCA CCG ACA CTA AC-3'
polyA3973dn	5'-TTT TTT TTT TTT TTT TTT TTT TTT TTT TTT TTT TTT TTT TTT TTAA TCT GCT GAC AAT GTC TGC T-3'
3729up	5'-TGA ACA TAC TGG CTG GTG AGG A-3'
4144dn	5'-GAA CAC TGA CTG AGG TAG CAG-3'
Sp63729up	5'-ATT TAG GTG ACA CTA TAG TGA ACA TAC TGG CTG GTG AGG A-3'
polyA4144dn	5'-TTT TTT TTT TTT TTT TTT TTT TTT TTT TTT TTT TTT TTT T GAA CAC TGA CTG AGG TAG CAG-3'
3939up	5'-AAC CAG TTG AGC CAG CAG AC-3'
4278dn	5'-CAC AAG GCA GAA CAG GCA TAC-3'
Sp63939up	5'-ATT TAG GTG ACA CTA TAG AAC CAG TTG AGC CAG CAG AC-3'
polyA4278dn	5'-TTT TTT TTT TTT TTT TTT TTT TTT TTT TTT TTT TTT TTT TCAC AAG GCA GAA CAG GCA TAC-3'
4109up	5'-GCA CTG AGC AGA GTC CTG CTA C-3'
4422dn	5'-GAT TGT GAA GTG CCA CTG AA-3'
Sp64109up	5'-ATT TAG GTG ACA CTA TAG GCA CTG AGC AGA GTC CTG CTA C-3'
polyA4422dn	5'-TTT TTT TTT TTT TTT TTT TTT TTT TTT TTT TTT TTT TTT T GAT TGT GAA GTG CCA CTG AA-3'
4250up	5'-GTC ACG AGG TAT GCC TGT TC-3'
bskpdn	5'-CCG CTC TAG AAC TAG TGG AT-3'
Sp64250up	5'-ATT TAG GTG ACA CTA TAG GTC ACG AGG TAT GCC TGT TC-3'
polyA2btail	5'-TTT TTT TTT TTT TTT TTT TTT TTT TTT TTT TTT TTT TTT T CCG CTC TAG AAC TAG TGG AT-3'

name	**TABLE VII. Primers for SERCA2b subfragments**
3560dn	5'- GGA GAC CCC CTC GGT GCA-3'
3546up	5'-ACC GAG GGG GTC TCC T-3'
3646dn	5'- AGT CAG GAC CAG AGC AGA-3'
Sp63546up	5'-ATT TAG GTG ACA CTA TAG ACC GAG GGG GTC TCC T-3'
3632up	5'-GCT CTG GTC CTG ACT GA-3'
3753dn	5'-ACC TCC TCA CCA GCC AGT-3'
Sp63632up	5'-ATT TAG GTG ACA CTA TAG GCT CTG GTC CTG ACT GA-3'
3545dn	5'-GCA CGC CCA CAA CGA GCA GGA-3'
3561up	5'-TGG CCG TTT GTG CTG CTC ATA G -3'
3631dn	5'-AGA TCA CTG AAG TTA GTG TCG G-3'
Sp63561up	5'-ATT TAG GTG ACA CTA TAG TGG CCG TTT GTG CTG CTC ATA G-3'
3647up	5'-GAC AGC TCC CTA AGA AGA TGT-3'
Sp63647up	5'-ATT TAG GTG ACA CTA TAG GAC AGC TCC CTA AGA AGA TGT-3'
3621up	5'-TTC AGT GAT CTG CTC TGG-3'
3681dn	5'-TGG GTT AAG TTA CAC ATC-3'
Sp63621up	5'- ATT TAG GTG ACA CTA TAG TTC AGT GAT CTG CTC TGG-3'
3596up	5'-GTG GGT CTA CAG CAC CGA-3'
Sp63596up	5'-ATT TAG GTG ACA CTA TAG GTG GGT CTA CAG CAC CGA-3'
3656dn	5'-GGA GCT GTC AGT CAG GAC-3'

location	name	**TABLE VIII. SERCA2B1 oligonucleotides**
3546	2B1-one	ACC GAG GGG GUC UCC
3632	2B1-two	GCU CUG GUC CUG ACU
3446	2B1-1	UCU CAU GGA CGA GAC UCU CAA GUU CGU GGC CCG CA
3471	2B1-2	GUG GCC CGC AAC UAC CUG GAA CCU GGU AAA GAG UG
3496	2B1-3	GUA AAG AGU GUG UGC AGC CUG CCC CCC AGU CCU GC
3521	2B1-4	CCA GUC CUG CUC GUU GUG GGC GUG CAC CGA GGG GG
3546	2B1-5	ACC GAG GGG GUC UCC UGG CCG UUU GUG CUG CUC AU
3571	2B1-6	UGC UGC UCA UAG UGC CCC UGG UGA UGU GGG UCU AC
3596	2B1-7	GUG GGU CUA CAG CAC CGA CAC UAA CUU CAG UGA UC
3621	2B1-8	UUC AGU GAU CUG CUC UGG UCC UGA CUG ACA GCU CC
3646	2B1-9	UGA CAG CUC CCU AAG AAG AUG UGU AAC UUA ACC CA
3671	2B1-10	ACU UAA CCC AUU AAU UUU UUA UUG UUU AAA GCA AG
3696	2B1-11	UUA AAG CAA GUG UCU UUC UGC UGA AUU UUC ACA UG
3721	2B1-12	UUU UCA CAU GAA CAU ACU GGC UGG UGA GGA GG U
3531	2B1-4 mini	UC GUU GUG GGC GUG C

CHAPTER THREE

RESULTS

3.1 SERCA2 half-life in cultured cells

The rate of transcription of SERCA2 is similar in LVM and SSM and yet LVM expresses SERCA2 mRNA at much higher level than SSM (76). Therefore, the working hypothesis was that differences in mRNA stability contribute to the discrepancy between the transcription levels and mRNA levels between the two tissues. The first step in proving this theory was to establish a difference between the mRNA decay rates *in vivo*. Even though LVM expresses SERCA2a and SSM expresses SERCA2b, the mRNA levels in both tissues can be monitored using a probe from the region conserved in the two splices. To this end, transcription was inhibited in primary cultures of LVM and SSM cells with 70 μM DRB and mRNA levels at 0 and 24 h after DRB addition were determined. DRB effectively inhibits transcription at 50-100 μM (110). Total RNA from LVM and SSM cells (6 and 60 μg, respectively) was used in RNase Protection Assays with the SERCA2 probe against bases 3064 to 3370. After 24 hours, SERCA2 mRNA was more stable in LVM cells than in SSM cells (Figure 7A). The stability at 0, 12, and 24 h after DRB addition was then investigated in order to estimate half-lives of SERCA2 mRNA in the two cell types (Figure 7B). SERCA2 mRNA had a significantly ($p<0.05$) longer half-life in LVM cells (27 ± 3 hours) than in SSM cells (13 ± 0.5 hours). As a control, the levels of 18S ribosomal RNA were

determined at various times after DRB addition. Using Northern Blots, the levels of 18S ribosomal RNA in LVM and SSM cells were not found to change significantly ($p>0.05$) over the time course (Figure 7C). Thus, in primary cell cultures, SERCA2 mRNA was more stable in LVM than in SSM cells.

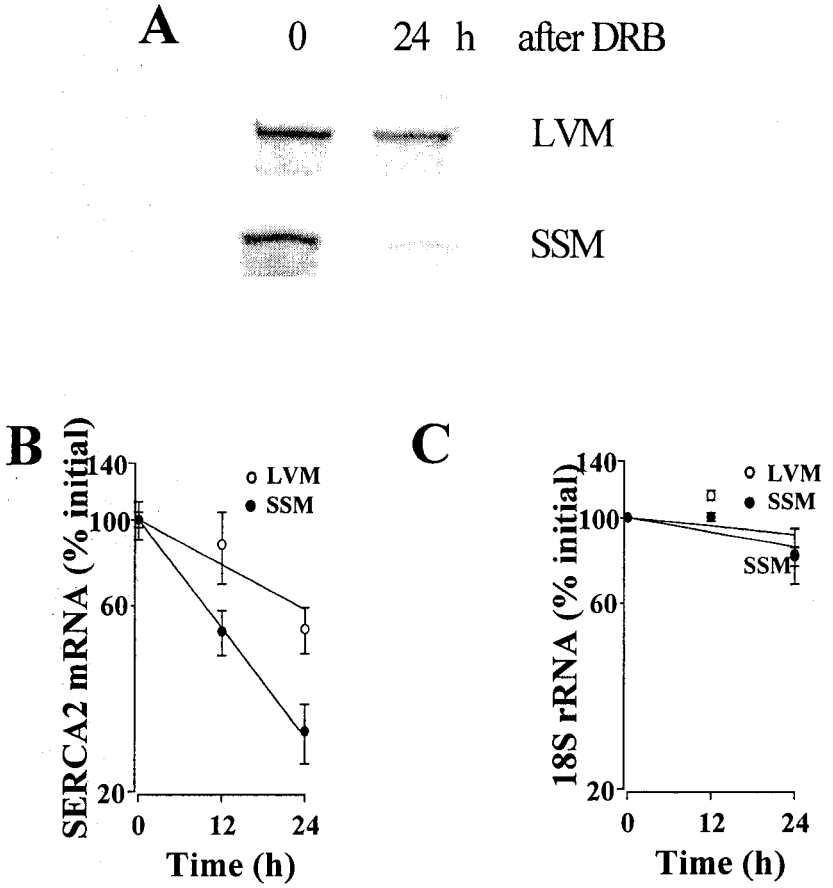

Figure 7. SERCA2 stability in cultured cells.

A. Representative RNase Protection Assay of SERCA2 RNA isolated 0 and 24 h after transcription inhibition in cardiac (LVM) and stomach smooth muscle (SSM) cells. **B. Time course of SERCA2 decay *in vivo*.** The values shown are mean ± SEM from 3-5 experiments. The half-lives of SERCA2 from LVM and SSM were estimated to be 27 ± 3 h and 13 ± 0.5 h, respectively. **C. Time course of 18S ribosomal RNA decay *in vivo*.** The abundance of 18S RNA in LVM cells at 24 h was not significantly different from 0 h or from the abundance in SSM cells at 24 h. Reprinted from (75) with permission from the American Physiological Society.

3.2 Nuclear and Cytoplasmic Abundance of SERCA2 RNA

Previous work showed SERCA2a mRNA in LVM to be 20-30X more abundant than SERCA2b mRNA in SSM (76). Based on these results, it was of interest to determine whether this difference in mRNA expression is initiated in the nucleus or in the cytoplasm. As such, the relative ratio of SERCA2 mRNA in the nucleus vs. SERCA2 mRNA in the cytoplasm was examined in both LVM and SSM.

In initial experiments, the purity of the cytoplasmic and nuclear cell fractions was analysed using appropriate markers. Nuclear and cytoplasmic abundance of total, 18S ribosomal, and poly A^+ RNA were determined. The total amount of RNA obtained per animal for LVM (411 ± 57 μg) and SSM (502 ± 51 μg) was comparable and nuclear RNA comprised approximately 10% of the total in either tissue (Figure 8A). It was expected that if the cell fractionation was done correctly, the majority of both ribosomal and poly A^+ RNA would be found in the cytoplasmic fractions. The results show that in SSM, the cytoplasmic ribosomal RNA abundance (68 ± 6 %) was significantly greater ($p<0.05$) than the nuclear ribosomal RNA abundance (37 ± 9 %). LVM showed similar differences in distribution between cytoplasm and nucleus as the SSM (Figure 8B). Similarly, both tissues showed a significantly greater ($p<0.05$) abundance of poly A^+ RNA in the cytoplasmic fraction as compared to the nuclear fraction (Figure 8C).

As additional confirmation of extract purity, the levels of histone H1 and α-tubulin were determined by ELISA and Western Blotting, respectively. Histones are found exclusively in the nucleus and, thus, served as a marker for nuclear contamination.

Conversely, α-tubulin provided a control for cytoplasmic contamination, as used in other studies (65). Figure 9A summarizes the ELISA data from 4 different protein preparations and shows the levels of nuclear histone H1 to be present in nuclear extracts of both LVM and SSM but not detectable in the cytoplasmic extracts of either tissue. Figure 9B shows the levels of α-tubulin present in cytoplasmic extracts at 20 μg and nuclear extracts at 80 μg protein. These results confirm that there was no detectable cytoplasmic contamination in the nuclear extracts and vice versa.

Figure 10A shows the levels of SERCA2 measured using RNase Protection Assays and expressed as the ratio between SERCA2 mRNA abundance and total RNA. The SERCA2 to total RNA ratio in the nuclear fraction is significantly ($p<0.05$) greater in LVM than that in the SSM. This difference in the nuclear abundance of SERCA2 between LVM and SSM was also observed when calculated as SERCA2 mRNA per ribosomal RNA or SERCA2 mRNA per poly A^+ RNA. Figure 10A also shows that the cytoplasmic abundance of SERCA2 is greater in LVM than in SSM. The abundance of SERCA2 did not differ between nuclear and cytoplasmic RNA in LVM or in SSM. As a control, the nuclear and cytoplasmic abundance of G3PDH mRNA was also determined in 3 experiments. As seen in Figure 10B, the G3PDH abundance did not differ significantly ($p>0.05$) a) between LVM and SSM, or b) between the nucleus and cytoplasm of LVM or SSM. This ensured that the nuclear regulation of SERCA2 mRNA was specific to this message and was not a global phenomenon. Thus, these experiments: (a) confirm the previous finding that SERCA2 mRNA is more abundant in LVM than in SSM, (b)

demonstrate that SERCA2 nuclear mRNA is more abundant in LVM than in SSM, indicating that the control of SERCA2 expression originates in the nucleus, and (c) shows the ratio of SERCA2 mRNA in the cytoplasm of LVM vs SSM is not significantly different from the ratio of SERCA2 mRNA in the nucleus of LVM vs SSM, indicating that the regulation of SERCA2 mRNA levels is continued in the cytoplasm.

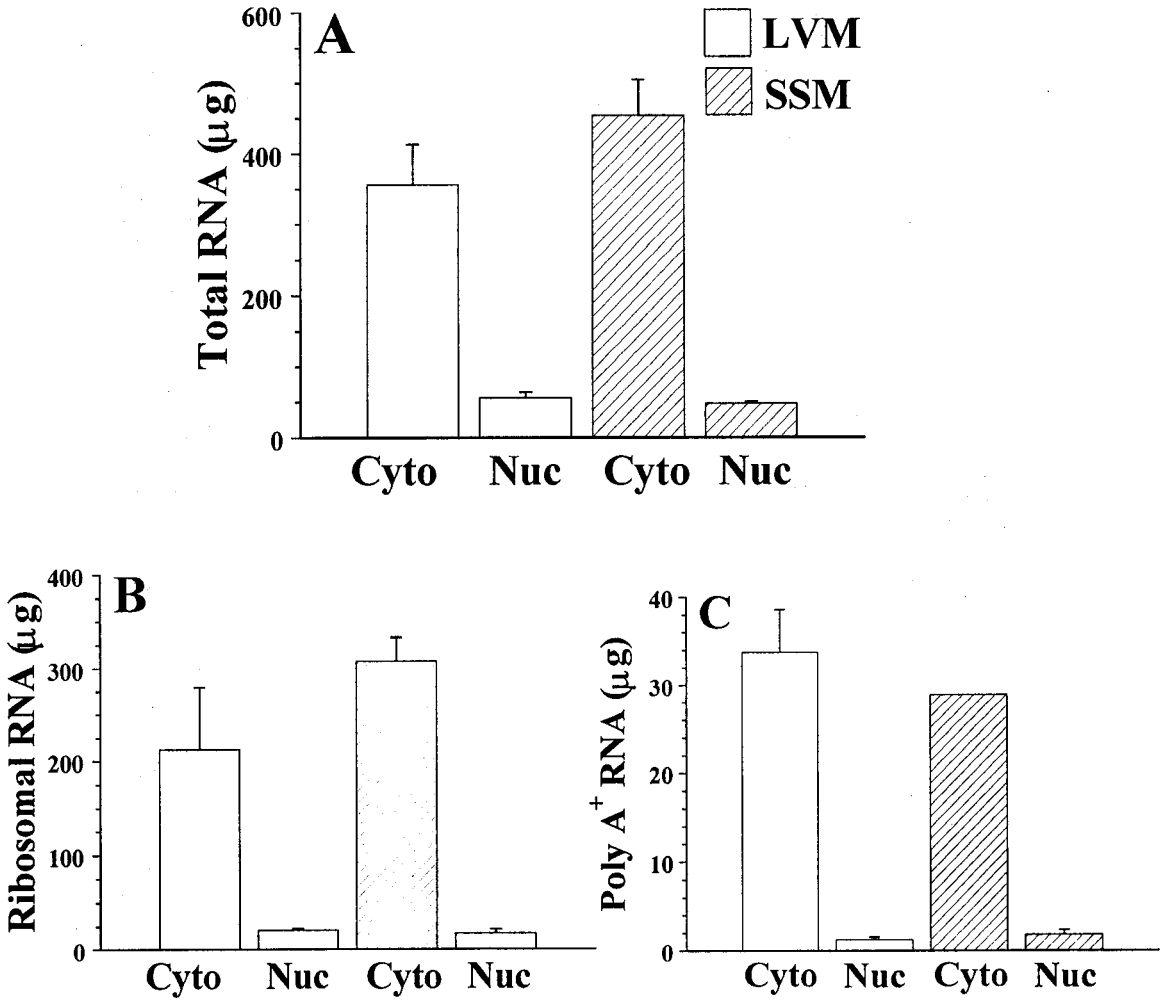

Figure 8. Characterization of cell extracts by RNA detection.

A. Total RNA. Approximately equal amounts of total RNA were recovered from both LVM and SSM, and the proportion of nuclear RNA was approximately 10 % in both. **B. 18S Ribosomal RNA. C. Poly A^+ RNA.** It was expected that a greater proportion of both ribosomal and poly A^+ RNA would be localized in the cytoplasm. This was true in both LVM and SSM. Cyto = cytoplasmic fraction, Nuc = nuclear fraction. Reprinted from (75) with permission from the American Physiological Society.

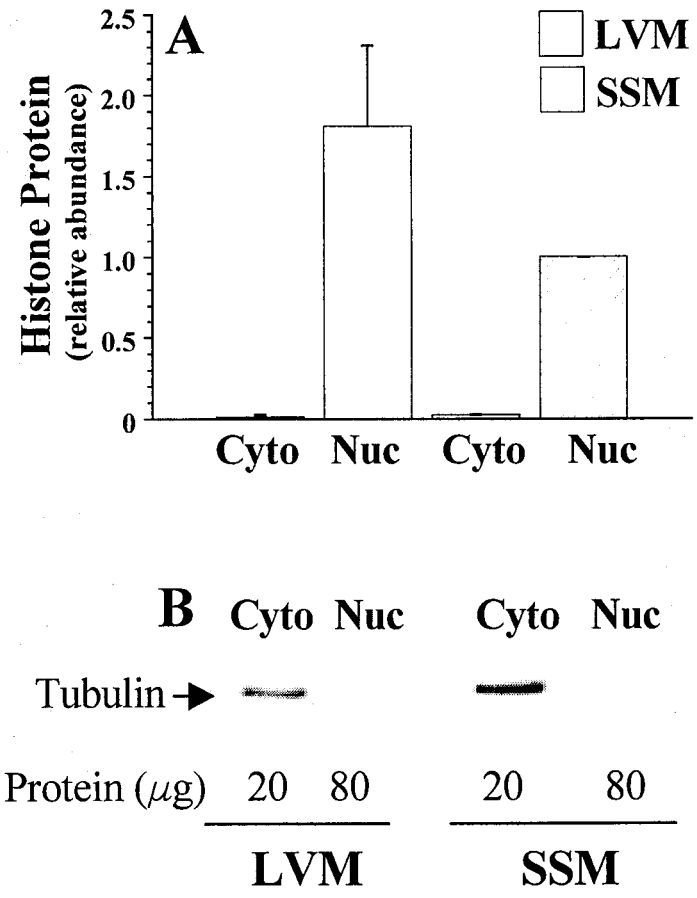

Figure 9. Characterization of cell extracts by protein detection.

A. Histone Protein. No significant amounts of the nuclear marker were detected in cytoplasmic extracts from either tissue using ELISA. **B. α-Tubulin Protein.** No significant amounts of the cytoplasmic marker were detected in nuclear extracts from either tissue, at even 4 times the amount of protein loaded in Western Blots. Cyto = cytoplasmic fraction, Nuc = nuclear fraction. Reprinted from (75) with permission from the American Physiological Society.

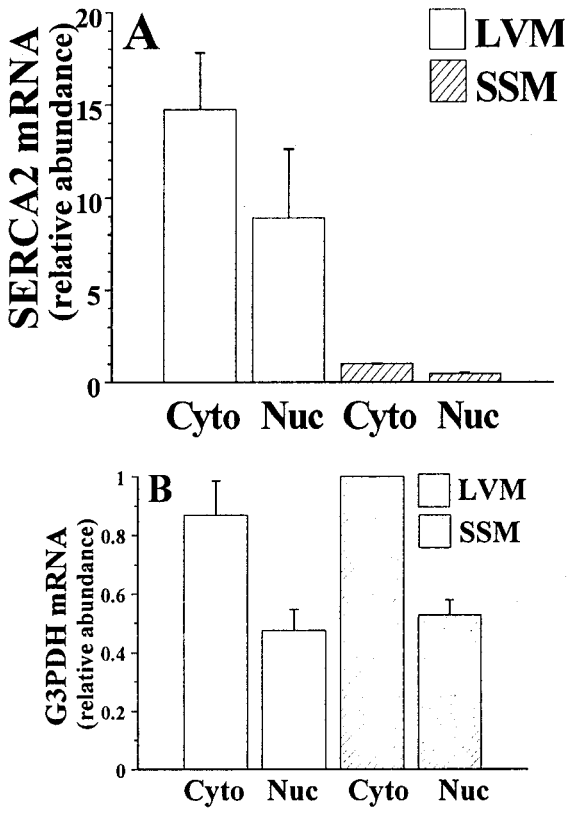

Figure 10. Relative nuclear and cytoplasmic RNA abundance.

A. Abundance of SERCA2 mRNA. The relative nuclear to cytoplasmic RNA abundance was determined by RNase Protection Assays and compared in LVM and SSM. In each experiment, the SERCA2 mRNA abundance was calculated as the amount of SERCA2 mRNA per total RNA. The abundance of the cytoplasmic SSM was taken as 1 and all the other values expressed relative to this value. The data shown are mean ± SEM of 3 preparations. **B. Abundance of G3PDH mRNA.** Computations were performed as in A. G3PDH in LVM is not significantly different from G3PDH in SSM. Cyto = cytoplasmic fraction, Nuc = nuclear fraction. Reprinted from (75) with permission from the American Physiological Society.

3.3 *In vitro* decay of synthetic 3'-region and full-length RNA

The SERCA2a and 2b transcripts are similar in their 5'-UTR and most of the coding region. The major difference in mRNA sequence of the two SERCA2 isoforms lies in the 3'-UTR due to alternative splicing. The next hypothesis was that proteins present in the two tissues and isoform-specific sequences in the 3'-region of SERCA2a and 2b may contribute to differences in the mRNA decay rates. To test this theory, the 3'-region from both transcripts was synthesized for use in *in vitro* decay experiments. Transcripts were synthesized *in vitro* including a 5' cap analogue and a 40 b poly A^+ tail to simulate protective influences found *in vivo* on full length mRNA. The 3'-end transcripts of SERCA2a and SERCA2b were incubated in: A) LVM cytoplasmic, B) LVM nuclear, C) SSM cytoplasmic, and D) SSM nuclear protein extracts for up to 60 min (Figure 11). Based on the decay rates obtained in primary cell cultures, it was expected that the 3'-region of SERCA2a would decay more slowly than that of SERCA2b. The results show that: (a) in general, the 3'-end of SERCA2a was more stable than the 3'-end of SERCA2b. One exception was noted in SSM cytoplasmic extracts, where the stabilities of SERCA2a and 2b 3'-region transcripts did not differ, (b) decay was more rapid in presence of nuclear protein extracts than with the cytoplasmic extracts, and (c) the largest difference between the stabilities of SERCA2a and SERCA2b 3'-ends was observed with LVM nuclear extracts. In similar *in vitro* decay experiments, when total RNA from LVM or SSM was incubated with the LVM nuclear protein extracts, SERCA2 mRNA from LVM decayed faster than SERCA2 mRNA from SSM. This experiment using native RNA, thus, validates the results obtained with the synthetic 3'-region RNA (Figure 11E).

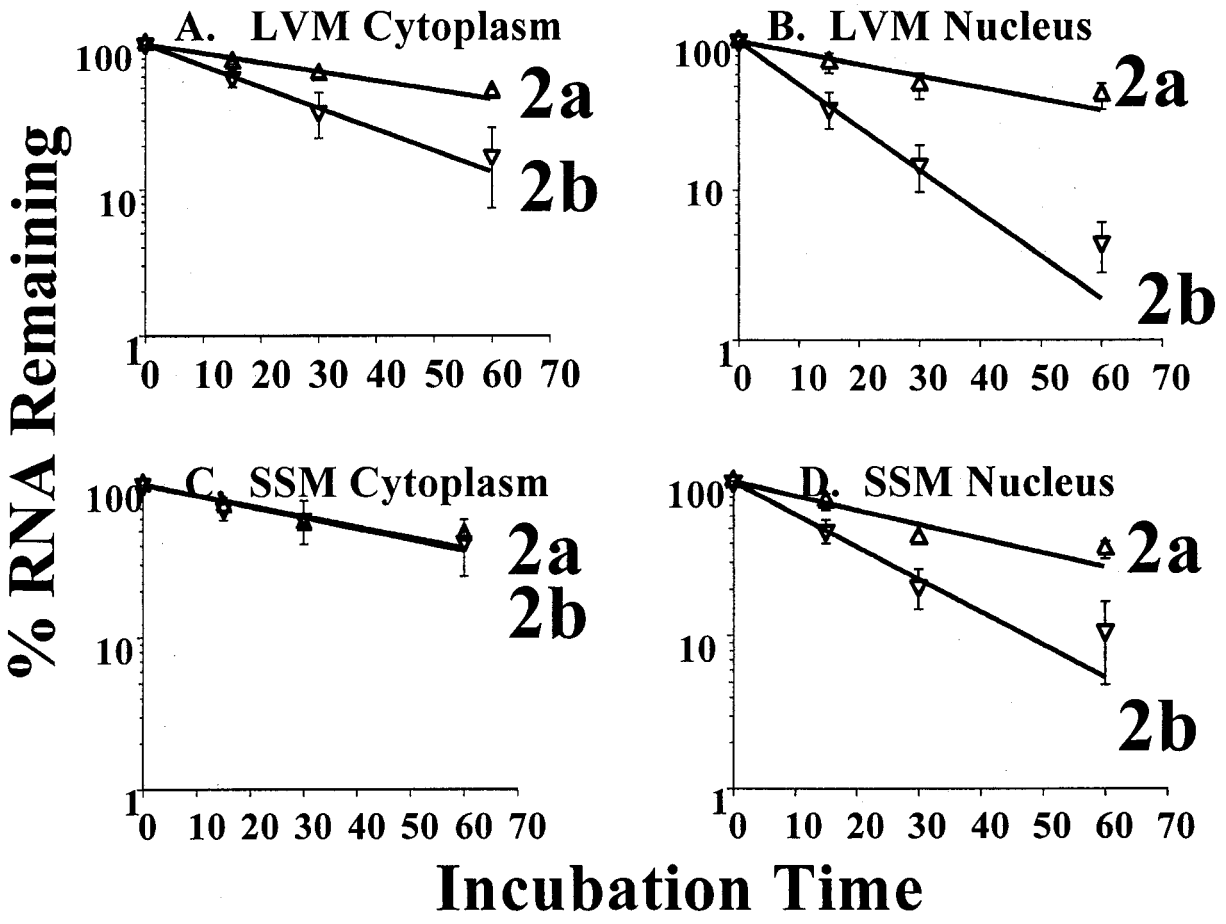
A. LVM Cytoplasm
B. LVM Nucleus
C. SSM Cytoplasm
D. SSM Nucleus
2a
2b
100
10
1
0 10 20 30 40 50 60 70
% RNA Remaining
Incubation Time

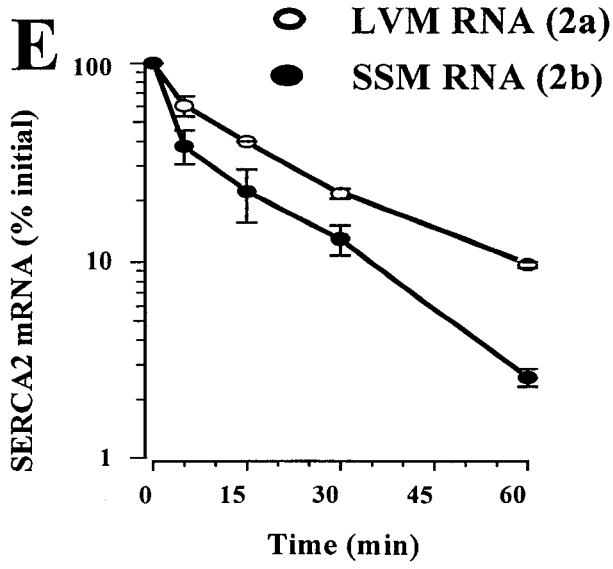
E
LVM RNA (2a)
SSM RNA (2b)
SERCA2 mRNA (% initial)
100
10
1
0 15 30 45 60
Time (min)

Figure 11. *In vitro* decay of synthetic 3'-region and full length RNA.

A. to D. *In vitro* decay of synthetic SERCA2 3'-region. For each experiment, the relative intensity at t = 0 min was taken as 100% and the mean relative intensity for other time points was calculated. Values shown are the mean ± SEM of 3-5 experiments. **E. *In vitro* decay of poly A^+ RNA from LVM and SSM.** The probe used was taken from the conserved region. For each experiment, the relative intensity at t = 0 min was taken as 100% and the mean relative intensity for other time points was calculated. Values shown are the mean ± SEM of 2 experiments. The values for 15, 30, and 60 min differed significantly ($p < 0.05$) between LVM and SSM but not the value for 5 min. Reprinted from (75) with permission from the American Physiological Society.

NOTE: these experiments were performed by Drs. James Mwanjewe and Lin Nie.

3.4 Effects of LVM Nuclear Extracts on SERCA2a stability

The above results showed that the capped, polyadenylated 3'-UTR of SERCA2a is significantly more stable than the capped, polyadenylated 3'-UTR of SERCA2b in the presence of all protein extracts except SSM cytoplasm. In the nuclear extracts from either tissue, the 3'-UTR of SERCA2a is more stable than the 3'-UTR of SERCA2b with the greatest difference being observed in LVM nuclear extracts. Hence, LVM nuclear extracts were used for further analysis of the sequences and proteins controlling SERCA2 stability.

For the following analysis of SERCA2a stability, 6 large, overlapping fragments were designed to span the full length of SERCA2a 3'-end (for schematic see Figure 12). Fragment 2A1 begins 52 bases upstream of the alternative splice site, thus, a portion of this fragment is shared with SERCA2b and bases of the coding region unique to SERCA2a are included. The exact start and end sites of each fragment, and sequence composition are given in Table IX.

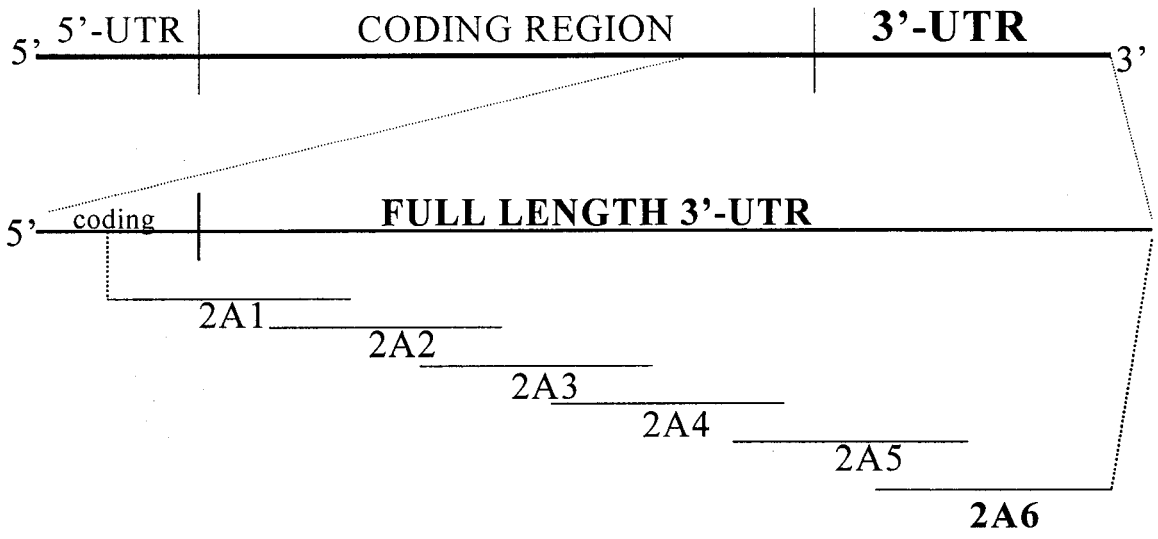

Figure 12. Schematic diagram of fragments from SERCA2a 3'-end.

The 3'-end sequence of SERCA2a was segmented into 6 overlapping fragments (2A1 to 2A6) for further analysis. These fragments were between 100 -250 bases long. For start and end sites, and sequence composition of each fragment see Table IX.

3.4.1 In vitro decay of synthetic 3'-end RNA fragments

To identify *cis*-acting elements of SERCA2a 3'-end that may influence the decay rate, the 6 large, overlapping fragments that span the unique coding region and full length of SERCA2a 3'-UTR were synthesized with a cap analogue at their 5' end and a 40 b poly A^+ tail at their 3' end for use in *in vitro* decay experiments similar to those described above. Each fragment was analysed over a 30 min time course in LVM nuclear extracts, where the largest difference between SERCA2a and 2b decay rates was noticed. In each experiment, duplicate samples of each time point were separated through denaturing polyacrylamide gels. Representative images of fragments 2A1 and 2A6 are shown in Figure 13A. The simplest assumption is that the mRNA decay depends on both protein and RNA concentrations as a first order reaction. In this case, the log RNA concentration versus time would be linear. Using this assumption, the decay rate constant for each experiment was calculated as in Figure 13B. For each of the 6 fragments, the decay rate constants from 3-5 experiments were averaged and are summarized in Figure 13C. The decay data were analysed using both a Student's t-test and ANOVA tests to determine statistical differences. The Student's t-test showed that the decay rate constants for isolated fragments from SERCA2a were similar except for 2A6 which was significantly greater (Figure 13C). Fragments 2A1-5 did not differ significantly ($p>0.05$) from each other or from G3PDH, used as a control. Thus, at least one fragment from the 3'-UTR of SERCA2a, 2A6, may have a destabilizing effect when analysed in isolation. Oneway ANOVA analysis confirmed these results.

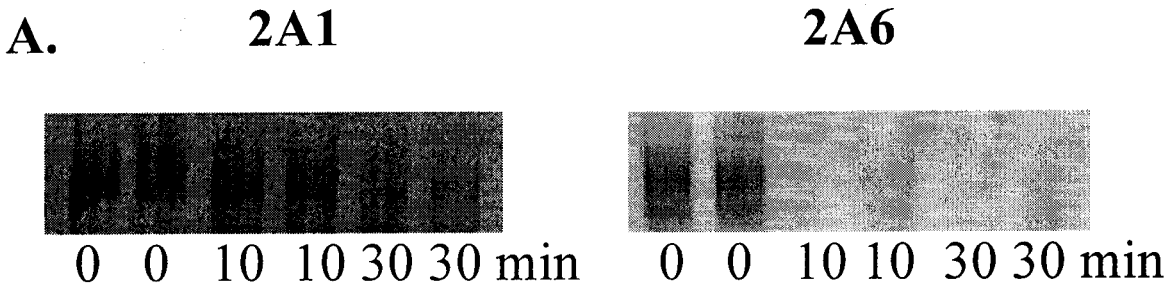
A.
2A1
2A6
0 0 10 10 30 30 min
0 0 10 10 30 30 min

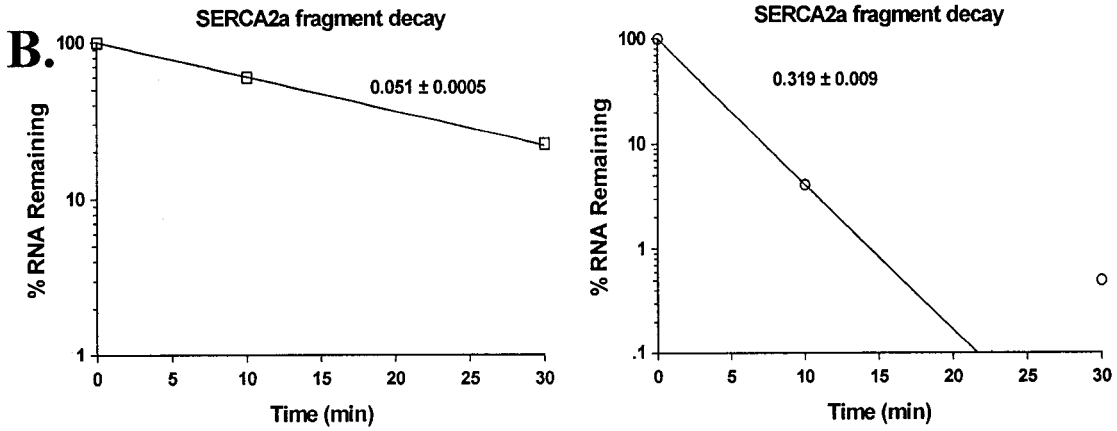
B.
SERCA2a fragment decay
0.051 ± 0.0005
% RNA Remaining
Time (min)
SERCA2a fragment decay
0.319 ± 0.009
% RNA Remaining
Time (min)

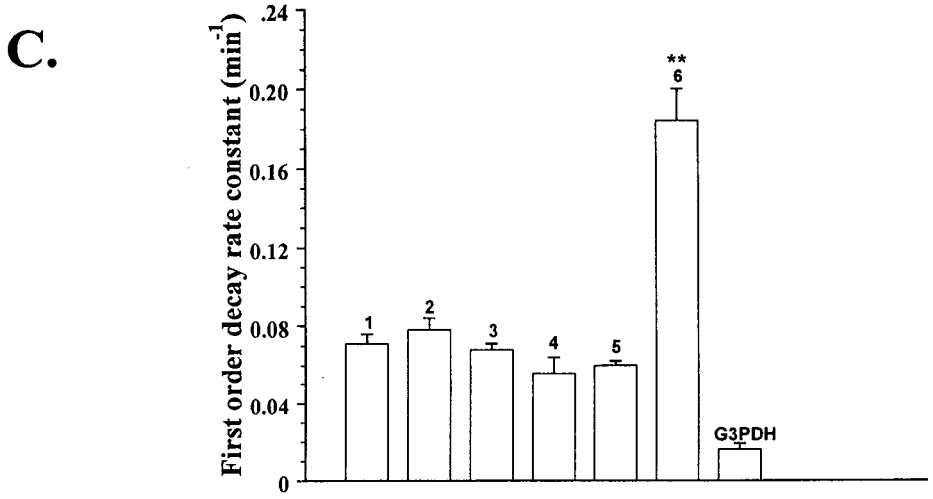
C.
First order decay rate constant (min-1)
1
2
3
4
5
**
6
G3PDH

Figure 13. *In vitro* decay of SERCA2a fragments.

A. PhosphorImages of decay experiments. Representative images for duplicate samples of 2A1 and 2A6 at t =0, 10, 30 min. **B. Calculation of decay rate constants.** Representative decay rate constants calculated for 2A1 and 2A6 (for images shown in A). **C. Decay rate constants of SERCA2a fragments**. Decay rate constants for 3-5 experiments were averaged for each fragment. The decay rate constant of fragment 2A6 was determined to be significantly different from all remaining fragments including G3PDH using both a student's t-test and a oneway ANOVA for analysis. The decay rate constants of fragments 2A1 to 2A5 did not differ significantly from each other or from the rate constant of G3PDH.

3.4.2 Context dependence of SERCA2a large fragments

As the stability of each of the fragments was examined in isolation, it was unclear what effect these fragments would have on the stability of the full length transcript as the decay rate may be context-dependent. To determine the effects of the unstable fragment, 2A6, on the stability of any mRNA transcript, hybrid fragments were constructed with the 2A6 at the 3' end. The sequence at the 5' end was a SERCA2-specific sequence (base) from the conserved region of the SERCA2 coding region or an unrelated sequence from G3PDH. In preliminary experiments, the stabilities of the isolated base transcript and of the G3PDH transcript alone were monitored in LVM nuclear extracts and both were found to be stable. As a control, similar hybrids were constructed with the stable fragment 2A1 instead of 2A6 but using the same base and G3PDH sequences. The *in vitro* decay experiments using the LVM nuclear protein extracts were repeated with the isolated fragments (2A1 and 2A6) and the appropriate hybrid fragments in parallel (base + 2A1, base + 2A6, G3PDH + 2A1, G3PDH + 2A6). Figure 14 shows the average rate constants obtained for these fragments. The rate constants for the decay of 2A1 and 2A6 alone were, 0.0767 ± 0.019 min^{-1} and 0.126 ± 0.006 min^{-1}, respectively. The addition of the stable SERCA base fragment had no significant effect on the decay rate constant of fragment 2A1 (0.0726 ± 0.004 min^{-1}) but made fragment 2A6 significantly ($p<0.05$) more stable (0.0323 ± 0.001 min^{-1}). The addition of either of these two SERCA fragments made the SERCA base significantly more unstable ($p<0.05$) relative to its decay rate constant alone (0.015 ± 0.008 min^{-1}). In comparison, addition of the stable G3PDH fragment caused fragment 2A1 to become more unstable

(0.1345 ± 0.0211 min^{-1}) and 2A6 to become more stable (0.066 ± 0.006 min^{-1}) ($p<0.05$ for both). Relative to the decay rate constant of G3PDH alone (0.024 ± 0.012 min^{-1}), the addition of either of these fragments made G3PDH significantly more unstable ($p<0.05$). Thus, the effect of adding the sequences 2A1 and 2A6 on the stability of the hybrids appeared to be context dependent.

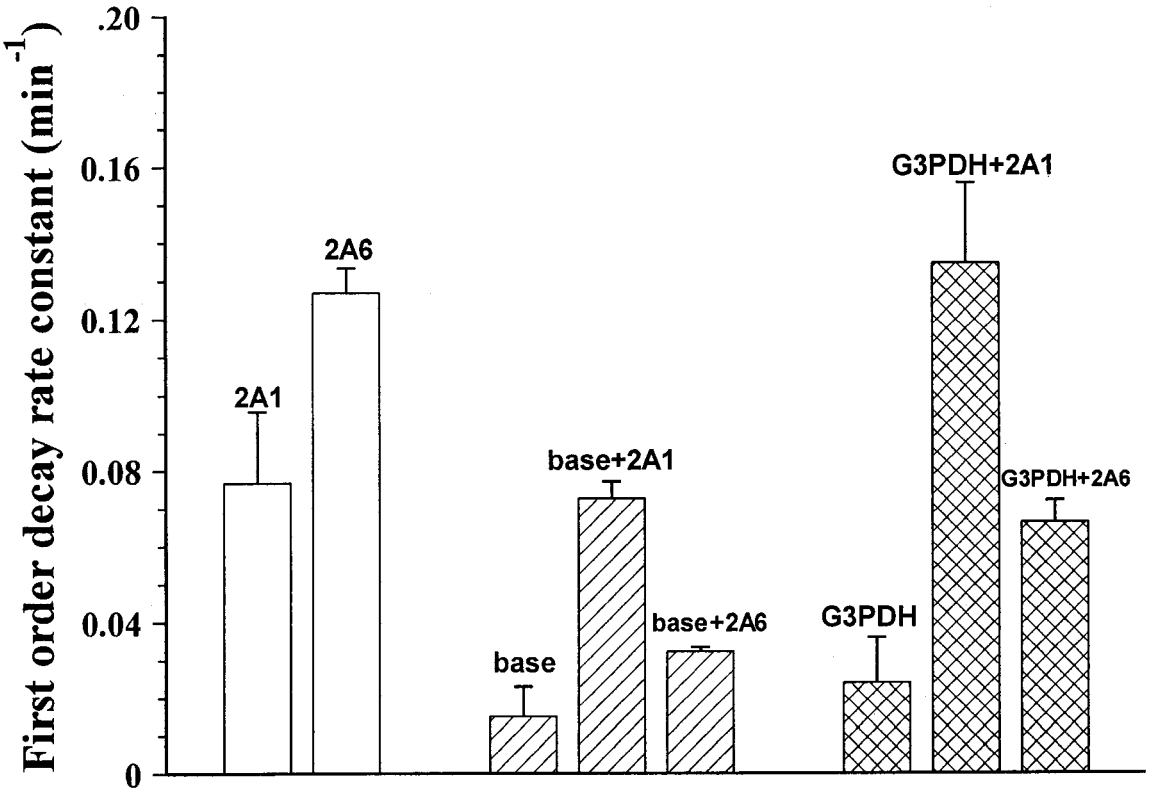

Figure 14. *In vitro* decay of SERCA2a fragments and hybrid fragments.

First order decay rate constants were calculated from 3-5 experiments for isolated fragments 2A1 and 2A6, and for the hybrid constructs. The average rate constants are shown and the relationships are described in the text. The rate constants for 2A1 and 2A6 alone were determined in parallel experiments with the hybrid constructs. The decay rate constants, shown here, do not differ significantly from the original decay rates determined for 2A1 and 2A6 as shown in Figure 13. Shown also are the decay rate constants calculated for the (SERCA) base transcript alone and the G3PDH transcript alone in LVM nuclear extracts.

3.4.3 Protein binding of SERCA2a large fragments

The *in vitro* decay experiments used protein extracts isolated from the LVM nuclei. The mRNA decay observed in these experiments would involve binding of the *cis*-acting elements within the 3'-region to specific *trans*-acting factors or proteins in the extracts. Therefore, the next issue was to determine the *cis*-acting elements that may bind to proteins in these extracts. Electrophoretic mobility shift assays were performed for all 6 fragments from SERCA2a 3'-end in LVM nuclear extracts. These fragments were identical in sequence to the fragments used in the *in vitro* decay assays except that they lacked the cap analogue or poly A^+ tail. These portions of the fragment were excluded in order to prevent binding to CBPs or to PABPs. Figure 15A shows the mobility shift assay for fragment 2A6 with increasing concentrations (0 to 25 μg) of the LVM nuclear protein extract. Increasing concentrations of the extract showed a sequential shift in the mobility of labelled 2A6 RNA with two bands of slower mobility appearing (Figure 15A). The mobility shift was further characterized in presence of excess unlabelled 2A6, poly C, poly U, and poly A RNA to determine the specificity of binding. For all competitive mobility shift assays, 2 μg protein and various amounts of each competitor RNA (ng) were used. Figure 15B shows these competitive mobility shift assays for 2A6. Excess unlabelled 2A6 RNA was able to reverse the mobility shift of labelled 2A6 while poly C RNA did not. Competitions performed with poly U RNA did not completely reverse the mobility shift of 2A6 but did show increased intensity of one of the higher bands. Interestingly, poly A RNA was also unable to completely reverse the shift but increased the intensity of the alternate slower mobility band.

Results for similar experiments with the remaining 5 fragments in SERCA2a are given in Appendix I (Figures A1 to A5). The sequence composition, decay rates, and mobility shift data for fragments 2A1 through 2A6 are summarized in Table IX, below. All large fragments from SERCA2a were found to shift in mobility with increasing amounts of protein, with the exception of fragment 2A4. In addition, some fragments may bind to more than one protein (2A3, 2A5, and 2A6) as shown by more than one band of slower mobility. The sizes of the two proteins bound by fragment 2A6 were estimated to be 90 ± 2 and 170 ± 8 kDa.

TABLE IX. SERCA2a fragments summary

Fragment	Start	End	A	U	C	G	Decay constant (min^{-1})	Proteins binding	Competition Self (IC_{50} ng/20µl)	C	U	A
2A1	3444	3558	28	30	29	27	0.071	1	25	-	-	+
2A2	3546	3783	56	73	50	58	0.078	1	50	-	-	-
2A3	3701	3870	38	51	41	39	0.068	2	40	-	-	-
2A4	3845	4082	68	79	45	45	0.055	0	n/a	n/a	n/a	n/a
2A5	4065	4207	41	43	29	29	0.06	2	50	-	-	-
2A6	4135	4243	33	33	20	22	0.184	2	10	-	p	p

The start and end site base numbers given correspond to the sequence in Figure 2. The exact base composition for each SERCA2a 3'-end fragment is summarized. Decay rates are taken from averages shown in Figure 13. Approximate binding constants were estimated from competitive mobility shift assays with self RNA. Ability of poly (N) RNA to compete for binding with labelled RNA are indicated by (-) = no competition, (+) = able to compete, (p) = partial competition, and (n/a) = not applicable.

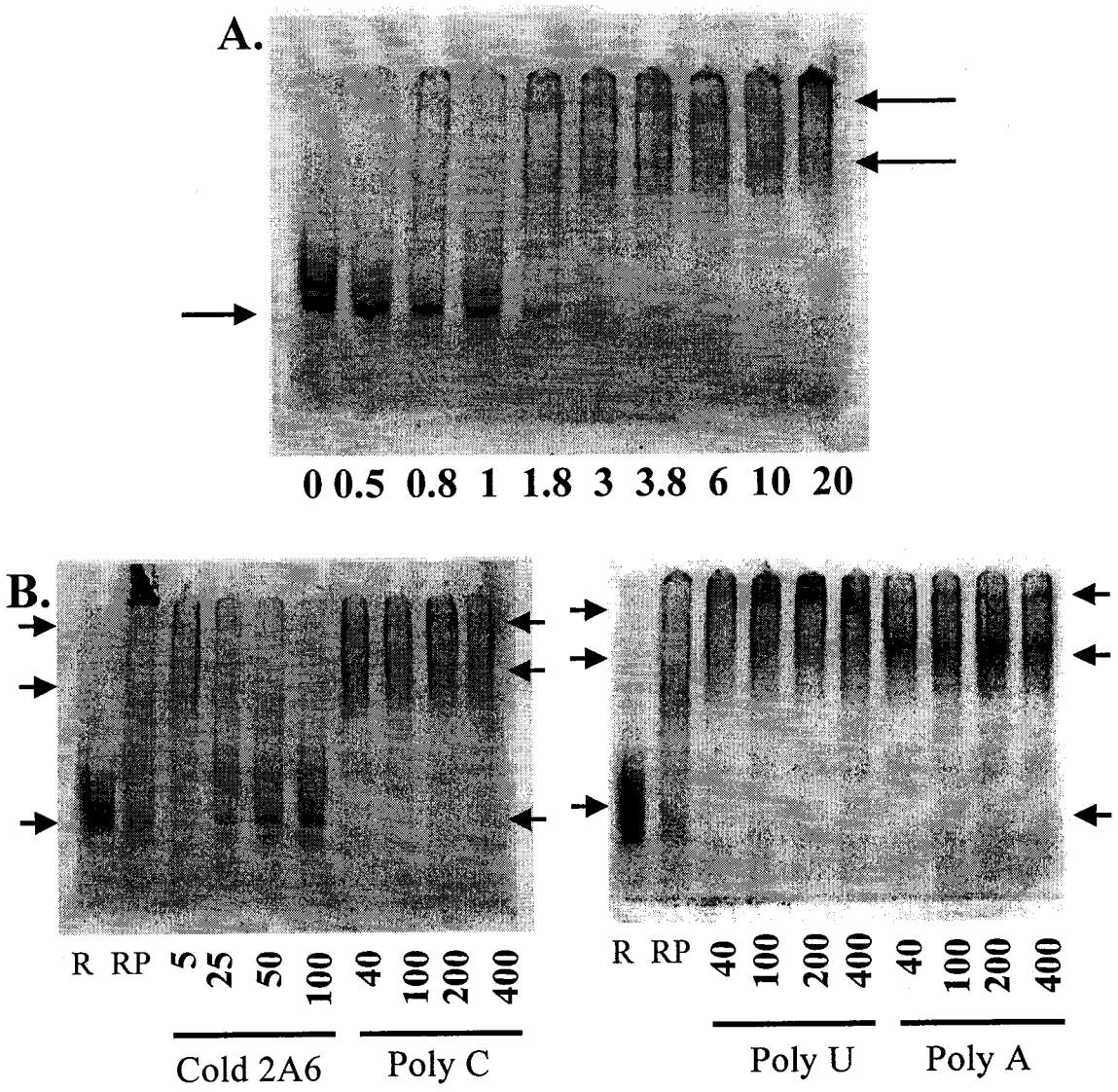

Figure 15. Mobility shift of fragment 2A6.

A. Concentration Curve. Increasing amounts of LVM nuclear protein extracts were used for incubation with 5 ng labelled 2A6 RNA / 20 µl reaction (exact amounts are given below each lane). All samples included 750 ng tRNA total as a non-specific competitor. **B. Competitions.** R= RNA alone, RP= RNA + protein. Concentrations of the competitor RNA are given below each lane.

3.4.4 Defining a minimum element in SERCA2 (fragment 2A6)

The decay pattern of fragment 2A6 in SERCA2a differed most from the others. Therefore, this domain was chosen for further analysis for minimum binding elements. Fragment 2A6 included the 118 b sequence of SERCA2a from 4135 to 4253. To define a minimum region of binding within 2A6, overlapping fragments within 2A6 were used in competitive mobility shift assays. Nine overlapping fragments, 20-30 bases in length, were designed to span the full length of fragment 2A6 (Figure 16). The criteria for the design of these fragments included length (most known minimum sequence elements are 15-25 bases long) and possible secondary structures predicted by the software, RNAdraw from http://rnadraw.base8.se/ (69). With 3 hairpin loops predicted, these loops were divided in some fragments and maintained in their entirety in others. A schematic of the 9 overlapping fragments and the negative controls used is shown in Figure 16.

Competitive mobility shift assays were performed with each of the 9 fragments against full length 2A6, however, due to their small size, these fragments were synthesized as RNA oligonucleotides rather than made through *in vitro* transcription. Figure 17 shows a competitive mobility shift assay performed with a single low and a single high concentration of each of the 9 unlabelled RNA competitors. All the fragments were able to compete for binding of labelled 2A6 with proteins from the nuclear extracts.

One plausible hypothesis, therefore, was that all 3 hairpins are involved in binding and that even partial sequences in these loops are able to bind proteins. To further evaluate this possibility, competitions were performed with different combinations of the fragments

to account for individual hairpins as well as all 3 hairpins. It was anticipated that the combination of fragments that included all 3 hairpins (fragments 2,5,8), would be able to compete for binding to a greater extent than any other combination of fragments comprising individual hairpins (fragments 1,2,3 or fragments 4,5,6 or fragments 7,8,9). The results of these combination experiments are seen in Figure 18. These experiments showed that the combination of fragments 2, 5, and 8 did compete to a greater extent than any of the individual hairpins but none of the combinations was able to completely reverse protein binding to fragment 2A6.

As the combination data still did not fully disprove or confirm the hypothesis, 3 negative control fragments were designed to test in similar competition mobility shift assays with 2A6. Two sequences within 2A6 but found outside the predicted hairpins (2A6-6 neg and 2A6-9neg, outlined by boxes in Figure 12), along with an unrelated 24 base sequence from large fragment 2A4 (2A4 neg), were used. Additionally, the 6 base "mini" overlap between small fragments 2A6-one, 2A6-two, and 2A6-three was also designed as a 10 base oligonucleotide (2A6 mini) and used in competitive assay with large fragment 2A6 to determine if this was the minimal element in this hairpin structure. None of the negative control sequences, nor the mini sequence were able to compete for 2A6 protein binding. This indicated that the binding of the 9 small oligonucleotides was, in fact, specific and that the binding region of the first three fragments is greater than 10 bases. The results of the control experiments are shown in Appendix I (Figure A6 and Figure A7) and the binding of all the 2A6 fragments are summarized in Table X.

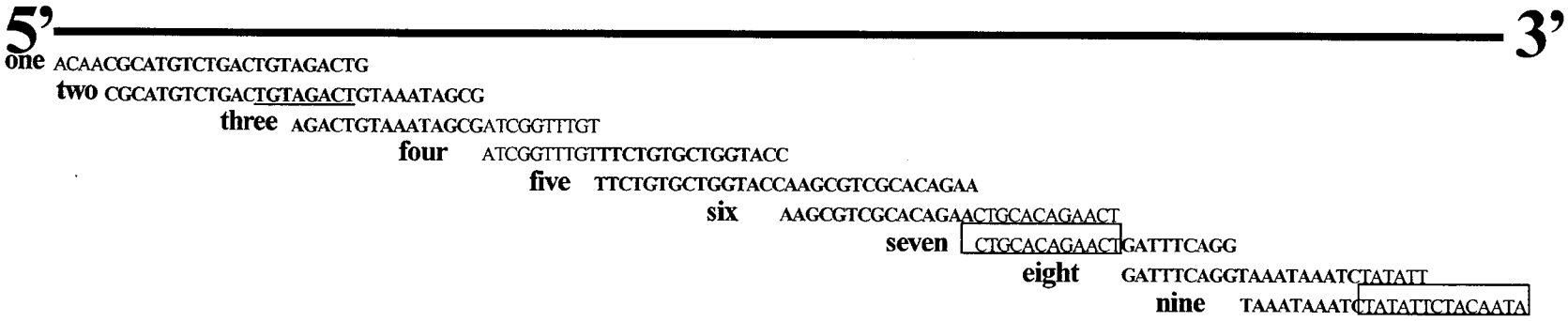

Figure 16. Schematic diagram of fragments from 2A6.

The fragment, 2A6, was segmented into 9 overlapping fragments for further analysis. These fragments were 20-30 bases long and were commercially synthesized. Bold regions indicate predicted hairpin loops, the underlined sequence indicates the "mini" overlap region, and sequences in boxes indicate regions used as negative controls.

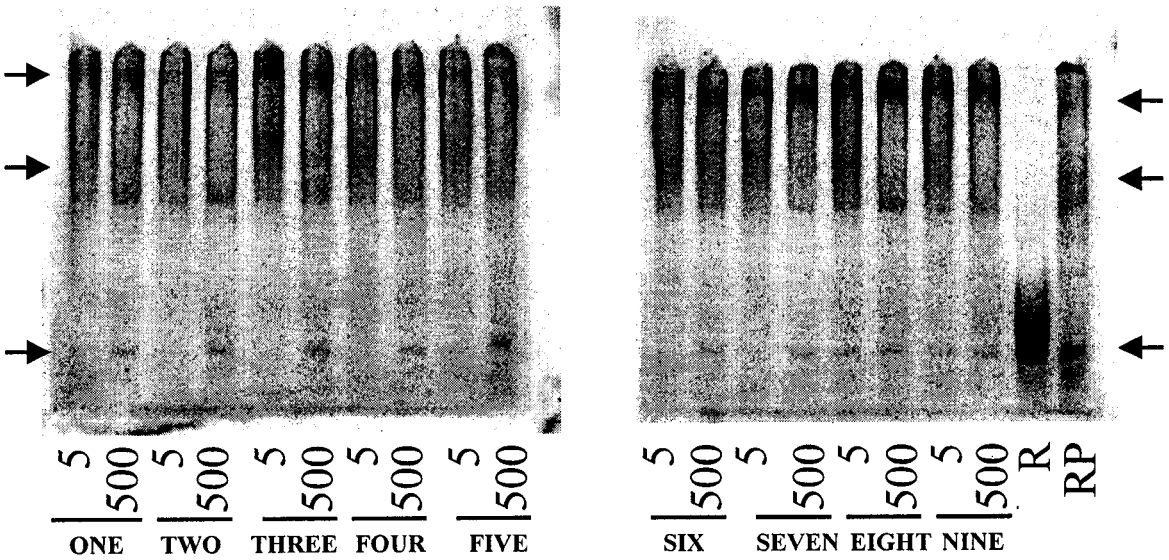

Figure 17. Competitive mobility shift of 2A6 with smaller fragments.

Competitive mobility shift assays with 2A6 against 9 overlapping fragments within this region. 5 or 500 ng of each competitor was used versus 5 ng labelled 2A6. Arrows indicate the bands of R = RNA alone and RP= RNA + protein.

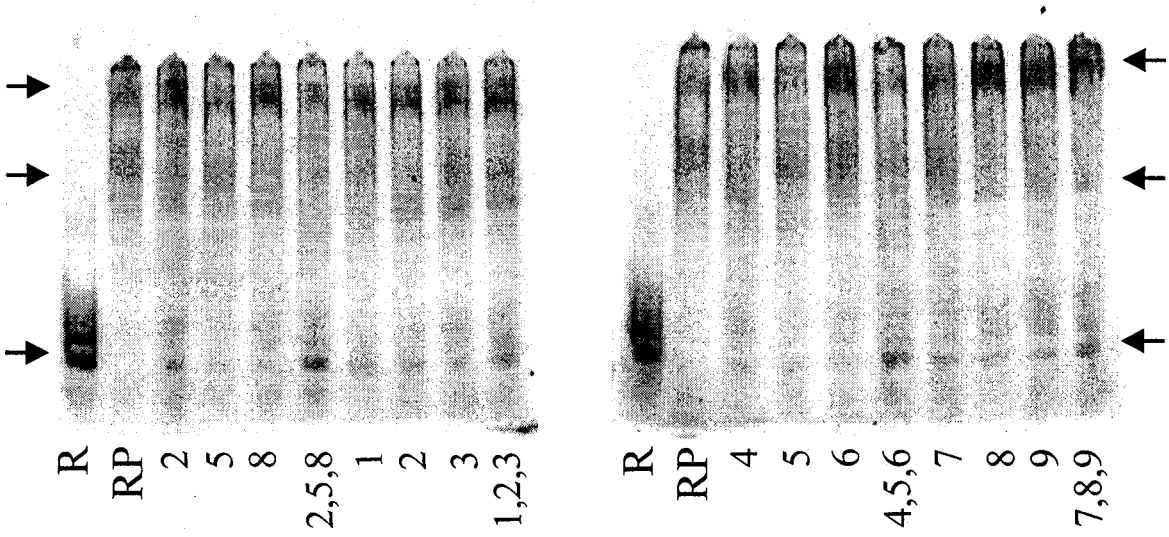

Figure 18. Competitive mobility shift of 2A6 with combinations of fragments.

Competitive mobility shift assays with 2A6 against individual fragments and combinations of fragments. Combinations of fragments were designed to simulate individual hairpins (1,2,3 or 4,5,6 or 7,8,9) or to include the loops of all three hairpins (2,5,8). Individual fragments were used at 500 ng / 20 µl reaction while 300 ng of each fragment was used in each of the combinations (to give 900 ng competitor RNA /20 µl) versus 5 ng labelled 2A6. Arrows indicate the bands of R = RNA alone and RP= RNA + protein.

TABLE X. SERCA2A6 small fragments summary

fragment	start	end	A	U	C	G	competition
2A6-one	4135	4159	7	6	6	6	+
2A6-two	4139	4168	8	8	6	8	+
2A6-three	4154	4178	7	8	3	7	+
2A6-four	4169	4193	2	10	4	7	+
2A6-five	4179	4208	7	7	8	8	+
2A6-six	4194	4211	10	3	8	6	+
2A6-seven	4211	4219	6	5	5	5	+
2A6-eight	4211	4235	10	10	2	3	+
2A6-nine	4220	4243	12	9	3	0	+
2A4-neg	3842	3862	5	5	6	5	-
2A6-6 neg	4209	4220	8	4	8	4	-
2A6-9 neg	4230	4243	6	6	2	0	-
2A6-mini	4152	4161	3	3	1	3	-

The start and end site base numbers given correspond to the sequence given in Figure 2. The exact base composition for each 2A6 fragment is given. Ability to compete with 2A6 is indicated by (-) = no competition, or (+) = ability to compete.

3.5 Effects of LVM Nuclear Extracts on SERCA2b stability

The results in section 3.3 indicated that in presence of the protein extracts from the LVM nucleus the capped, polyadenylated 3'-region of SERCA2b is significantly less stable than the capped, polyadenylated 3'-region of SERCA2a. Hence, LVM nuclear extracts were used for further analysis of the sequences and proteins controlling SERCA2b stability. To determine which domains of the SERCA3'-end contribute to its decay, the unique bases of the coding region and the full length of the SERCA2b 3'-UTR was divided into 6 large, overlapping fragments. Fragment 2B1 begins 52 bases upstream of the alternative splice site, thus, a portion of this fragment is shared with SERCA2a (for schematic see Figure 19). The exact start and end sites of each fragment, and sequence composition are given in Table XI.

3.5.1 In vitro decay of synthetic 3'-end RNA fragments

The *in vitro* decay experiments were repeated with the 6 capped and polyadenylated fragments from SERCA2b. Representative images of fragments 2B1 and 2B2 are shown in Figure 20A. The decay rate constant for each experiment was calculated as in Figure 20B. For each of the 6 fragments, the decay rate constants from 3-5 experiments were averaged and are summarized in Figure 20C. In contrast to SERCA2a, the relationship between the fragments of SERCA2b was more complex. All the fragments were more unstable than G3PDH used as control. The data was analysed using both the student's t-test and a oneway ANOVA. Using the student's t-test, fragment 2B1 was the most unstable and differed significantly ($p<0.05$) from all fragments in SERCA2B, except 2B3. However, 2B3 is not significantly different ($p>0.05$) from 2B4 and 2B5. Similarly, fragment 2B2 is most stable

and differed significantly ($p < 0.05$) from all fragments in SERCA2B, except 2B6. However, fragment 2B6 is not significantly different ($p > 0.05$) from 2B4 and 2B5. Analysis with the ANOVA showed that fragment 2B1 is significantly different from only fragment 2B2, 2B6, and G3PDH. Thus, at least one fragment from the 3'-end of SERCA2b, 2B1, may have been less stable than the others and another, 2B2, more stable than the others. The decay rate constants for 2B2 compared with that of 2A1, 2A2, 2A3, 2A4 and 2A5 (shown earlier in Figure 13C), while that of 2B1 compared with that of 2A6.

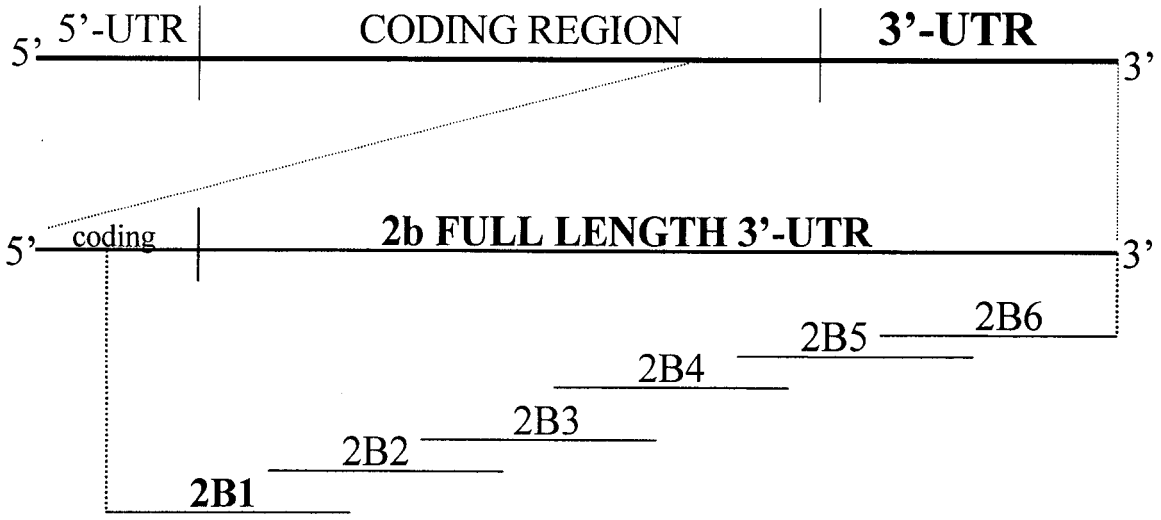

Figure 19. Schematic diagram of fragments from SERCA2b 3'-end.

The 3'-end sequence of SERCA2b was segmented into 6 overlapping fragments for further analysis. These fragments were between 300 -500 bases long.

A. 2B1 2B2

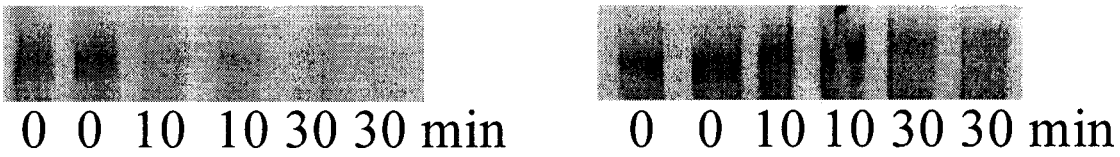
0 0 10 10 30 30 min
0 0 10 10 30 30 min

B.

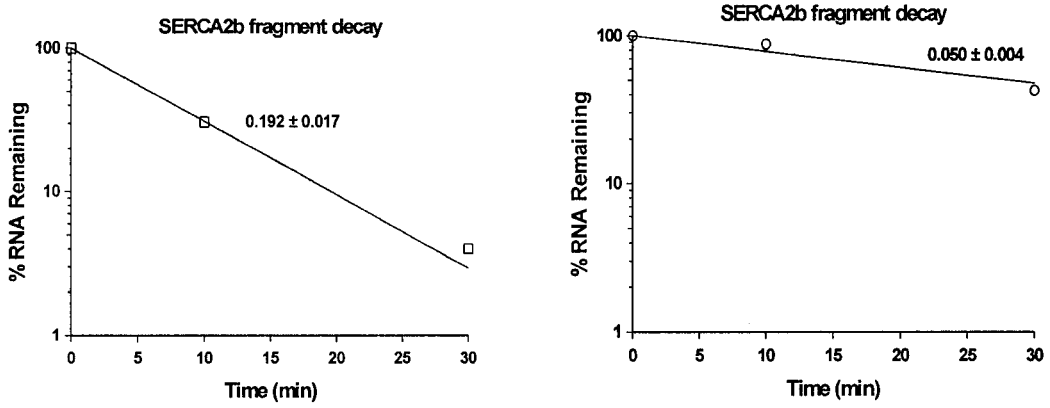
SERCA2b fragment decay
% RNA Remaining
100
10
1
0.192 ± 0.017
0 5 10 15 20 25 30
Time (min)
SERCA2b fragment decay
% RNA Remaining
100
10
1
0.050 ± 0.004
0 5 10 15 20 25 30
Time (min)

C.

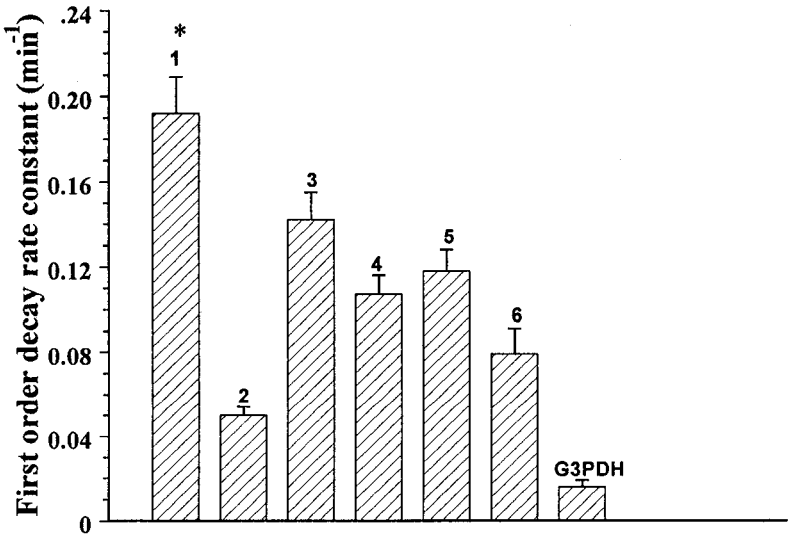
First order decay rate constant (min-1)
.24
0.20
0.16
0.12
0.08
0.04
0
*
1
2
3
4
5
6
G3PDH

Figure 20. *In vitro* decay of SERCA2b fragments.

A. PhosphorImages of decay experiments. Representative images for duplicate samples of 2B1 and 2B2 at t =0, 10, 30 min. **B. Calculation of decay rate constants.** Representative decay rate constant calculations for 2B1 and 2B2 (for images shown in A). **C. Decay rate constants of SERCA2b fragments.** Decay rates for 3-5 experiments were averaged for each fragment. Combining the analysis of both a student's t-test and a oneway ANOVA, fragment 2B1 was found to be significantly different from the stable G3PDH. The complex relationship of these fragments is given in the text.

3.5.2 Context dependence of SERCA2b large fragments

As with SERCA2a, hybrid fragments were constructed to determine the effects of SERCA2b fragments on the stability of any mRNA transcript. Both the SERCA2-specific sequence (base) and the non-specific sequence from G3PDH was placed upstream of the unstable fragment, 2B1 and the stable control fragment, 2B2. The above *in vitro* decay experiments were repeated with the isolated fragments (2B1 and 2B2) and the appropriate hybrid fragments in parallel (base + 2B1, base + 2B2, G3PDH + 2B1, G3PDH + 2B2). Figure 21 summarizes the hybrid data obtained for 2B1 and 2B2. The addition of the stable SERCA base fragment to the unstable fragment 2B1 (0.183 ± 0.004 min^{-1}) did not significantly change its stability alone (0.112 ± 0.001 min^{-1}), but made the stable fragment 2B2 (0.0717 ± 0.004 min^{-1}) significantly more unstable (0.1212 ± 0.004). The addition of either of these two fragments made the SERCA base significantly ($p<0.05$) more unstable relative to its decay rate constant alone (0.015 ± 0.008 min^{-1}). In comparison, addition of the stable G3PDH fragment also stabilized fragment 2B1 (0.0656 ± 0.010 min^{-1}) and caused fragment 2B2 to become more unstable (0.0973 ± 0.002 min^{-1}) ($p<0.05$ for both). Relative to the decay rate constant of G3PDH alone (0.024 ± 0.012 min^{-1}), the addition of either of these fragments made G3PDH significantly more unstable. Thus, the effect of adding the sequences 2B1 and 2B2 on the stability of the hybrids appeared to be context dependent.

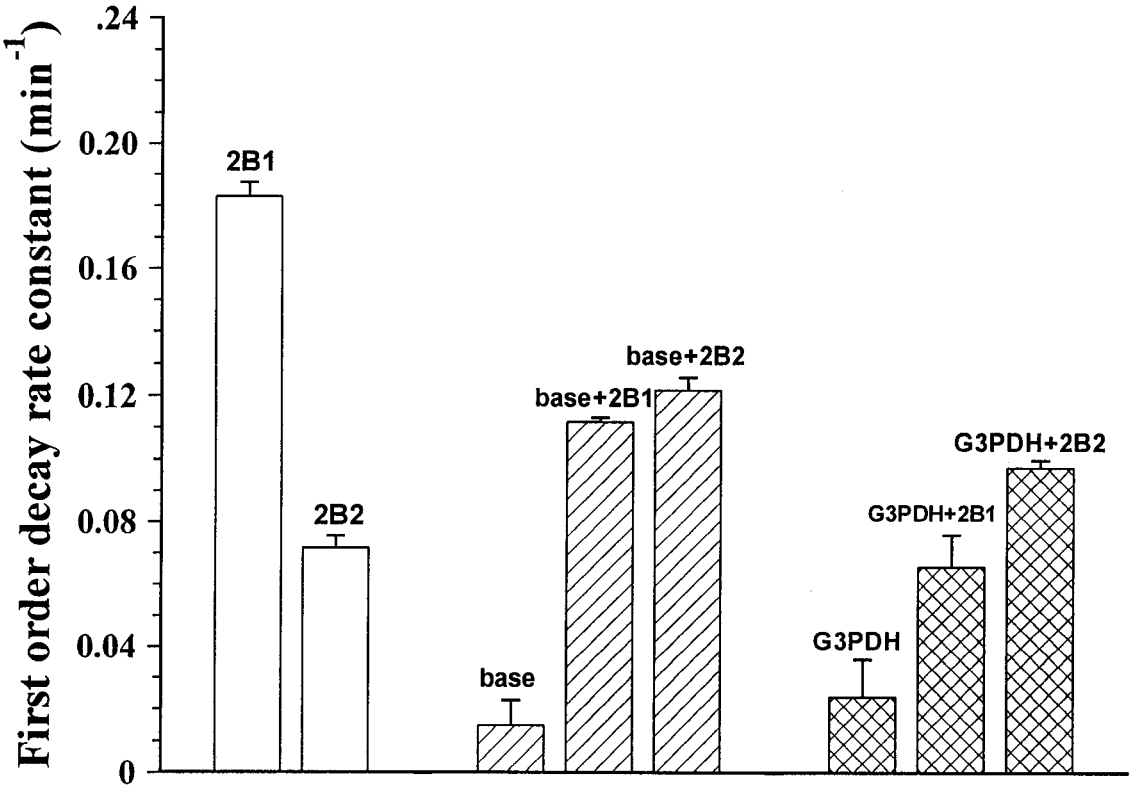

Figure 21. *In vitro* decay of SERCA2b fragments and hybrid fragments.

First order decay rate constants were calculated from 3-5 experiments for the fragments 2B1 and 2B2, and for the hybrid constructs. The average rate constants are shown and their relationships are described in the text. The rates for 2B1 and 2B2 alone were determined in parallel experiments with the hybrid constructs. These decay rate constants, shown here, did not differ significantly from the original decay rates determined for 2B1 and 2B2 as shown in Figure 21. Shown also are the decay rate constants calculated for the (SERCA) base transcript alone and the G3PDH transcript alone in LVM nuclear extracts.

3.5.2 Protein binding of SERCA2b large fragments

Mobility shift assays were performed for all 6 fragments from SERCA2b 3'-end in LVM nuclear protein extracts. These fragments were identical in sequence to the fragments used in the *in vitro* decay assays except that they lacked the cap analogue and poly A^+ tail. These portions of the fragment were excluded in order to prevent binding to CBPs or to PABPs. For each fragment, the experiments were examined at different protein concentrations. Figure 22A shows the mobility shift assay for fragment 2B1 with increasing concentrations (0 to 20 μg) of the LVM nuclear protein extract. Increasing concentrations of protein extracts showed a sequential shift in the mobility of labelled 2B1 RNA with a band of slower mobility appearing. The mobility shift was further characterized in presence of excess unlabelled 2B1, poly C, poly U, and poly A RNA to determine the specificity of binding. For all competitive mobility shift assays, 2 μg protein and various amounts of each competitor RNA (ng) were used. Figure 22B shows these competitive assays for 2B1. Excess unlabelled 2B1 RNA was able to reverse the mobility shift of labelled 2B1 while poly C RNA did not. Competitions performed with poly U and poly A RNA may have reversed the mobility shift of 2B1 at high concentrations, indicating the possibility of a slightly non-specific binding protein (Figure 22C). Similar experiments were also performed with the fragments 2B2 to 2B6. (See Appendix I, Figures A8 to A12). All large fragments from SERCA2b were found to shift in mobility with increasing amounts of protein. No fragments from SERCA2b 3'-end appeared to bind more than one protein. The sizes of the protein bound by fragment 2B1 was estimated to be 201 ± 20 kDa. The sequence composition,

decay rates, and mobility shift data for fragments 2B1 through 2B6 are summarized in Table XI.

TABLE XI. SERCA2b fragments summary

Fragment	Start	End	A	U	C	G	Decay Constant (min^{-1})	Proteins binding	Competition self (IC_{50}/20 µl)	C	U	A
2B1	3446	3753	62	88	78	80	0.192	1	50	-	+	+
2B2	3601	3973	107	129	71	65	0.05	1	25	-	-	-
2B3	3729	4144	117	154	67	77	0.142	1	60	-	-	-
2B4	3939	4278	71	115	84	69	0.107	1	50	-	-	-
2B5	4109	4422	62	107	84	59	0.118	1	10	-	-	-
2B6	4232	bskp	83	85	41	49	0.079	1	25	-	-	-

The start and end site base numbers given correspond to the sequence given in Figure 2. The exact base composition for each SERCA2b 3'-end fragment is summarized. Decay rates are those taken from Figure 20. Approximate binding constants were estimated from competitive mobility shift assays with self RNA. Bskp = BlueScript SK+ plasmid. Poly (N) RNA competitions are indicated by (-) = no competition, and (+) = ability to compete.

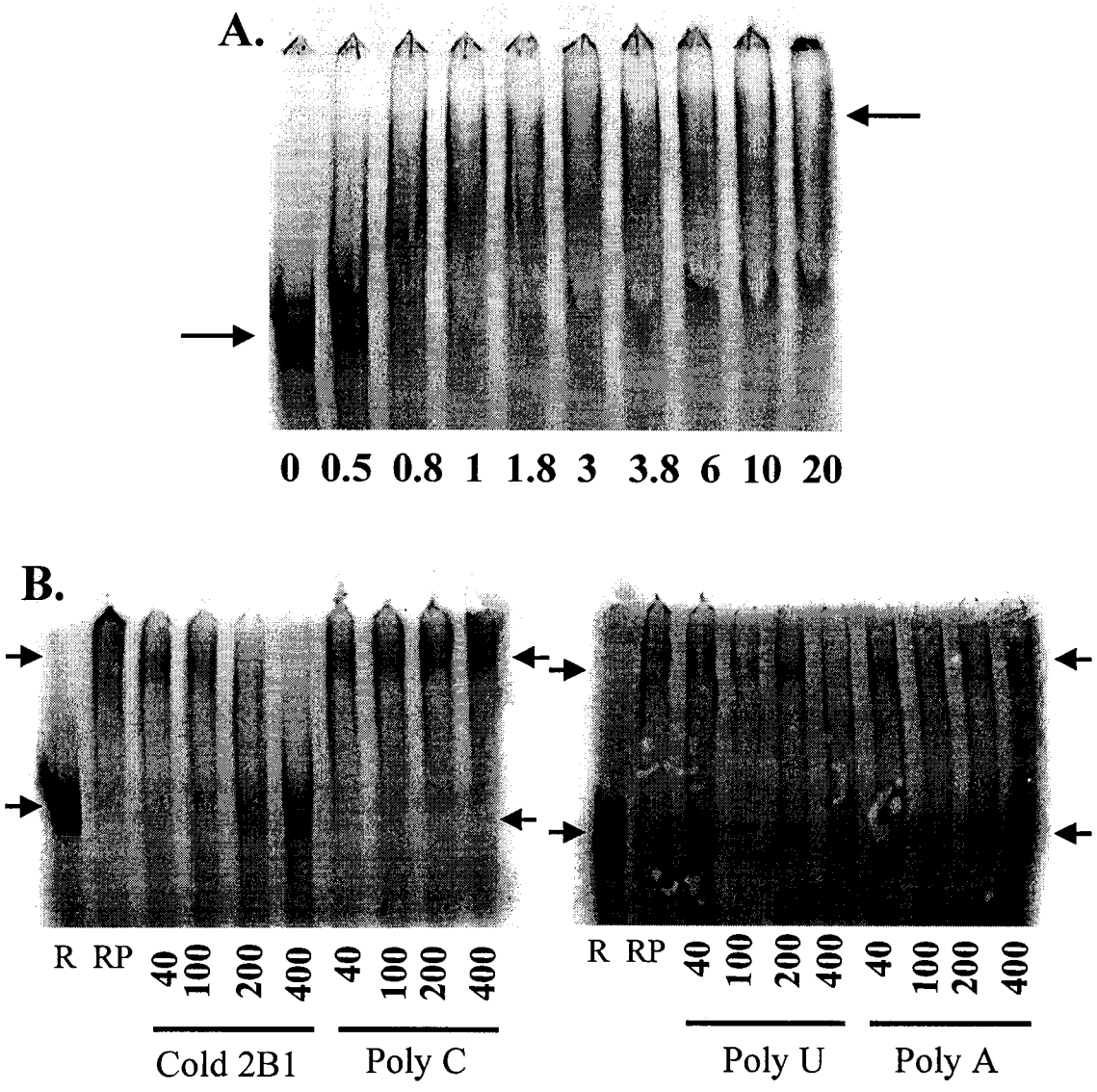

Figure 22. Mobility shift of fragment 2B1.

A. Concentration Curve. Increasing amounts of LVM nuclear protein extracts were used for incubation with 5 ng labelled 2B1 RNA / 20 µl reaction (exact amounts are given below each lane). All samples included 750 ng tRNA total as a non-specific competitor. **B. Competitions.** R= RNA alone, RP= RNA + protein. Concentrations of the competitor RNA are given below each lane.

3.5.3 Defining a minimum element in SERCA2 (fragment 2B1)

Based on the decay pattern of fragments from SERCA2b, the most unstable fragment (2B1) was chosen for further analysis. This fragment included the 307 b sequence of SERCA2b from the conserved region site 3446 to the 2b-specific site, 3753. To define a minimum region of binding within 2B1, the same approach of overlapping fragments used in competitive mobility shift assays was taken as for 2A6. Figure 23 is a schematic diagram of the overlapping fragments designed for 2B1. Initially, 3 overlapping fragments each more than 100 b long (2B1a, 2B1b, 2B1c) were synthesized by *in vitro* transcription. Initially, protein concentration dependence of LVM nuclear protein binding was determined for all three fragments. The protein concentration curve for fragment 2B1b only is shown in Figure 24A and others are presented in Appendix I (Figure A13). These experiments show that all three fragments were able to bind at least one protein present in LVM nuclear extracts, suggesting at least two sites of binding in the full length 2B1. This was unexpected, as the concentration dependence data for 2B1 did not indicate binding of more than one protein. In addition, the concentration curve of 2B1b showed one distinct band but a possible second region of protein binding (dashed arrows in Figure 24). Binding of fragment 2B1c may also have been to more than one protein but fragment 2B1a gave only one distinct band of slower mobility (Appendix I, Figure A13). Thus, in order to determine if these fragments all bound the same protein, competitive shift assays were performed using labelled 2B1b as the hot RNA and cold 2B1a, 2B1b and 2B1c as competitors. As a negative control, poly C RNA was also used as a competitor. The competition data obtained with 2B1a and 2B1c is shown in

Figure 24B and summarized in Table XII (for 2B1b self competition see Appendix I, Figure A14). The sequence composition and mobility shift data for 2B1a, 2B1b, and 2B1c are also summarized in Table XII.

These experiments suggested the binding element of 2B1 may reside in two distinct domains since 2B1b competes with both 2B1a and 2B1c. Interestingly, this also suggested that the two binding sequences lie in the overlaps between 2B1a and 2B1b, and between 2B1b and 2B1c. The two short overlapping regions (one and two) were ordered as RNA oligonucleotides for use in competitive mobility shift assays with 2B1b. These fragments, however, did not compete with 2B1b for protein binding (see Appendix I, Figure A15). Also, negative control fragments (2B1a neg, 2B1b neg, 2B1c neg) spanning the 3 regions separated by the two small oligonucleotides were designed. These were also used in competitive assays and were able to compete with 2B1b for protein binding (Appendix I, Figure A14). This confirmed that the two fragments of 15 bases are not the minimum binding elements in fragment 2B1.

In order to better define the elements of binding within 2B1, the approach using sequential overlapping fragments was taken. In this case, 12 fragments of 35 bases with 10 base overlaps were designed to span the full length of 2B1 (see Figure 23). Competitive mobility shift assays were performed against full length 2B1 with a single low and a single high concentration of each of the 12 cold RNA competitors. The results are summarized in Figure 25 and in Table XIII. The results of the competitive mobility shift confirmed a region of binding within the overlap region between fragments 2B1a and 2B1b, in small fragment

4. As this binding was not seen with the small fragment, one, it implies that the minimum sequence required for binding is between bases 3521 to 3556 but is greater than only the 15 bases between 3546 and 3560.

The competitive mobility shift data showed that small fragments 3 (3496 to 3530) and 5 (3546 to 3580) were not able to fully compete with 2B1 for protein binding but small fragment 4 (3521 to 3555) was able. As there are overlaps between these fragments in the first and last 10 bases, only 15 bases of small fragment 4 are unique. To determine whether these 15 bases (4 mini) are sufficient for protein binding, a competitive mobility shift assay against 2B1 was performed. The results are summarized in Figure 26 and in Table XIII. This experiment showed that 4 mini was unable to compete for binding. Thus, the minimal binding sequence for a protein in 2B1 is between 3521 and 3555 but is greater than the 15 bases between 3531 and 3545.

Conversely, these data did not show a second region of binding within the overlap region between fragments 2B1b and 2B1c. It was expected that either fragment 8 or 9, encompassing the overlap region, would compete for 2B1 binding. As this did not occur, one possible explanation was that the protein requires a sequence greater than 35 bases for binding. To test this theory, a fragment was synthesized to include the full length from fragments 8 and 9 (called 89). This fragment was then used as a competitor in mobility shift assays with 2B1 but also did not compete for protein binding (see Appendix I, Figure A16). As a further possible explanation, the protein may require a longer sequence or a different portion of this sequence. In order to test both these theories, two additional fragments were

transcribed. The first fragment (called 789) included the sequences from the start of fragment 7 to the end of fragment 9. The second fragment (78) included a different portion of the sequence in this region, from the beginning of fragment 7 to the end of fragment 8. These fragments were also used in competitive assays but were not able to compete with 2B1 for protein binding. Thus, while the original competitive mobility shift assays with the 3 large overlapping fragments (2B1a, 2B1b, 2B1c) would have suggested a second region of protein binding in 2B1, the remaining experiments were unable to define this region. Figure 27 shows a summary of the binding patterns of the various fragments used to define regions in 2B1. Additionally, the binding of all the small 2B1 fragments are summarized in Table XIII.

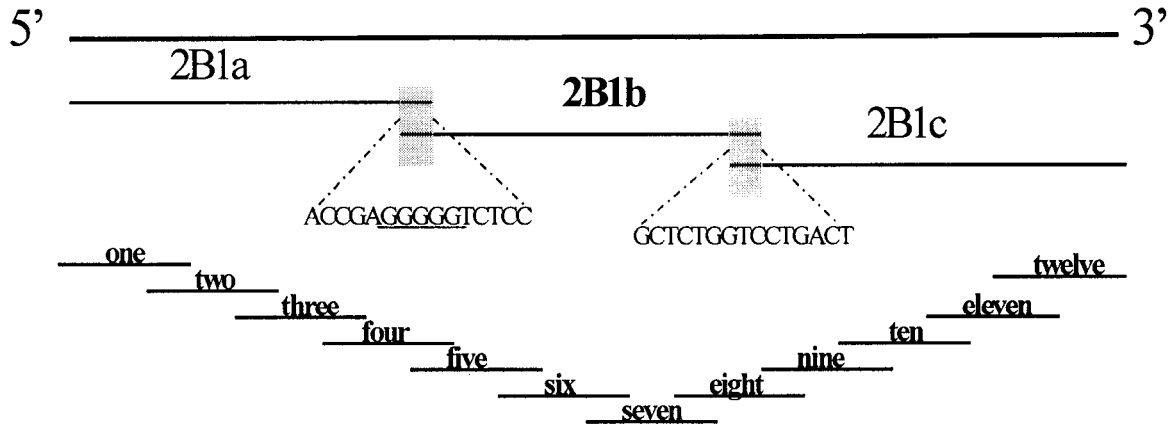

Figure 23. Schematic diagram of fragments from 2B1.

The fragment, 2B1, was segmented into 3 overlapping fragments for further analysis (2B1a, 2B1b, and 2B1c). These fragments were approximately 100 b long and were synthesized by *in vitro* transcription. The two shaded regions indicate the 15 b overlaps between these large fragments. These sequences were synthesized as oligonucleotides. An additional 12 small overlapping fragments, each approximately 35 b long, were synthesized as oligoribonucleotides to better define binding elements.

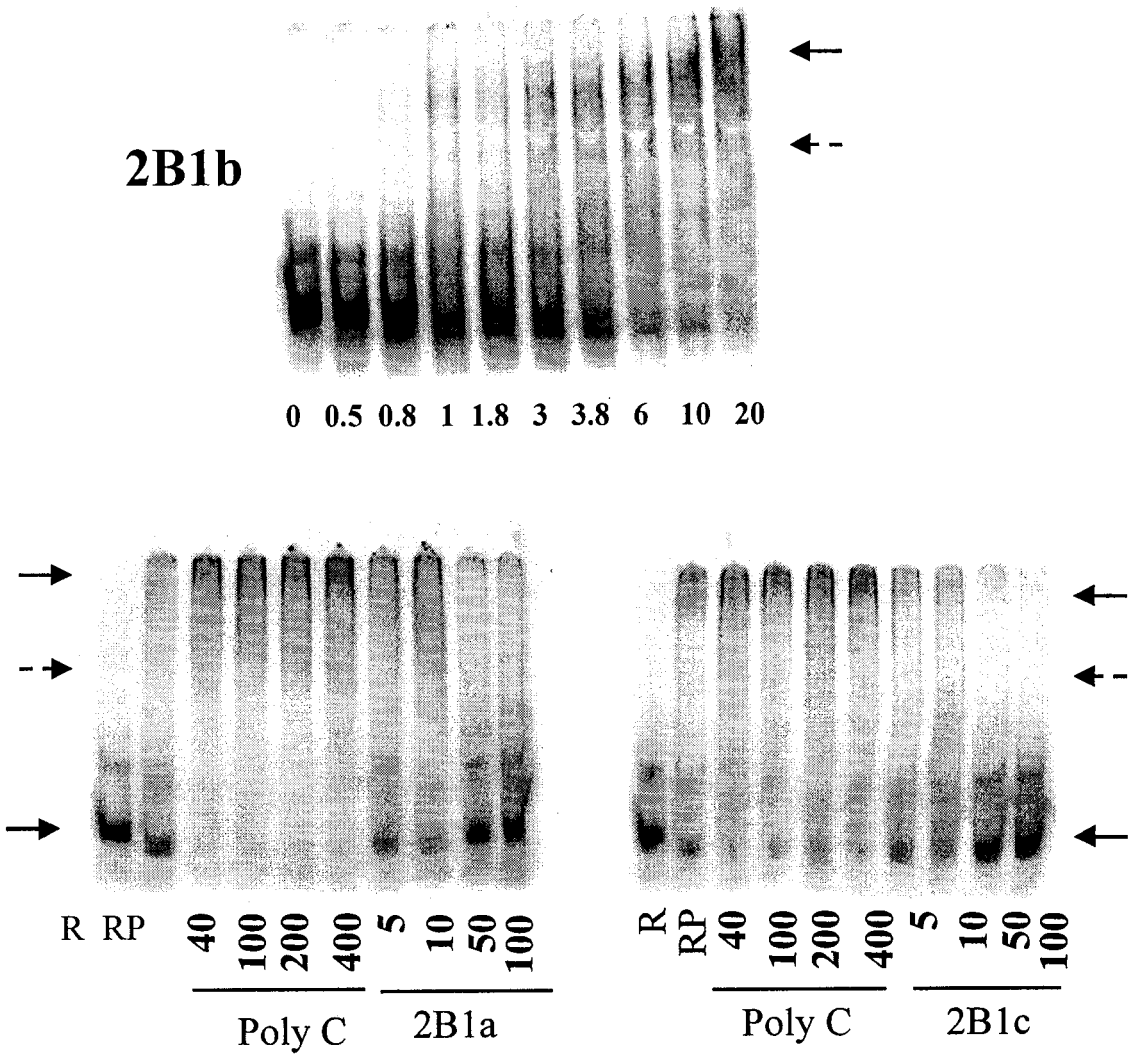

Figure 24. Protein Binding and competition of 2B1b.

A. Concentration Dependence of 2B1b protein binding. Increasing amounts of LVM nuclear protein extracts were used for incubation with 5 ng labelled 2B1b RNA (exact amounts are given below each lane). All samples included 750 ng tRNA as a non-specific competitor. A dashed arrow indicates a possible second band of slower mobility. **B. Competition of 2B1b.** R= RNA alone, RP= RNA + protein. Amounts of the competitor RNA per 20 μl are given below each lane.

Table XII. Summary of SERCA2B1 (large fragments)

fragment	start	end	A	U	C	G	protein binding
2B1-a	3446	3560	19	25	36	35	1
2B1-b	3546	3646	15	28	29	29	2
2B1-c	3632	3753	31	42	22	25	1

The start and end site numbers correspond to the SERCA2 numbering in Figure 2. The base composition is given as well as information about protein binding.

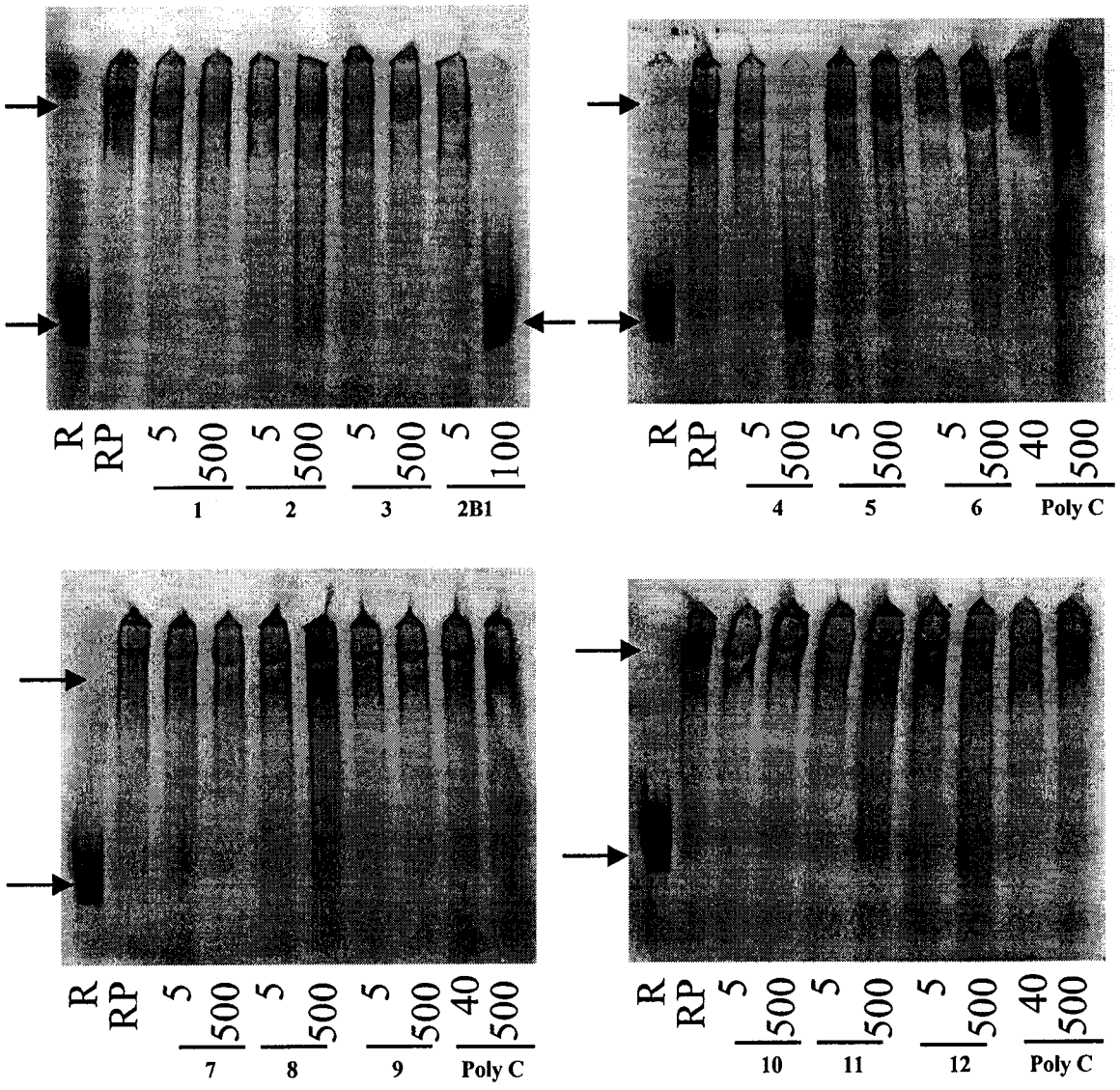

Figure 25. Competitive mobility shift of 2B1 with smaller fragments.

Competitive mobility shift assays with 2B1 against 12 overlapping fragments within this region. Only two concentrations (5 and 500 ng) of each competitor was used versus 5 ng labelled 2B1 in 20 µl. Arrows indicate the bands of R = RNA alone and RP= RNA + protein.

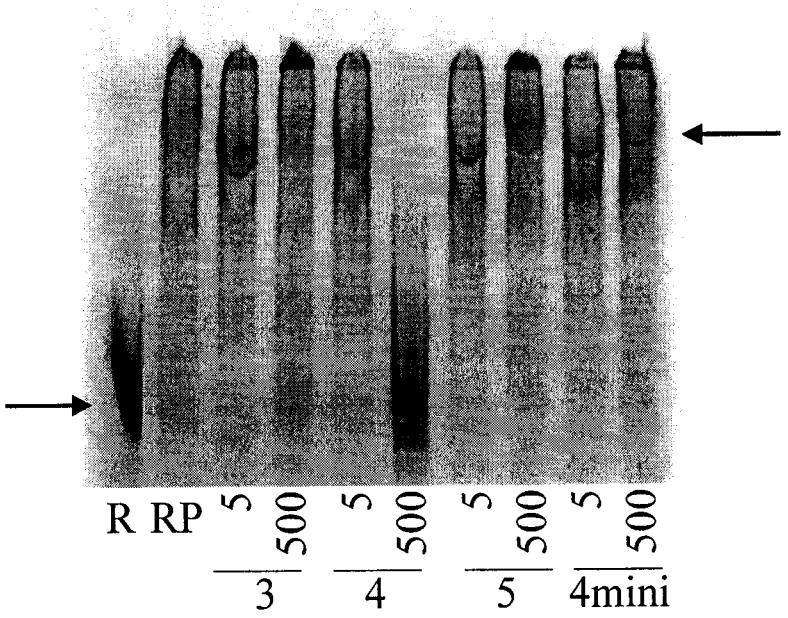

Figure 26. Competitive mobility shift of 2B1 with minimal element.

Competitive mobility shift assays with 2B1 against the unique 15 bases of small fragment 4. Small fragments 3 and 5 were used as negative controls and fragment 4 as a positive control. Only two concentrations (5 and 500 ng) of each competitor was used versus 5 ng labelled 2B1 in 20 µl. Arrows indicate the bands of R = RNA alone and RP= RNA + protein.

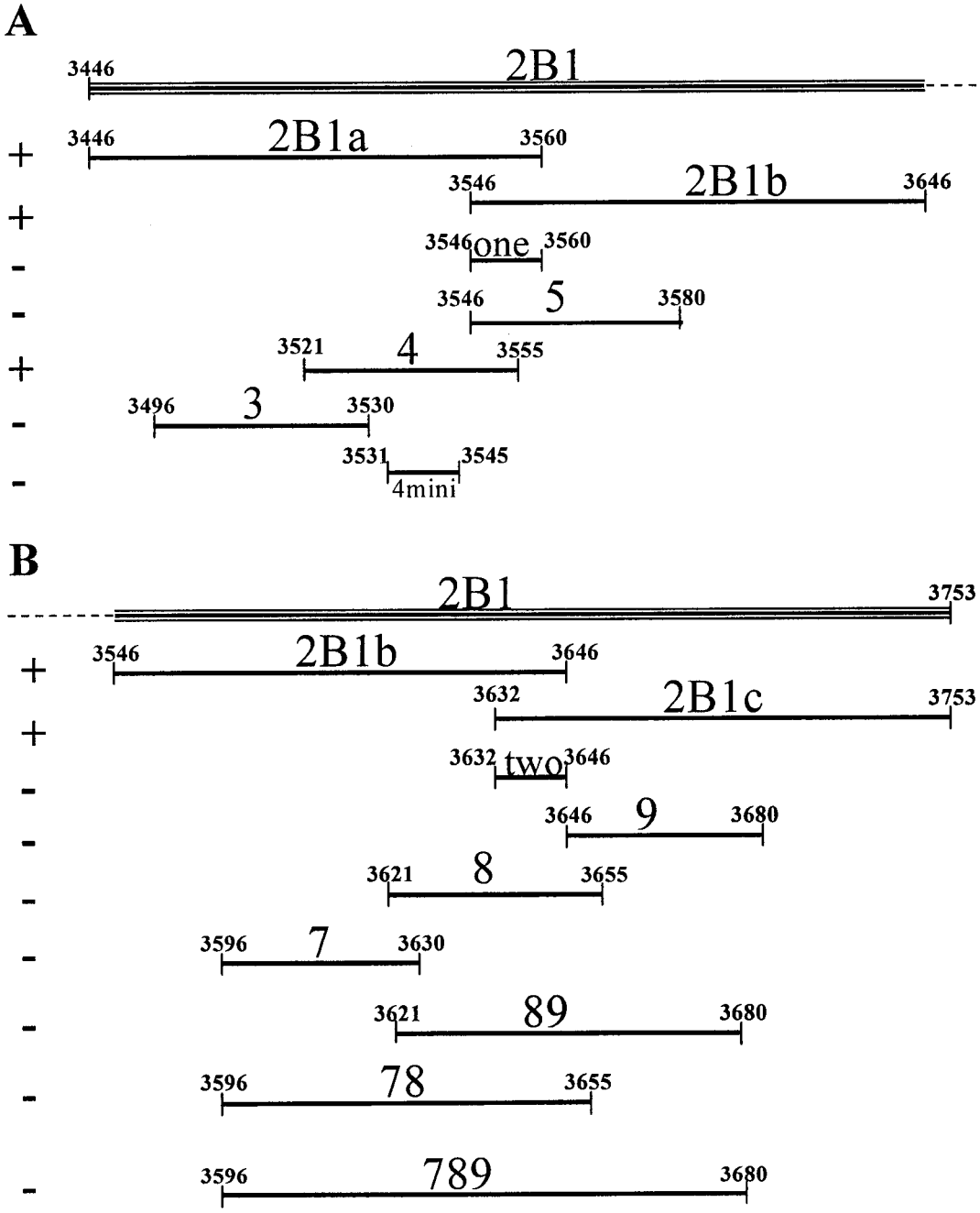

Figure 27. Competitive mobility shift of 2B1 with selected smaller fragments.

Ability and sequence location of fragments used to compete are shown for the first region (A) and second region (B) of 2B1 by (+) = able to compete and (-) = no competition.

TABLE XIII. Summary of SERCA2B1 (small fragments)

fragment	start	end	A	U	C	G	competition
2B1-one	3546	3560	2	2	5	6	-
2B1-two	3632	3646	1	5	4	4	-
2B1-1	3446	3480	7	8	11	9	-
2B1-2	3471	3505	9	6	9	11	-
2B1-3	3496	3530	6	7	12	10	-
2B1-4	3521	3555	3	7	10	15	+
2B1-5	3546	3580	3	10	10	12	-
2B1-6	3571	3605	4	11	9	11	-
2B1-7	3596	3630	9	8	10	8	-
2B1-8	3621	3655	5	11	11	8	-
2B1-9	3646	3680	12	8	9	6	-
2B1-10	3671	3705	12	15	5	3	-
2B1-11	3696	3730	9	14	6	6	-
2B1-12	3721	3753	8	10	5	10	-
89	3621	3680	17	19	20	14	-
789	3596	3680	26	27	30	22	-
78	3596	3655	21	16	19	14	-
2B1-4mini	3531	3545	0	5	3	7	-

The start and end site base numbers given correspond to the sequence given in Figure 2. The exact base composition for each 2B1 fragment is summarized. Ability to compete with 2B1 are indicated by (-) = no competition or (+) = ability to compete.

CHAPTER FOUR

DISCUSSION

SERCA2 mRNA in LVM is 20-30X more abundant than in SSM but the transcription initiation rates in the two tissues do not differ significantly (57;58;76). Thus, the key step in SERCA2 regulation is post-transcriptional. The Discussion focuses on the following key observations made in this study: a) SERCA2 mRNA decay in cultured cells is faster in SSM than in LVM, b) different rates of SERCA2 decay originate in the nucleus, c) the difference in decay rates is associated with the 3'-end of the SERCA2 mRNA molecule, which is different in SERCA2a and 2b, although there is also some tissue-dependence of the decay, (d) the decay of SERCA2a and SERCA2b is associated with different domains within the 3'-region, and (e) SERCA2a and SERCA2b subfragments bind proteins from nuclear extracts of LVM and this binding is associated with minimal elements which have not been previously identified. Validity of the methods used, comparison with the literature, implications of the findings, summary models and possible future directions are presented.

4.1 SERCA2 mRNA decay in cultured cells

Steady state levels of mRNA depend on both its synthesis and decay. The SERCA2

transcription initiation rates are known to be similar in LVM and SSM (75). Hence, we examined the mRNA decay in primary cultures of LVM and SSM treated with a transcription inhibitor. SERCA2 mRNA in LVM and SSM had half-lives of 27 ± 3 h and 13 ± 0.5 h, respectively. This difference in half-lives was specific for SERCA2 as it was not observed for the rRNA used as a control.

Obvious pitfalls in this approach are possible phenotypic changes of cells in culture and the use of transcription inhibitors to monitor the half-lives of mRNA. In initial experiments, unpublished results from this lab showed culturing the cells did not alter the SERCA mRNA abundance. Furthermore, in histochemical studies, the LVM cells retained their cardiac phenotype and the SSM cells retained their smooth muscle phenotype (75). Therefore, the possibility of phenotypic changes is not a likely explanation for the observed difference in the half-life of SERCA2 mRNA in LVM and SSM. Some controversy has arisen over the use of transcription inhibitors to monitor mRNA decay because of their possible effects on RNA-binding proteins. The argument is that shuttling proteins, such as HuR, accumulate in the cytoplasm when transcription is blocked (20-22;89). This effect, however, varies depending on the class of mRNA being monitored and also with the sequence specificity of the binding proteins in question. For example, class II mRNA are affected to a lesser extent than class I and U-rich binding proteins are among those that relocate to the nucleus (20). The observed mRNA stabilization may also depend on other conditions, including stress, used in the treatment of the cells. For example, ARE-containing mRNA show increased protein binding after serum induction, possibly due to

phosphorylation of the protein (134). In the absence of other factors, it is speculated that treatment with the transcription inhibitor, actinomycin D, reveals the normal rate of poly A^+ tail shortening and decay (111). The redistribution effect also appears to vary with the transcription inhibitor used, with DRB having less of a stabilizing effect than actinomycin D (107). DRB, used at concentrations between 50 and 100 μM, effectively inhibits transcription without a known stabilizing effect on RNA (110). Also, despite these arguments, it has not been clearly demonstrated that any other method for determining mRNA half-life gives results which are more reliable. Additionally, the half-life reported in the literature for rat heart cells is similar to that observed here for LVM (95). Similarly, the half-life of SERCA2 reported in vascular smooth muscle cells is similar to that observed in SSM (129). It is also noted the half-lives observed here are consistent with the SERCA2 mRNA being relatively stable compared to the mRNA for short-lived signal molecules, such as cytokines and early genes.

There can be many reasons for differences in SERCA2 abundance in LVM and SSM. Nuclear run-on experiments have ruled out the possibility of differences in transcription initiation rates in the two tissues, however, defects in nuclear transport may also contribute. The differences in SERCA2 mRNA stability observed in this study would also contribute to the difference in abundance between LVM and SSM.

The literature shows many factors that may influence mRNA decay. The relative stabilities of some mRNA species have been correlated with the lengths of their poly A^+ tails (83). β-globin transcripts with short poly A^+ tails are more susceptible to endonucleolytic

cuts in their 3'-UTR than those with longer tails (123). The poly A^+ tail shortening of c-*myc* mRNA precedes degradation in an *in vitro* system, and inhibiting polyadenylation (with 3'-deoxyadenosine) of newly synthesized mRNA does not prevent these unadenylated mRNAs from entering the cytoplasm but it does decrease their half-lives (63). Data obtained recently (Lin Nie, unpublished) show that the lengths of the poly A^+ tails of SERCA2a and 2b are different, with SERCA2a (42 b) being longer than 2b (21 b). The stability of dihydrofolate reductase mRNA also correlates with the polyadenylation signals used, that is a strong polyadenylation site increases the half-life of the mRNA (83;106). Since SERCA2a and 2b use different polyadenylation sites, this may affect their relative stabilities (71). In addition to effects of the poly A^+ tail, both *cis*-acting elements (RNA sequences) and *trans*-acting factors (RNA-binding proteins) may contribute to the regulation of mRNA stability. As SERCA2a and SERCA2b differ in their 3'-region and their tissue-specific expression, the contributions from elements in this region and from tissue-specific proteins factors also needs to be considered. Therefore, the mechanism and locale for the difference in SERCA2 mRNA stability between LVM and SSM are considered next.

4.2 Nuclear origin of SERCA2 mRNA decay

SERCA2 mRNA is 20-30X more abundant in LVM than in SSM (76). Even though the transcription initiation rate of SERCA2 is the same in the two tissues, one can not exclude the possibility that this difference in abundance originates in the nucleus - whether due to differences in nuclear decay or other factors. The results show that SERCA2 mRNA

abundance in LVM nuclei is already close to 20 times more abundant than in SSM nuclei. A similar ratio is maintained in the cytoplasm. *In vitro* decay experiments using the synthetic 3'-UTR of SERCA2a and 2b in nuclear and cytoplasmic protein extracts from LVM and SSM confirm that the primary difference in decay rates is initiated in the nucleus, and also show that the greatest difference is observed in nuclear extracts from LVM.

As RNA is constantly being transported from the nucleus, extraction of cytoplasmic RNA in nuclear fractions may give artificial results. Several controls for the purity of both the nuclear and cytoplasmic fractions ensured that these results were not due to cross-contamination of either the RNA or protein samples during isolation. Despite these controls one can not rule out that some of the cytoplasmic RNA may be associated with the nuclei. This argument, however is negated because, unlike the SERCA2 mRNA, the nuclear to cytoplasmic ratio of G3PDH was not different between the two tissues. An alternative approach to the study of mRNA distribution may have been *in situ* hybridization, however, this method is not as quantitative as the approach taken here. In this study, the *in vitro* decay experiments also confirm the nuclear origin of the difference in the SERCA2 abundance between the two tissues.

The Results show that the difference in SERCA2 mRNA levels between LVM and SSM originates in the nucleus. In most studies, however, mRNA decay has been shown to be cytoplasmic. The importance of nuclear decay is being recognized more recently, although the pathways identified so far are mainly for RNA processing, as is the case for degradation of introns, or for quality control, as in the case of nonsense-mediated mRNA

decay (78). HuR is present in both the nucleus and the cytoplasm but it functions primarily in the protection rather than the decay of mRNA (37). Several other RNA-binding factors have been identified in the nucleus and cytoplasm, however, their role in mRNA degradation is mainly cytoplasmic (79;124;125). In contrast, the p42 and p45 isoforms of the AUF1 protein are known to have a destabilizing function and are restricted to the nucleus through their association with a scaffolding protein (3). Exosomal decay, mediated by ten to eleven proteins, also has a nuclear-specific component (78). Thus, it is possible that the nuclear factors controlling SERCA2 decay have not been previously identified and may reveal novel information about the mechanism of specific nuclear mRNA decay proteins.

The mRNA ratios of SERCA2a and 2b were studied in their native tissue extracts while in the *in vitro* decay experiments the decay of both transcripts in the same extract was examined. Thus, the results from both experiments can be combined to determine the most probable model of SERCA2 expression. The first issue raised in the abundance experiments is that of compartment-specific versus shuttling proteins in LVM and SSM. The results of the *in vitro* decay experiments, however, show specifically that the 3'-UTR of SERCA2b is much more stable in extracts from SSM cytoplasm than it is in those from SSM nucleus, pointing to nuclear-specific decay factors and fewer of these same proteins or the existence of stabilizing proteins in the cytoplasm. Another question raised by the results of the abundance experiments is in regards to the tissue specificity of protein factors. Again, the stability of SERCA2b 3'-UTR in SSM cytoplasmic extracts and instability in LVM cytoplasmic extracts would suggest that the proteins between the two tissues are different or

that, at the least, the proteins are found at different concentrations within LVM and SSM. Based on the results showing that a 20-fold greater abundance of SERCA2 exists in the nucleus of LVM versus SSM, another possible model would have SERCA2 mRNA being exported from SSM nuclei at a faster rate than from LVM nuclei with SSM-specific cytoplasmic decay factors to maintain this ratio. The *in vitro* stability of SERCA2b 3'-UTR in SSM cytoplasmic extracts shows the second half of this theory to be invalid, thus, it is unlikely that SERCA2 expression differences result from differences in mRNA export rates. The combined data, therefore, suggest **the difference in SERCA2 mRNA abundance is regulated primarily by destabilizing factors in the nucleus of SSM**. This is surprising, as much of the literature points to co-translational decay in the cytoplasm (1;27;40;99;104). The results, however, are not exclusive of additional tissue-specific influences on decay.

4.3 Isoform-dependence versus tissue-dependence of SERCA2 mRNA decay

As mRNA decay is regulated by both *cis*-acting and *trans*-acting factors, the *in vitro* experiments comparing the decay rate of both SERCA2 3'-regions in protein extracts from both tissues allowed us to determine the influence of each of these factors. Although the 3'-end from SERCA2a was signifcantly more stable than 2b in most extracts, in extracts taken from the SSM cytoplasm the two transcripts decay at the same rate. This suggests the mRNA decay rates depend on the isoform-specific sequences in the 3'-region but also, to some extent, on tissue-specific factors in the nucleus or cytoplasm of LVM and SSM.

The results with both the 3'-regions indicate that SERCA2 mRNA decay is both

isoform-dependent and tissue-dependent. An alternative approach would have been to use transfected cells to confirm this finding *in vivo*, we were unable to do so due to difficulties in culturing LVM cells for many generations. Another alternative would have been to use an immortalized cell line that is easily transfected, such as HEK293 cells. However, this would have proceeded in only evaluating the influence of isoform-specific sequences if the decay rates differed in this cell type and would have yielded no information on the protein factors from LVM and SSM. Thus, the approach taken is more likely to reveal influences that occur *in vivo* in the tissues examined. It will be interesting to confirm these results at a later time when stable lines are available for both LVM and SSM cells.

These results propose isoform-specific control of SERCA2 stability via the 3'-region. These sequence-specific effects may have important implications during development and disease. The expression of SERCA2a in cardiac muscle is developmentally-regulated and switched from SERCA2b to SERCA2a prenatally (70). This developmentally-regulated shift in isoform expression may be accompanied or explained by a similar shift in expression of mRNA stability factors. In transgenic mice, replacing SERCA2a with SERCA2b decreases the expression to approximately 50%, with impaired relaxation in isolated cells and severe cardiac pathology produced in mice (119). The 3'-region sequences may also play a role in diseases such as congestive heart failure. Levels of the SERCA2a protein are down-regulated in this disease. Levels of β-adrenergic receptor protein and mRNA are also decreased (6;88). It is possible that sequences common to the AU-rich 3'-region of SERCA2a, the β-adrenergic receptor, and other integral cardiovascular proteins are controlled in heart failure by the up-

regulation of destabilizing mRNA binding proteins. Increased levels of AUF1 have already been found in heart failure, thus, a general mechanistic switch may control mRNA stability in this disease (88). Since the different 3'-UTR of SERCA2a and 2b arise from alternative splicing, the key to control of SERCA2 protein expression can be attributed to this process. This may introduce a novel view of the purpose of splicing: in addition to determining the type of protein (SERCA2a or SERCA2b), alternative splicing may also determine the level of protein expression via effects on mRNA stability. These experiments have not examined poly A^+ tail length, transcriptional pause due to secondary structure, or other sequence related factors that may provide additional influences on stability. Further substantiation of this model of SERCA2 regulation will come with characterization of the *trans*-acting factors in LVM and SSM, and identification of specific *cis*-acting sequences in SERCA2a and 2b.

4.4 Decay of 3'-region fragments

The 3'- terminal fragment, 2A6, in SERCA2a RNA and the proximal fragment, 2B1, in SERCA2b have the fastest *in vitro* decay rates. These fragments were able to decrease the stability of a stable SERCA or G3PDH sequence placed upstream. However, the control experiments also gave similar results and hence their role in degrading any upstream RNA was inconclusive.

Many studies have used β-globin reporter constructs to show the influence of an identified instability element (13). This approach has been used in cells in which β-globin RNA is very stable. We found β-globin to be unstable in LVM nuclear extracts (data not

shown), thus, there may be some dependence of β-globin stability on the system being used. The approach used here was similar, using the stable G3PDH sequence to test the effects of the 3'-region sequences on stability. The addition of either 2A6 or 2B1 decreased the stability of the G3PDH fragment, however, the addition of stable fragments (2A1 and 2B2) also caused decay of G3PDH. The results were similarly inconclusive using an upstream mRNA sequence from SERCA, also known to be stable in our system, thus, more consideration must be given to constructs used to study the effects of proposed *cis*-elements on decay. Since neither of these upstream sequences has been compared with β-globin in determining the role of *cis*-acting elements, one can not rule out that the upstream sequences used in this study interact with the *cis*-acting elements to give context-dependent effects. This is not without precedence as a similar context-dependent effect has been observed in other β-globin studies due to possible changes in RNA conformation (127).

4.5 Protein binding to 3'-region RNA

Fragments 2A1, 2, 3, 5 and 6 of SERCA2a and fragments 2B1-6 of SERCA2b were able to specifically bind a *trans*-acting factor in LVM nuclear extracts. The regions encompassed by fragments 2A6 and 2B1 were examined in more detail to identify minimal binding elements. Competitive mobility shift assays revealed that 3 specific elements within the 108 bases of 2A6 (30, 30 and 19 bases in length) were able to bind proteins of approximately 90 and 170 kDa. In the 327 base fragment, 2B1, a specific 35 base region was found to bind to a 201 kDa protein.

Our results confirm that several regions in the 3'-end of both SERCA2a and 2b are targets of binding proteins. However, these experiments do not rule out the existence of other unique factors contributing to the stability of SERCA2 in other extracts, nor does it mean that the sequences identified here are solely responsible for SERCA2 stability. Particularly for SERCA2b, it is likely that sequences and proteins other than those identified here play a role in its *in vivo* decay as these experiments were not performed in its native extract. The results of this study are important, nonetheless, because they highlight difference between SERCA2a and 2b when all other conditions are the same. Thus, the data here place more of an emphasis on the *cis*-acting elements than the *trans*-acting factors affecting SERCA2b stability.

Although positive and negative controls were used to ensure the specificity of binding in the mobility shift assays, these experiments do not indicate whether binding of these elements would occur in the context of the full message. The length of the full length mRNA or even the 3'-region, however, does not permit mobility shift experiments. It will, thus, be important to confirm the *in vivo* binding specificity of these elements through competitions with the full length mRNA or the full length 3'-region. Additionally, these assays do not show a functional role for these regions of binding in decay. *In vitro* decay experiments with deletion constructs are needed to confirm that the proteins bound by these elements are also involved in stability.

Of the many studies that have started to identify sequences involved in the regulation of mRNA stability, ARE have been reported in unstable mRNAs and C-rich elements have been similarly reported in stable mRNAs (1;19;20;28;46). GA-rich elements have also been

found to bind a protein that regulates developmental stability of elastin mRNA and a purine-rich sequence is necessary for c-*fos* destabilization (23;45). The 3'-UTR of SERCA2a and 2b are both AU-rich and contain some of the known consensus sequences for AUBPs, however, the presence of consensus motifs in an AU-rich region does not always guarantee an RNA-destabilizing for this element (19). At least three specific sequences have been discovered in SERCA2a: the 30 base sequence from 4139 to 4168 (CGC AUG UCU GAC UGU AGA CUG UAA AUA GCG), the 30 base sequence from 4179 to 4208 (UUC UGU GCU GGU ACC AAG CGU CGC ACA GAA), and the 19 base sequence from 4211 to 4230 (GAU UUC AGG UAA AUA AAU C). Only the 19 base sequence is significantly AU-rich and even this region does not contain any of the known consensus sequences. Similarly, one region in SERCA2b has been identified: the 35 bases from 3521 to 3555 (CCA GUC CUG CUC GUU GUG GGC GUG CAC CGA GGG GG). This element is decidedly GC-rich and also does not resemble known binding sites. Thus, the elements identified here in SERCA2a and 2b are novel. These elements and their location in the full length SERCA2 are shown in Figures 28 and 29.

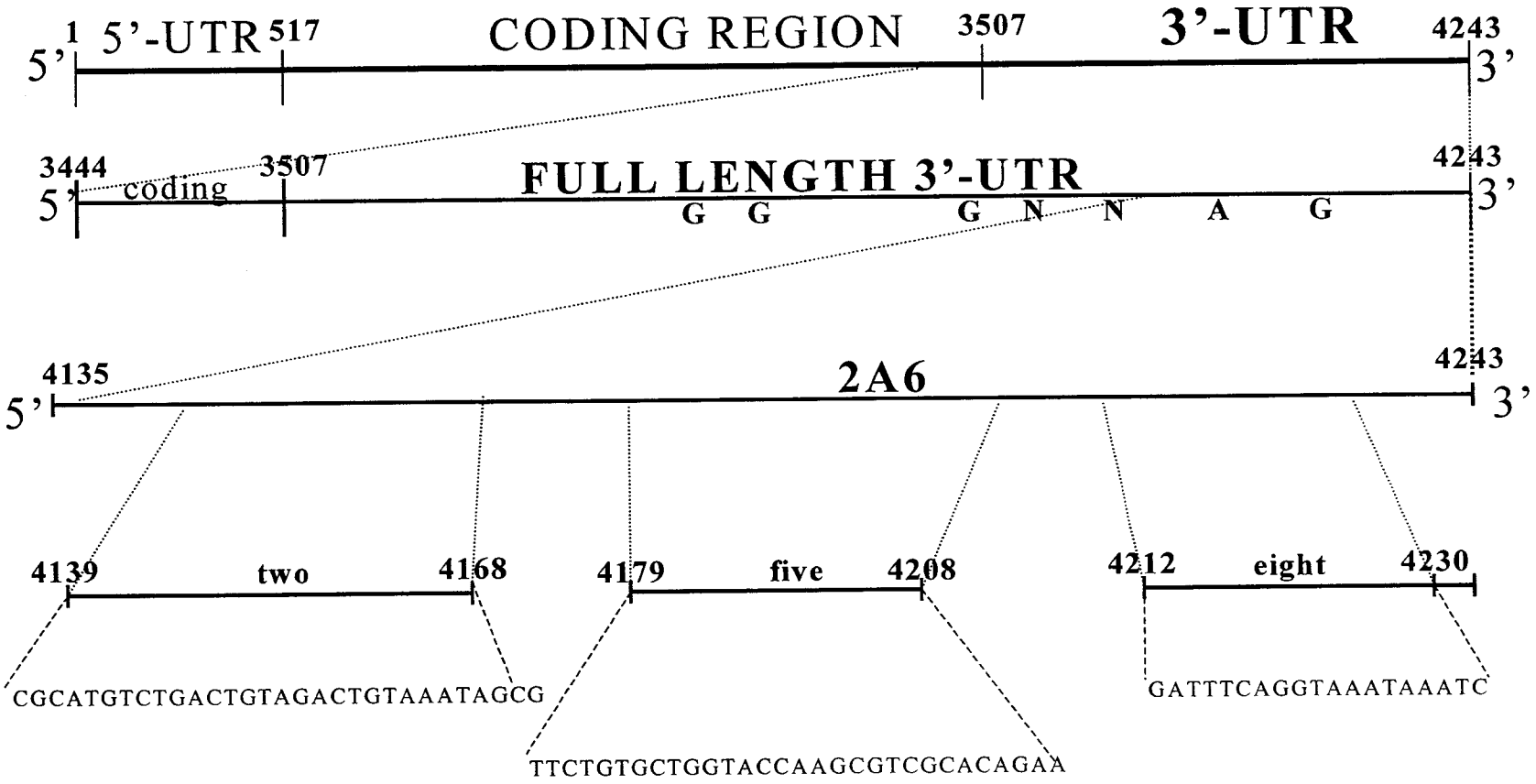

Figure 28. Sequence elements in SERCA2a.

The numbers given correspond to the sequence in Figure 2. Approximate locations of known GUUUG (G) elements at 3716, 3765, 3919, and 4173, the AUUUA (A) element at 4100, and the nonamer (N) motifs at 3925 and 4044 are shown in addition to the sequences of the 3 elements identified in 2A6 (4139 to 4168, 4179 to 4208, and 4212 to 4230).

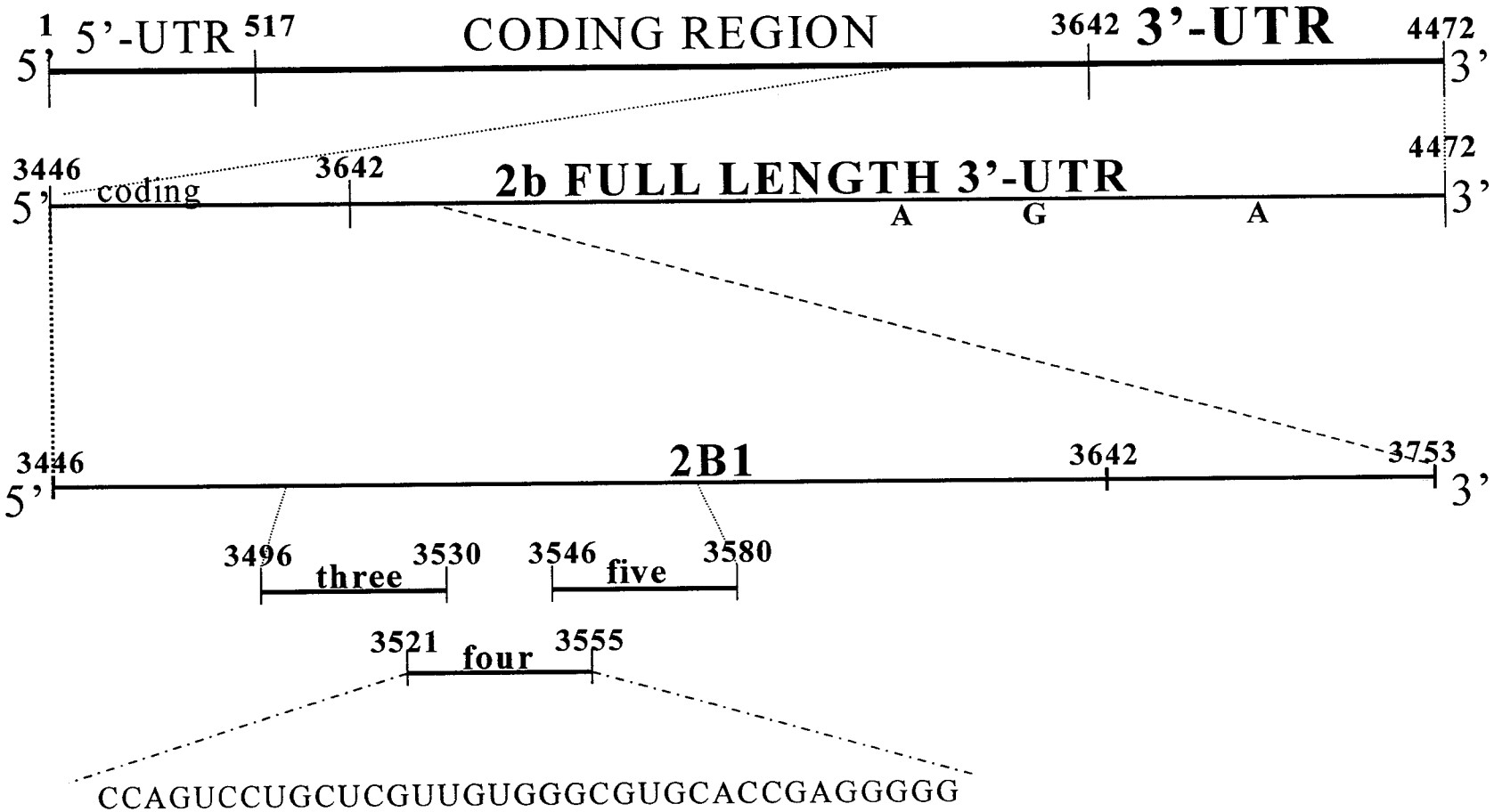

Figure 29. Sequence elements in SERCA2b.

The numbers given correspond to the sequence in Figure 2. Approximate locations of the known GUUUG (G) element at 4188, and AUUUA (A) elements at 4060 and 4342 are shown in addition to the sequence of the element identified in 2B1 (3521 to 3555).

Since the combination of all three regions in SERCA2a (fragments 2, 5, and 8) competed more strongly than the individual fragments or other combinations of fragments, this also supports the hypothesis that more than one protein or more than one binding site is involved in the protein binding of fragment 2A6. However, the combination of all three regions was still unable to completely reverse a shift in mobility, thus, there may be other factors influencing binding in this region.

Fragment 2A6 gave more than one band of slower mobility, suggesting that this fragment may bind more than one protein or there may have multiple binding sites on the same protein. Another explanation for more than one mobility complex is that there are two forms of the protein resulting from post-translational modification. The stem loop binding protein is able to bind histone mRNA in both the nuclear and polyribosomal fractions, and two forms of the protein are detected by Western blotting in either extract. These two protein forms, also observed through doublets in mobility shift assays, are attributed to either post-translational modifications or proteolysis of the protein from the amino terminus (124). Based on the estimated sizes of the proteins (90 and 170 kDa), it is also feasible that the higher band reflects the formation of a dimer of the smaller protein. The protein bound by fragment 2B1 (201 kDa) is significantly larger than most of the known RNA-binding proteins, which range from 20 to 50 kDa, and is also larger than the protein(s) bound by 2A6 (114). This suggests that the proteins bound by these regions of SERCA2 are distinct from any previously identified protein factors and are likely also different from each other. These proteins should be characterized by a more quantitative means, such as UV crosslinking, to

confirm these results.

The competitive mobility shift assays between fragment 2B1 and the 3 large overlapping fragments (2B1a, 2B1b, and 2B1c) suggested the binding of two proteins. As this was contradictory to the initial finding of one protein bound by 2B1, we instead used the original 2B1 for further analysis and no second region was found. As a possible explanation for the absence of any competition for binding in the second half of the 2B1 molecule, the secondary structure of each of these smaller fragments was predicted with the program, RNAdraw, and compared to the structures of 2B1b and 2B1c. The folding patterns showed a distinct hairpin structure at the very end of the fragment of 2B1b and at the beginning of 2B1c, within the overlapping region. This structure was not present in any of the smaller fragments, thus, it is possible that the downstream element of binding is only seen with fragments 2B1b and 2B1c due to a unique hairpin loop that is targeted for binding by a protein. Regions of secondary structure are known to be sights of binding for proteins that play a role in both stability and decay. A large region of stable secondary structure in the 3'-UTR of chicken elastin mRNA is specifically bound by a cytoplasmic protein (44). The abundance of this protein during development was then correlated with circumstances in which elastin mRNA is stable (45). Similarly, hairpin loops have been found as targets of proteins that control decay rather than stability. It is proposed protein factors bound to secondary structures may unravel these hairpins and make them targets for endonucleases (63;105). Our results imply, however, that the secondary structure and protein binding properties of an mRNA sequence may change in the context of the full message. The

structure of mRNA was shown to vary in the presence of different Mg^{2+} concentrations, confirming that alternative mRNA structures are possible in different conditions (128).

While fragment 2A6 is at the very end of the 3'-UTR of SERCA2a, fragment 2B1 contains bases common to both SERCA2a and 2b, the unique coding region sequence of SERCA2b, and part of the SERCA2b 3'-UTR. Thus, this study shows a novel GC-rich element within the coding region and 3'-UTR that may function in the decay of SERCA2b. This has an important implication, as binding in the coding region may affect downstream secondary structure and subsequent protein binding. Coding region elements in c-*myc* and c-*fos* are required for protein binding in the 3'-UTR and in other messages, long range interactions exist between AU-rich sequences and other parts of the RNA before they are able to function as destabilizing elements (19;21;92). This may prove to be the case in SERCA2b, as there may be additional influences of the 2B1 element on downstream binding in the 3'-end of SERCA2b. While this is promising, the complexity of SERCA2b, due to the finding of many unstable fragments, leaves much still to uncover.

4.6 Summary and future considerations

This work has led to significant progress in the study of the regulation of SERCA2 gene expression. It has shown the relative stability of SERCA2a and the nuclear decay of SERCA2b by two different methods. This is interesting given that most research points to cytoplasmic decay of mRNA. Additionally, we have shown the effect of specific sequences in the 3' regions of both the SERCA2 isoforms on decay and have begun to correlate these

data with the initial identification of *trans*-acting proteins in nuclear extracts from LVM. Toward this end, we have also discovered specific regions in SERCA2a and 2b, and novel sequences in 2 of these regions, that may have important roles in SERCA2 stability.

This study has, thus, begun the important task of identifying the *cis*-acting elements and *trans*-acting factors that regulate SERCA2 decay. Much work, however, still remains. As priorities, it will be important to determine the *in vivo* relevance of these binding studies through competition with full length transcripts and decay of deletion constructs. This is especially important in the study of SERCA2b where the effect of the coding region element may be considered. As another issue to be resolved, it would be interesting to determine the differences in factors between LVM nucleus and SSM cytoplasm that lead to similar decay rates of SERCA2a and 2b in the latter extract. This comparison may help identify factors that are key to destabilizing and/or stabilizing SERCA2b. As long term goals, the characterization of SERCA2 RNA-binding proteins and their comparison in other species may help determine their evolutionary importance. Once these proteins have been characterized it will then be possible to test their roles in development and disease.

REFERENCES

1. **Aharon, T. and R. J. Schneider.** Selective destabilization of short-lived mRNAs with the granulocyte- macrophage colony-stimulating factor AU-rich 3' noncoding region is mediated by a cotranslational mechanism. *Mol.Cell Biol.* 13: 1971-1980, 1993.

2. **Andersen, J. P. and B. Vilsen.** Structure-function relationships of cation translocation by Ca(2+)- and Na+, K(+)-ATPases studied by site-directed mutagenesis. *FEBS Lett.* 359: 101-106, 1995.

3. **Arao, Y., R. Kuriyama, F. Kayama, and S. Kato.** A nuclear matrix-associated factor, SAF-B, interacts with specific isoforms of AUF1/hnRNP D. *Arch.Biochem.Biophys.* 380: 228-236, 2000.

4. **Barritt, G. J.** Receptor-activated Ca2+ inflow in animal cells: a variety of pathways tailored to meet different intracellular Ca2+ signalling requirements. *Biochem.J.* 337 (Pt 2): 153-169, 1999.

5. **Berchtold, M. W., H. Brinkmeier, and M. Muntener.** Calcium ion in skeletal muscle: its crucial role for muscle function, plasticity, and disease. *Physiol Rev.* 80: 1215-1265, 2000.

6. **Blaxall, B. C., A. C. Pellett, S. C. Wu, A. Pende, and J. D. Port.** Purification and characterization of beta-adrenergic receptor mRNA- binding proteins. *J.Biol.Chem.* 275: 4290-4297, 2000.

7. **Blencowe, B. J.** Exonic splicing enhancers: mechanism of action, diversity and role in human genetic diseases. *Trends Biochem.Sci.* 25: 106-110, 2000.

8. **Boheler, K. R., C. Chassagne, X. Martin, C. Wisnewsky, and K. Schwartz.** Cardiac expressions of alpha- and beta-myosin heavy chains and sarcomeric alpha-actins are regulated through transcriptional mechanisms. Results from nuclear run-on assays in isolated rat cardiac nuclei. *J.Biol.Chem.* 267: 12979-12985, 1992.

9. **Brawerman, G.** Determinants of messenger RNA stability. *Cell* 48: 5-6, 1987.

10. **Brawerman, G.** mRNA decay: finding the right targets. *Cell* 57: 9-10, 1989.

11. **Brewer, G.** Characterization of c-myc 3' to 5' mRNA decay activities in an in vitro system. *J.Biol.Chem.* 273: 34770-34774, 1998.

12. **Brewer, G.** Evidence for a 3'-5' decay pathway for c-myc mRNA in mammalian cells. *J.Biol.Chem.* 274: 16174-16179, 1999.

13. **Brewer, G. and J. Ross.** Poly(A) shortening and degradation of the 3' A+U-rich sequences of human c-myc mRNA in a cell-free system. *Mol.Cell Biol.* 8: 1697-1708, 1988.

14. **Buzby, J. S., G. Brewer, and D. J. Nugent.** Developmental regulation of RNA transcript destabilization by A + U- rich elements is AUF1-dependent. *J.Biol.Chem.* 274: 33973-33978, 1999.

15. **Carafoli, E.** Calcium pump of the plasma membrane. *Physiol Rev.* 71: 129-153, 1991.

16. **Carafoli, E.** The calcium pumping ATPase of the plasma membrane. *Annu.Rev.Physiol* 53: 531-547, 1991.

17. **Carpousis, A. J., N. F. Vanzo, and L. C. Raynal.** mRNA degradation. A tale of poly(A) and multiprotein machines. *Trends Genet.* 15: 24-28, 1999.

18. **Chen, C. Y., T. M. Chen, and A. B. Shyu.** Interplay of two functionally and structurally distinct domains of the c-fos AU-rich element specifies its mRNA-

destabilizing function. *Mol.Cell Biol.* 14: 416-426, 1994.

19. **Chen, C. Y. and A. B. Shyu.** Selective degradation of early-response-gene mRNAs: functional analyses of sequence features of the AU-rich elements. *Mol.Cell Biol.* 14: 8471-8482, 1994.

20. **Chen, C. Y. and A. B. Shyu.** AU-rich elements: characterization and importance in mRNA degradation. *Trends Biochem.Sci.* 20: 465-470, 1995.

21. **Chen, C. Y., N. Xu, and A. B. Shyu.** mRNA decay mediated by two distinct AU-rich elements from c-fos and granulocyte-macrophage colony-stimulating factor transcripts: different deadenylation kinetics and uncoupling from translation. *Mol.Cell Biol.* 15: 5777-5788, 1995.

22. **Chen, C. Y., N. Xu, and A. B. Shyu.** Highly selective actions of HuR in antagonizing AU-rich element- mediated mRNA destabilization. *Mol.Cell Biol.* 22: 7268-7278, 2002.

23. **Chen, C. Y., Y. You, and A. B. Shyu.** Two cellular proteins bind specifically to a purine-rich sequence necessary for the destabilization function of a c-fos protein-coding region determinant of mRNA instability. *Mol.Cell Biol.* 12: 5748-5757, 1992.

24. **Chin, D. and A. R. Means.** Calmodulin: a prototypical calcium sensor. *Trends Cell Biol.* 10: 322-328, 2000.

25. **Chkheidze, A. N., D. L. Lyakhov, A. V. Makeyev, J. Morales, J. Kong, and S. A. Liebhaber.** Assembly of the alpha-globin mRNA stability complex reflects binary interaction between the pyrimidine-rich 3' untranslated region determinant and poly(C) binding protein alphaCP. *Mol.Cell Biol.* 19: 4572-4581, 1999.

26. **Clapham, D. E.** Calcium signaling. *Cell* 80: 259-268, 1995.

27. **Coller, J. M., N. K. Gray, and M. P. Wickens.** mRNA stabilization by poly(A) binding protein is independent of poly(A) and requires translation. *Genes Dev.* 12: 3226-3235, 1998.

28. **Curatola, A. M., M. S. Nadal, and R. J. Schneider.** Rapid degradation of AU-rich element (ARE) mRNAs is activated by ribosome transit and blocked by secondary structure at any position 5' to the ARE. *Mol.Cell Biol.* 15: 6331-6340, 1995.

29. **Daneholt, B.** A look at messenger RNP moving through the nuclear pore. *Cell* 88: 585-588, 1997.

30. **Day, D. A. and M. F. Tuite.** Post-transcriptional gene regulatory mechanisms in

eukaryotes: an overview. *J.Endocrinol.* 157: 361-371, 1998.

31. **Decker, C. J. and R. Parker.** Mechanisms of mRNA degradation in eukaryotes. *Trends Biochem.Sci.* 19: 336-340, 1994.

32. **DeMaria, C. T., Y. Sun, B. J. Wagner, L. Long, and G. A. Brewer.** Structural determination in AUF1 required for high affinity binding to A + U-rich elements. *Nucleic Acids Symp.Ser.* 12-14, 1997.

33. **Dode, L., F. Wuytack, P. F. Kools, F. Baba-Aissa, L. Raeymaekers, F. Brike, W. J. van de Ven, R. Casteels, and F. Brik.** cDNA cloning, expression and chromosomal localization of the human sarco/endoplasmic reticulum Ca(2+)-ATPase 3 gene. *Biochem.J.* 318 (Pt 2): 689-699, 1996.

34. **East, J. M.** Sarco(endo)plasmic reticulum calcium pumps: recent advances in our understanding of structure/function and biology (review). *Mol.Membr.Biol.* 17: 189-200, 2000.

35. **Eisner, D. A., A. W. Trafford, M. E. Diaz, C. L. Overend, and S. C. O'Neill.** The control of Ca release from the cardiac sarcoplasmic reticulum: regulation versus autoregulation. *Cardiovasc.Res.* 38: 589-604, 1998.

36. **Fan, X. C. and J. A. Steitz.** HNS, a nuclear-cytoplasmic shuttling sequence in HuR. *Proc.Natl.Acad.Sci.U.S.A* 95: 15293-15298, 1998.

37. **Fan, X. C. and J. A. Steitz.** Overexpression of HuR, a nuclear-cytoplasmic shuttling protein, increases the in vivo stability of ARE-containing mRNAs. *EMBO J.* 17: 3448-3460, 1998.

38. **Fortea, M. I., F. Soler, and F. Fernandez-Belda.** Unravelling the interaction of thapsigargin with the conformational states of Ca(2+)-ATPase from skeletal sarcoplasmic reticulum. *J.Biol.Chem.* 276: 37266-37272, 2001.

39. **Furuichi, Y., A. LaFiandra, and A. J. Shatkin.** 5'-Terminal structure and mRNA stability. *Nature* 266: 235-239, 1977.

40. **Grosset, C., C. Y. Chen, N. Xu, N. Sonenberg, H. Jacquemin-Sablon, and A. B. Shyu.** A mechanism for translationally coupled mRNA turnover: interaction between the poly(A) tail and a c-fos RNA coding determinant via a protein complex. *Cell* 103: 29-40, 2000.

41. **Gu, H., J. D. Gupta, and D. R. Schoenberg.** The poly(A)-limiting element is a conserved cis-acting sequence that regulates poly(A) tail length on nuclear pre-

mRNAs. *Proc.Natl.Acad.Sci.U.S.A* 96: 8943-8948, 1999.

42. **Guo, W., G. J. Mulligan, S. Wormsley, and D. M. Helfman.** Alternative splicing of beta-tropomyosin pre-mRNA: cis-acting elements and cellular factors that block the use of a skeletal muscle exon in nonmuscle cells. *Genes Dev.* 5: 2096-2107, 1991.

43. **Helenius, A., E. S. Trombetta, D. N. Hebert, and J. F. Simons.** Calnexin, calreticulin and the folding of glycoproteins. *Trends Cell Biol.* 7: 200, 1997.

44. **Hew, Y., Z. Grzelczak, C. Lau, and F. W. Keeley.** Identification of a large region of secondary structure in the 3'- untranslated region of chicken elastin mRNA with implications for the regulation of mRNA stability. *J.Biol.Chem.* 274: 14415-14421, 1999.

45. **Hew, Y., C. Lau, Z. Grzelczak, and F. W. Keeley.** Identification of a GA-rich sequence as a protein-binding site in the 3'-untranslated region of chicken elastin mRNA with a potential role in the developmental regulation of elastin mRNA stability. *J.Biol.Chem.* 275: 24857-24864, 2000.

46. **Holcik, M. and S. A. Liebhaber.** Four highly stable eukaryotic mRNAs assemble

3' untranslated region RNA- protein complexes sharing cis and trans components. *Proc.Natl.Acad.Sci.U.S.A* 94: 2410-2414, 1997.

47. **Huang, Y. and G. G. Carmichael.** Nucleocytoplasmic mRNA transport. *Results Probl.Cell.Differ.* 34:139-155, 2001.

48. **Jackson, R. J. and N. Standart.** Do the poly(A) tail and 3' untranslated region control mRNA translation? *Cell* 62: 15-24, 1990.

49. **Jacobson, A. and S. W. Peltz.** Interrelationships of the pathways of mRNA decay and translation in eukaryotic cells. *Annu.Rev.Biochem.* 65: 693-739, 1996.

50. **Jacobson, A. and S. W. Peltz.** Tools for turnover: methods for analysis of mRNA stability in eukaryotic cells [editorial]. *Methods* 17: 1-2, 1999.

51. **Jarmolowski, A., W. C. Boelens, E. Izaurralde, and I. W. Mattaj.** Nuclear export of different classes of RNA is mediated by specific factors. *J.Cell Biol.* 124: 627-635, 1994.

52a. **Jarzembowski, J. A., L. E. Rajagopalan, H. C. Shin, and J. S. Malter.** The 5'-untranslated region of GM-CSF mRNA suppresses translational repression mediated by the 3' adenosine-uridine-rich element and the poly(A) tail. *Nucleic Acids Res.* 27:

3660-3666, 1999.

52b. **Jarrousse, A. S., F. Petit, C. Kreutzer-Schmid, R. Gaedigk, and H. P. Schmid.** Possible involvement of proteasomes (prosomes) in AUUUA-mediated mRNA decay. *J.Biol.Chem.* 274: 5925-5930, 1999.

53. **John, L. M., J. D. Lechleiter, and P. Camacho.** Differential modulation of SERCA2 isoforms by calreticulin. *J.Cell Biol.* 142: 963-973, 1998.

54. **Kadambi, V. J. and E. G. Kranias.** Phospholamban: a protein coming of age. *Biochem.Biophys.Res.Commun.* 239: 1-5, 1997.

55. **Kajita, Y., J. Nakayama, M. Aizawa, and F. Ishikawa.** The UUAG-specific RNA binding protein, heterogeneous nuclear ribonucleoprotein D. Common modular structure and binding properties of the 2xRBD-Gly family. *J.Biol.Chem.* 270: 22167-22175, 1995.

56. **Karp, G.** Cell and Molecular Biology: Concepts and Experiments. Toronto, John Wiley & Sons, Inc. 1996.

57. **Khan, I. and A. K. Grover.** Abundance of heteronuclear and messenger RNA for internal Ca pump in stomach smooth muscle and myocardium. *Cell Calcium* 14: 17-

23, 1993.

58. **Khan, I., G. G. Spencer, S. E. Samson, P. Crine, G. Boileau, and A. K. Grover.** Abundance of sarcoplasmic reticulum calcium pump isoforms in stomach and cardiac muscles. *Biochem.J.* 268: 415-419, 1990.

59. **Koss, K. L., I. L. Grupp, and E. G. Kranias.** The relative phospholamban and SERCA2 ratio: a critical determinant of myocardial contractility. *Basic Res.Cardiol.* 92 Suppl 1: 17-24, 1997.

60. **Koss, K. L. and E. G. Kranias.** Phospholamban: a prominent regulator of myocardial contractility. *Circ.Res.* 79: 1059-1063, 1996.

61. **Krause, K. H. and M. Michalak.** Calreticulin. *Cell* 88: 439-443, 1997.

62. **Laroia, G., R. Cuesta, G. Brewer, and R. J. Schneider.** Control of mRNA decay by heat shock-ubiquitin-proteasome pathway. *Science* 284: 499-502, 1999.

63. **Lee, C. H., P. Leeds, and J. Ross.** Purification and characterization of a polysome-associated endoribonuclease that degrades c-myc mRNA in vitro. *J.Biol.Chem.* 273: 25261-25271, 1998.

64. **Liu, H., N. D. Rodgers, X. Jiao, and M. Kiledjian.** The scavenger mRNA decapping enzyme DcpS is a member of the HIT family of pyrophosphatases. *EMBO J.* 21: 4699-4708, 2002.

65. **Loflin, P., C. Y. Chen, and A. B. Shyu.** Unraveling a cytoplasmic role for hnRNP D in the in vivo mRNA destabilization directed by the AU-rich element. *Genes Dev.* 13: 1884-1897, 1999.

66. **Ludtke, J. J., G. Zhang, M. G. Sebestyen, and J. A. Wolff.** A nuclear localization signal can enhance both the nuclear transport and expression of 1 kb DNA. *J.Cell.Sci.* 112 (Pt 2):2033-2041, 1999.

67. **Lytton, J., A. Zarain-Herzberg, M. Periasamy, and D. H. MacLennan.** Molecular cloning of the mammalian smooth muscle sarco(endo)plasmic reticulum Ca2+-ATPase. *J.Biol.Chem.* 264: 7059-7065, 1989.

68. **Maquat, L. E.** Molecular biology. Skiing toward nonstop mRNA decay. *Science* 295: 2221-2222, 2002.

69. **Matzura, O. and A. Wennbrg.** RNAdraw: an integrated program for RNA secondary structure calculation and analysis under 32-bit Microsoft Windows.

Computer Applications in the Biosciences (CABIOS) 12: 247-249, 1996.

70. **Mearow, K. M., B. G. Thilander, I. Khan, R. E. Garfield, and A. K. Grover.** In situ hybridization and immunocytochemical localization of SERCA2 encoded Ca2+ pump in rabbit heart and stomach. *Mol.Cell Biochem.* 121: 155-165, 1993.

71. **Mertens, L., B. L. Van den, H. Verboomen, F. Wuytack, H. De Smedt, and J. Eggermont.** Sequence and spatial requirements for regulated muscle-specific processing of the sarco/endoplasmic reticulum Ca(2+)-ATPase 2 gene transcript. *J.Biol.Chem.* 270: 11004-11011, 1995.

72. **Miller, R. J.** Voltage-sensitive Ca2+ Channels. *J.Biol.Chem.* 267: 1403-1406, 1992.

73. **Misquitta, C. M., V. R. Iyer, E. S. Werstiuk, and A. K. Grover.** The role of 3'-untranslated region (3'-UTR) mediated mRNA stability in cardiovascular pathophysiology. *Mol.Cell Biochem.* 224: 53-67, 2001.

74. **Misquitta, C. M., D. P. Mack, and A. K. Grover.** Sarco/endoplasmic reticulum Ca2+ (SERCA)-pumps: link to heart beats and calcium waves. *Cell Calcium* 25: 277-290, 1999.

75. **Misquitta, C. M., J. Mwanjewe, L. Nie, and A. K. Grover.** Sarcoplasmic

reticulum Ca(2+) pump mRNA stability in cardiac and smooth muscle: role of the 3'-untranslated region. *Am.J.Physiol Cell Physiol* 283: C560-C568, 2002.

76. **Misquitta, C. M., A. Sing, and A. K. Grover.** Control of sarcoplasmic/ endoplasmic-reticulum Ca2+ pump expression in cardiac and smooth muscle. *Biochem.J.* 338 (Pt 1): 167-173, 1999.

77. **Missiaen, L., F. Wuytack, L. Raeymaekers, H. De Smedt, G. Droogmans, I. Declerck, and R. Casteels.** Ca2+ extrusion across plasma membrane and Ca2+ uptake by intracellular stores. *Pharmacol.Ther.* 50: 191-232, 1991.

78. **Moore, M. J. Nuclear RNA turnover.** *Cell* 108: 431-434, 2002.

79. **Nakamaki, T., J. Imamura, G. Brewer, N. Tsuruoka, and H. P. Koeffler.** Characterization of adenosine-uridine-rich RNA binding factors. *J.Cell Physiol* 165: 484-492, 1995.

80. **Nakielny, S. and G. Dreyfuss.** Transport of proteins and RNAs in and out of the nucleus. *Cell* 99: 677-690, 1999.

81. **Nakielny, S., U. Fischer, W. M. Michael, and G. Dreyfuss.** RNA transport. *Annu.Rev.Neurosci.* 20: 269-301, 1997.

82. **Narayanan, N. and A. Xu.** Phosphorylation and regulation of the Ca(2+)-pumping ATPase in cardiac sarcoplasmic reticulum by calcium/calmodulin-dependent protein kinase. *Basic Res.Cardiol.* 92 Suppl 1: 25-35, 1997.

83. **Noe, V., C. J. Ciudad, and L. A. Chasin.** Effect of differential polyadenylation and cell growth phase on dihydrofolate reductase mRNA stability. *J.Biol.Chem.* 274: 27807-27814, 1999.

84. **Odermatt, A., S. Becker, V. K. Khanna, K. Kurzydlowski, E. Leisner, D. Pette, and D. H. MacLennan.** Sarcolipin regulates the activity of SERCA1, the fast-twitch skeletal muscle sarcoplasmic reticulum Ca2+-ATPase. *J.Biol.Chem.* 273: 12360-12369, 1998.

85. **Odermatt, A., P. E. Taschner, S. W. Scherer, B. Beatty, V. K. Khanna, D. R. Cornblath, V. Chaudhry, W. C. Yee, B. Schrank, G. Karpati, M. H. Breuning, N. Knoers, and D. H. MacLennan.** Characterization of the gene encoding human sarcolipin (SLN), a proteolipid associated with SERCA1: absence of structural mutations in five patients with Brody disease. *Genomics* 45: 541-553, 1997.

86. **Olson, S., M. G. Wang, E. Carafoli, E. E. Strehler, and O. W. McBride.** Localization of two genes encoding plasma membrane Ca2(+)-transporting ATPases

to human chromosomes 1q25-32 and 12q21-23. *Genomics* 9: 629-641, 1991.

87. **Parekh, A. B. and R. Penner.** Store depletion and calcium influx. *Physiol Rev.* 77: 901-930, 1997.

88. **Pende, A., K. D. Tremmel, C. T. DeMaria, B. C. Blaxall, W. A. Minobe, J. A. Sherman, J. D. Bisognano, M. R. Bristow, G. Brewer, and J. Port.** Regulation of the mRNA-binding protein AUF1 by activation of the beta- adrenergic receptor signal transduction pathway. *J.Biol.Chem.* 271: 8493-8501, 1996.

89a. **Peng, S. S., C. Y. Chen, N. Xu, and A. B. Shyu.** RNA stabilization by the AU-rich element binding protein, HuR, an ELAV protein. *EMBO J.* 17: 3461-3470, 1998.

89b. **Peng, S. S., C. Y. Chen, and A. B. Shyu.** Functional characterization of a non-AUUUA AU-rich element from the c-jun proto-oncogene mRNA: evidence for a novel class of AU-rich elements. *Mol.Cell Biol.* 16: 1490-1499, 1996.

90. **Periasamy, M.** Adenoviral-mediated serca gene transfer into cardiac myocytes: how much is too much? *Circ.Res.* 88: 373-375, 2001.

91. **Periasamy, M. and S. Huke.** SERCA pump level is a critical determinant of Ca(2+)homeostasis and cardiac contractility. *J.Mol.Cell Cardiol.* 33: 1053-1063,

2001.

92. **Piechaczyk, M., J. M. Blanchard, A. Bonnieu, P. Fort, N. Mechti, J. Rech, M. Cuny, L. Marty, F. Ferre, B. Lebleu, and P. Jeanteur.** Role of RNA structures in c-myc and c-fos gene regulations. *Gene* 72: 287-295, 1988.

93. **Pollock, J. A., A. Assaf, A. Peretz, C. D. Nichols, M. H. Mojet, R. C. Hardie, and B. Minke.** TRP, a protein essential for inositide-mediated Ca2+ influx is localized adjacent to the calcium stores in Drosophila photoreceptors. *J.Neurosci.* 15: 3747-3760, 1995.

94. **Putney, J. W., Jr., L. M. Broad, F. J. Braun, J. P. Lievremont, and G. S. Bird.** Mechanisms of capacitative calcium entry. *J.Cell Sci.* 114: 2223-2229, 2001.

95. **Qi, M., J. W. Bassani, D. M. Bers, and A. M. Samarel.** Phorbol 12-myristate 13-acetate alters SR Ca(2+)-ATPase gene expression in cultured neonatal rat heart cells. *Am.J.Physiol* 271: H1031-H1039, 1996.

96. **Rajagopalan, L. E. and J. S. Malter.** Modulation of granulocyte-macrophage colony-stimulating factor mRNA stability in vitro by the adenosine-uridine binding factor. *J.Biol.Chem.* 269: 23882-23888, 1994.

97. **Ross, J.** mRNA stability in mammalian cells. *Microbiol.Rev.* 59: 423-450, 1995.

98. **Ross, J.** Control of messenger RNA stability in higher eukaryotes. *Trends Genet.* 12: 171-175, 1996.

99. **Ross, J.** A hypothesis to explain why translation inhibitors stabilize mRNAs in mammalian cells: mRNA stability and mitosis. *Bioessays* 19: 527-529, 1997.

100. **Ross, J., G. Kobs, G. Brewer, and S. W. Peltz.** Properties of the exonuclease activity that degrades H4 histone mRNA. *J.Biol.Chem.* 262: 9374-9381, 1987.

101. **Sachs, A. and E. Wahle.** Poly(A) tail metabolism and function in eucaryotes. *J.Biol.Chem.* 268: 22955-22958, 1993.

102. **Sachs, A. B.** Messenger RNA degradation in eukaryotes. *Cell* 74: 413-421, 1993.

103. **Sambrook, J., E. F. Fritsch, and T.** Maniatis. Molecular Cloning: A Laboratory Manual. New York, Cold Spring Harbor Laboratory Press. 1989.

104. **Savant-Bhonsale, S. and D. W. Cleveland.** Evidence for instability of mRNAs containing AUUUA motifs mediated through translation-dependent assembly of a > 20S degradation complex. *Genes Dev.* 6: 1927-1939, 1992.

105. **Schiavone, N., P. Rosini, A. Quattrone, M. Donnini, A. Lapucci, L. Citti, A. Bevilacqua, A. Nicolin, and S. Capaccioli.** A conserved AU-rich element in the 3' untranslated region of bcl-2 mRNA is endowed with a destabilizing function that is involved in bcl-2 down-regulation during apoptosis. *FASEB J.* 14: 174-184, 2000.

106. **Setzer, D. R., M. McGrogan, and R. T. Schimke.** Nucleotide sequence surrounding multiple polyadenylation sites in the mouse dihydrofolate reductase gene. *J.Biol.Chem.* 257: 5143-5147, 1982.

107. **Sinn, P. L. and C. D. Sigmund.** Human Renin mRNA Stability Is Increased in Response to cAMP in Calu-6 Cells. *Hypertension* 33: 900-905, 1999.

108. **Stokes, D. L.** Keeping calcium in its place: Ca(2+)-ATPase and phospholamban. *Curr.Opin.Struct.Biol.* 7: 550-556, 1997.

109. **Strehler, E. E. and D. A. Zacharias.** Role of alternative splicing in generating isoform diversity among plasma membrane calcium pumps. *Physiol Rev.* 81: 21-50, 2001.

110. **Tamm, I., R. Hand, and L. A. Caliguiri.** Action of dichlorobenzimidazole riboside on RNA synthesis in L-929 and HeLa cells. *J.Cell Biol.* 69: 229-240, 1976.

111. **Theodorakis, N. G. and A. De Maio.** Cx32 mRNA in rat liver: effects of inflammation on poly(A) tail distribution and mRNA degradation. *Am.J.Physiol* 276: R1249-R1257, 1999.

112. **Toyofuku, T., K. K. Curotto, N. Narayanan, and D. H. MacLennan.** Identification of Ser38 as the site in cardiac sarcoplasmic reticulum Ca(2+)-ATPase that is phosphorylated by Ca2+/calmodulin-dependent protein kinase. *J.Biol.Chem.* 269: 26492-26496, 1994.

113. **Toyofuku, T., K. Kurzydlowski, M. Tada, and D. H. MacLennan.** Identification of regions in the Ca(2+)-ATPase of sarcoplasmic reticulum that affect functional association with phospholamban. *J.Biol.Chem.* 268: 2809-2815, 1993.

114. **Vakalopoulou, E., J. Schaack, and T. Shenk.** A 32-kilodalton protein binds to AU-rich domains in the 3' untranslated regions of rapidly degraded mRNAs. *Mol.Cell Biol.* 11: 3355-3364, 1991.

115. **van Breemen, C. and K. Saida.** Cellular mechanisms regulating [Ca2+]i smooth muscle. *Annu.Rev.Physiol* 51: 315-329, 1989.

116. **van Breemen, C., K. Saida, H. Yamamoto, K. Hwang, and C. Twort.** Vascular

smooth muscle sarcoplasmic reticulum. Function and mechanisms of Ca2+ release. *Ann.N.Y.Acad.Sci.* 522: 60-73, 1988.

117. **Van den Bosch, L., J. Eggermont, H. De Smedt, L. Mertens, F. Wuytack, and R. Casteels.** Regulation of splicing is responsible for the expression of the muscle-specific 2a isoform of the sarco/endoplasmic-reticulum Ca(2+)-ATPase. *Biochem.J.* 302 (Pt 2): 559-566, 1994.

118. **van Hoof, A., P. A. Frischmeyer, H. C. Dietz, and R. Parker.** Exosome-mediated recognition and degradation of mRNAs lacking a termination codon. *Science* 295: 2262-2264, 2002.

119. **Ver, H. M., S. Heymans, G. Antoons, T. Reed, M. Periasamy, B. Awede, J. Lebacq, P. Vangheluwe, M. Dewerchin, D. Collen, K. Sipido, P. Carmeliet, and F. Wuytack.** Replacement of the muscle-specific sarcoplasmic reticulum Ca(2+)-ATPase isoform SERCA2a by the nonmuscle SERCA2b homologue causes mild concentric hypertrophy and impairs contraction-relaxation of the heart. *Circ.Res.* 89: 838-846, 2001.

120. **Verboomen, H., F. Wuytack, B. L. Van den, L. Mertens, and R. Casteels.** The functional importance of the extreme C-terminal tail in the gene 2 organellar

Ca(2+)-transport ATPase (SERCA2a/b). *Biochem.J.* 303 (Pt 3): 979-984, 1994.

121. **Wagner, B. J., C. T. DeMaria, Y. Sun, G. M. Wilson, and G. Brewer.** Structure and genomic organization of the human AUF1 gene: alternative pre-mRNA splicing generates four protein isoforms. *Genomics* 48: 195-202, 1998.

122. **Wang, X., M. Kiledjian, I. M. Weiss, and S. A. Liebhaber.** Detection and characterization of a 3' untranslated region ribonucleoprotein complex associated with human alpha-globin mRNA stability. *Mol.Cell Biol.* 15: 1769-1777, 1995.

123. **Wang, Z. and M. Kiledjian.** The poly(A)-binding protein and an mRNA stability protein jointly regulate an endoribonuclease activity.

124. **Wang, Z. F., M. L. Whitfield, T. C. Ingledue, III, Z. Dominski, and W. F. Marzluff.** The protein that binds the 3' end of histone mRNA: a novel RNA-binding protein required for histone pre-mRNA processing. *Genes Dev.* 10: 3028-3040, 1996.

125. **Wilkinson, M. F. and A. B. Shyu.** Multifunctional regulatory proteins that control gene expression in both the nucleus and the cytoplasm. *Bioessays* 23: 775-787, 2001.

126. **Wilson, G. M. and G. Brewer.** Identification and characterization of proteins binding A + U-rich elements. *Methods* 17: 74-83, 1999.

127. **Wilson, G. M., Y. Sun, H. Lu, and G. Brewer.** Assembly of AUF1 Oligomers on U-rich RNA Targets by Sequential Dimer Association. *J.Biol.Chem.* 274: 33374-33381, 1999.

128. **Wilson, G. M., K. Sutphen, K. Chuang, and G. Brewer.** Folding of A+U-rich RNA elements modulates AUF1 binding. Potential roles in regulation of mRNA turnover. *J.Biol.Chem.* 276: 8695-8704, 2001.

129. **Wu, K. D., D. Bungard, and J. Lytton.** Regulation of SERCA Ca2+ pump expression by cytoplasmic Ca2+ in vascular smooth muscle cells. *Am.J.Physiol Cell Physiol* 280: C843-C851, 2001.

130. **Wuytack, F., L. Raeymaekers, H. De Smedt, J. A. Eggermont, L. Missiaen, B. L. Van den, S. De Jaegere, H. Verboomen, L. Plessers, and R. Casteels.** Ca(2+)-transport ATPases and their regulation in muscle and brain. *Ann.N.Y.Acad.Sci.* 671: 82-91, 1992.

131. **Wuytack, F., B. L. Van den, H. M. Ver, F. Baba-Aissa, L. Raeymaekers, and R.**

Casteels. Regulation of alternative splicing of the SERCA2 pre-mRNA in muscle. *Ann.N.Y.Acad.Sci.* 853: 372-375, 1998.

132. **Xu, N., C. Y. Chen, and A. B. Shyu.** Modulation of the fate of cytoplasmic mRNA by AU-rich elements: key sequence features controlling mRNA deadenylation and decay. *Mol.Cell Biol.* 17: 4611-4621, 1997.

133. **Yang, H., C. S. Duckett, and T. Lindsten.** iPABP, an inducible poly(A)-binding protein detected in activated human T cells. *Mol.Cell Biol.* 15: 6770-6776, 1995.

134. **You, Y., C. Y. Chen, and A. B. Shyu.** U-rich sequence-binding proteins (URBPs) interacting with a 20- nucleotide U-rich sequence in the 3' untranslated region of c-fos mRNA may be involved in the first step of c-fos mRNA degradation. *Mol.Cell Biol.* 12: 2931-2940, 1992.

135. **Zhang, W., B. J. Wagner, K. Ehrenman, A. W. Schaefer, C. T. DeMaria, D. Crater, K. DeHaven, L. Long, and G. Brewer.** Purification, characterization, and cDNA cloning of an AU-rich element RNA-binding protein, AUF1. *Mol.Cell Biol.* 13: 7652-7665, 1993.

136. **Zhang, Y., J. Fujii, M. S. Phillips, H. S. Chen, G. Karpati, W. C. Yee, B.**

Schrank, D. R. Cornblath, K. B. Boylan, and D. H. MacLennan.

Characterization of cDNA and genomic DNA encoding SERCA1, the Ca(2+)-ATPase of human fast-twitch skeletal muscle sarcoplasmic reticulum, and its elimination as a candidate gene for Brody disease. *Genomics* 30: 415-424, 1995.

APPENDIX I:

Supplementary Figures

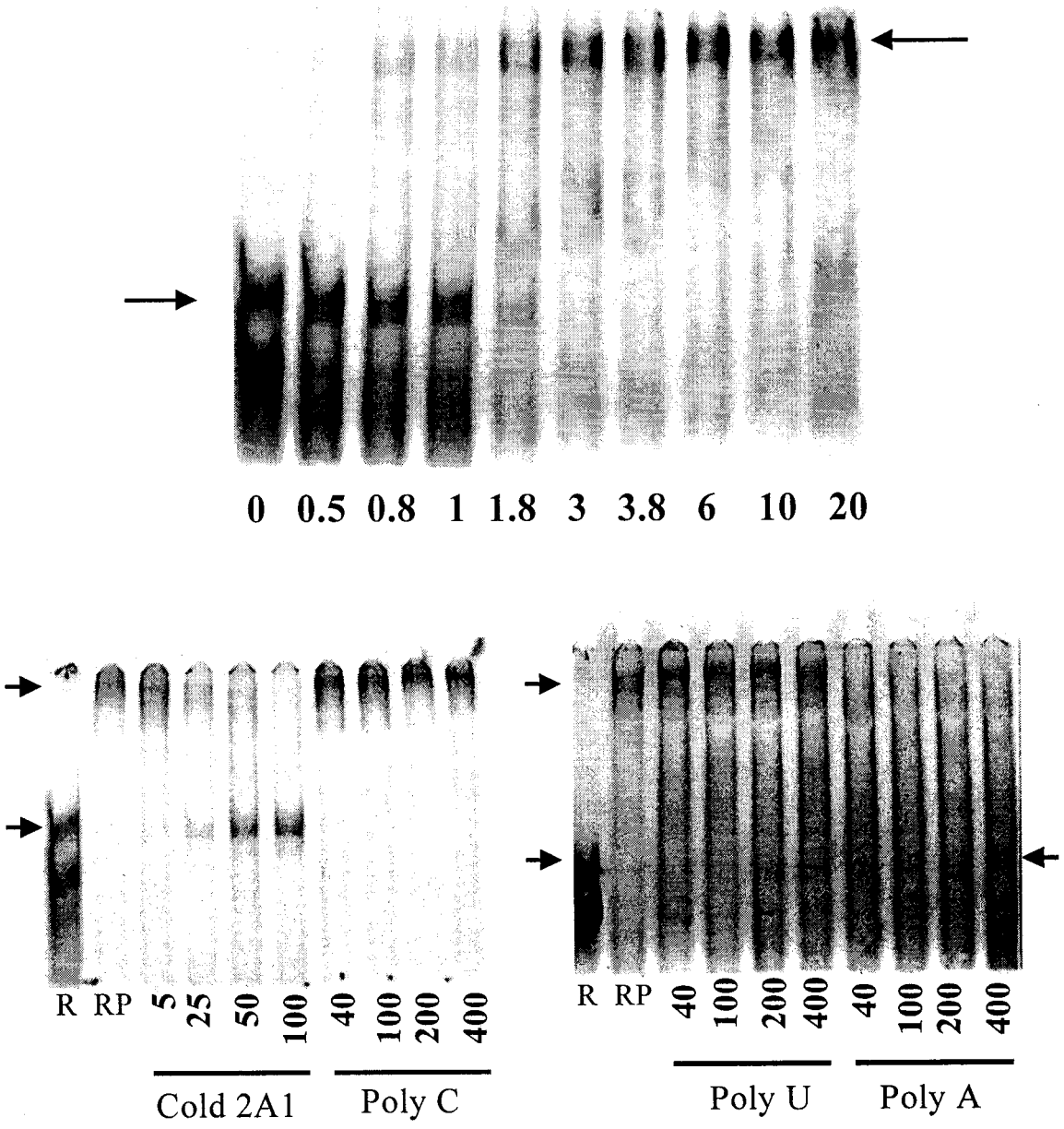

Figure A1. Mobility shift of fragment 2A1.

See Fig.15 for experimental details.

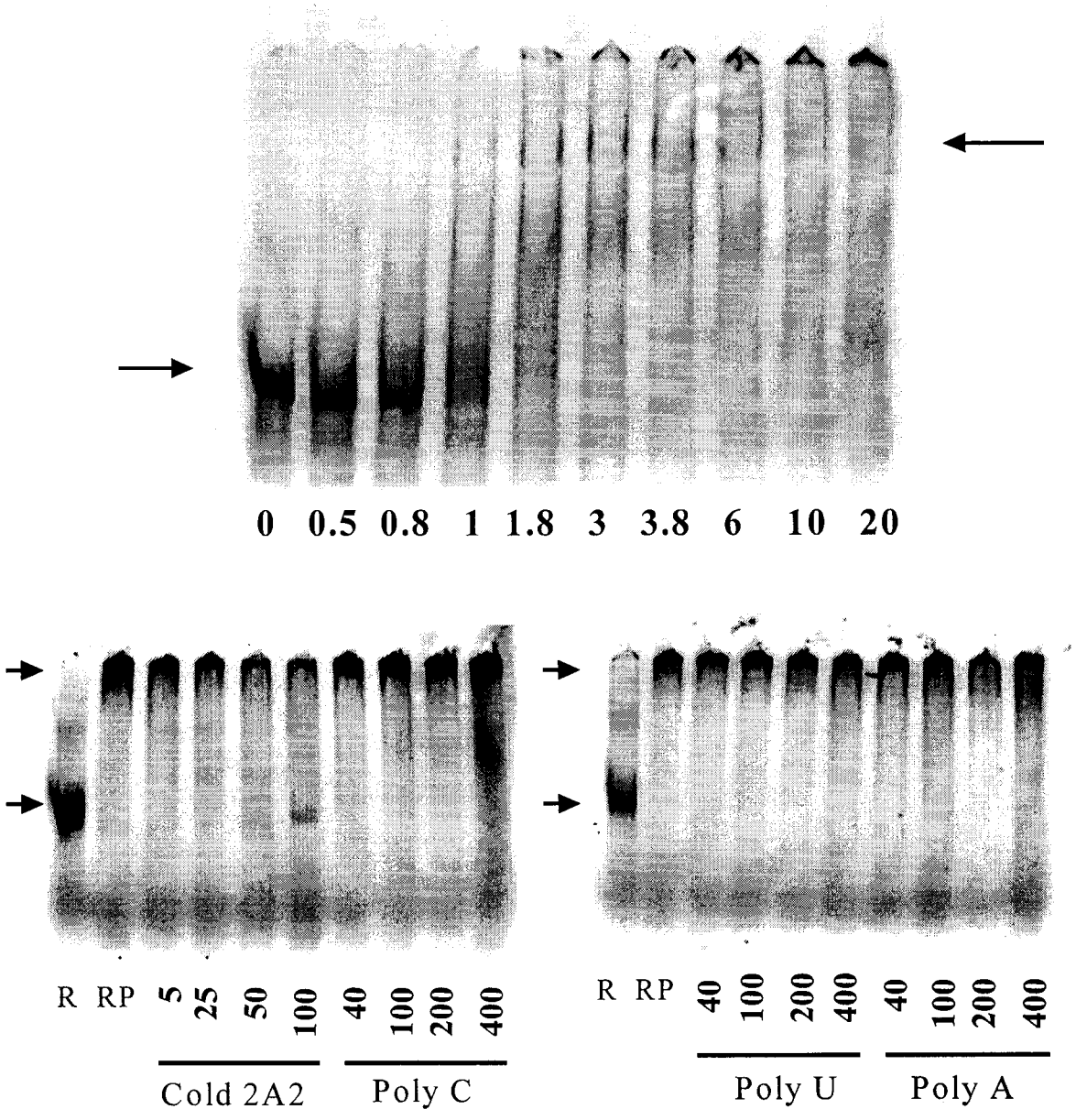

Figure A2. Mobility shift of fragment 2A2.

See Fig.15 for experimental details.

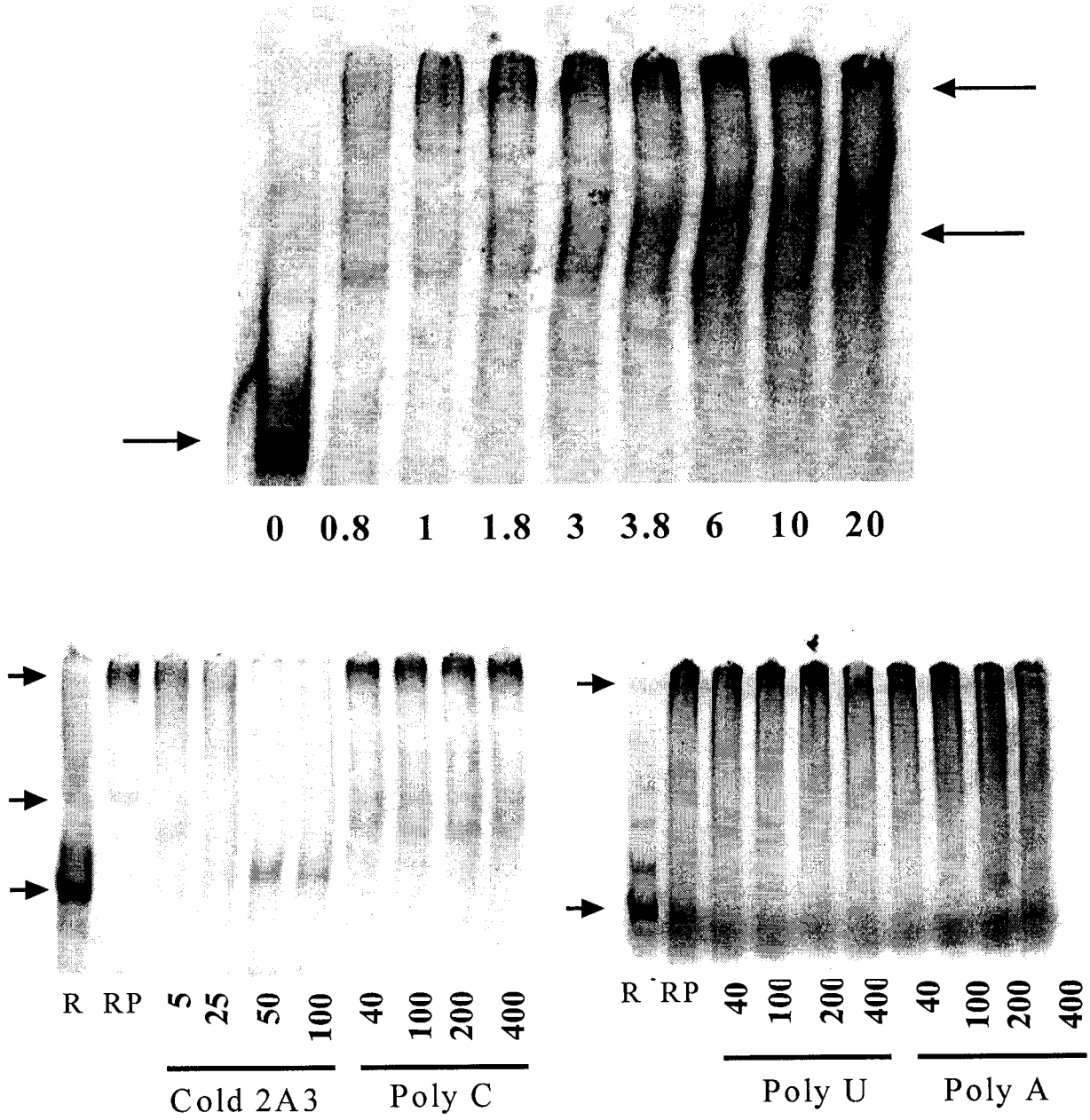

Figure A3. Mobility shift of fragment 2A3.

See Fig.15 for experimental details.

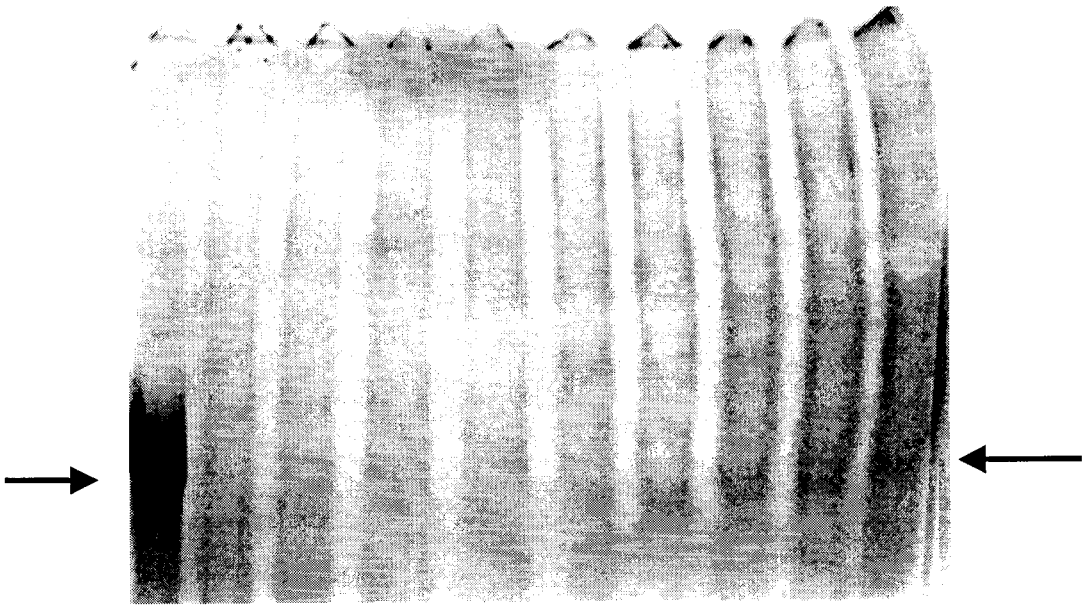

Figure A4. Mobility shift of fragment 2A4.

See Fig.15 for experimental details.

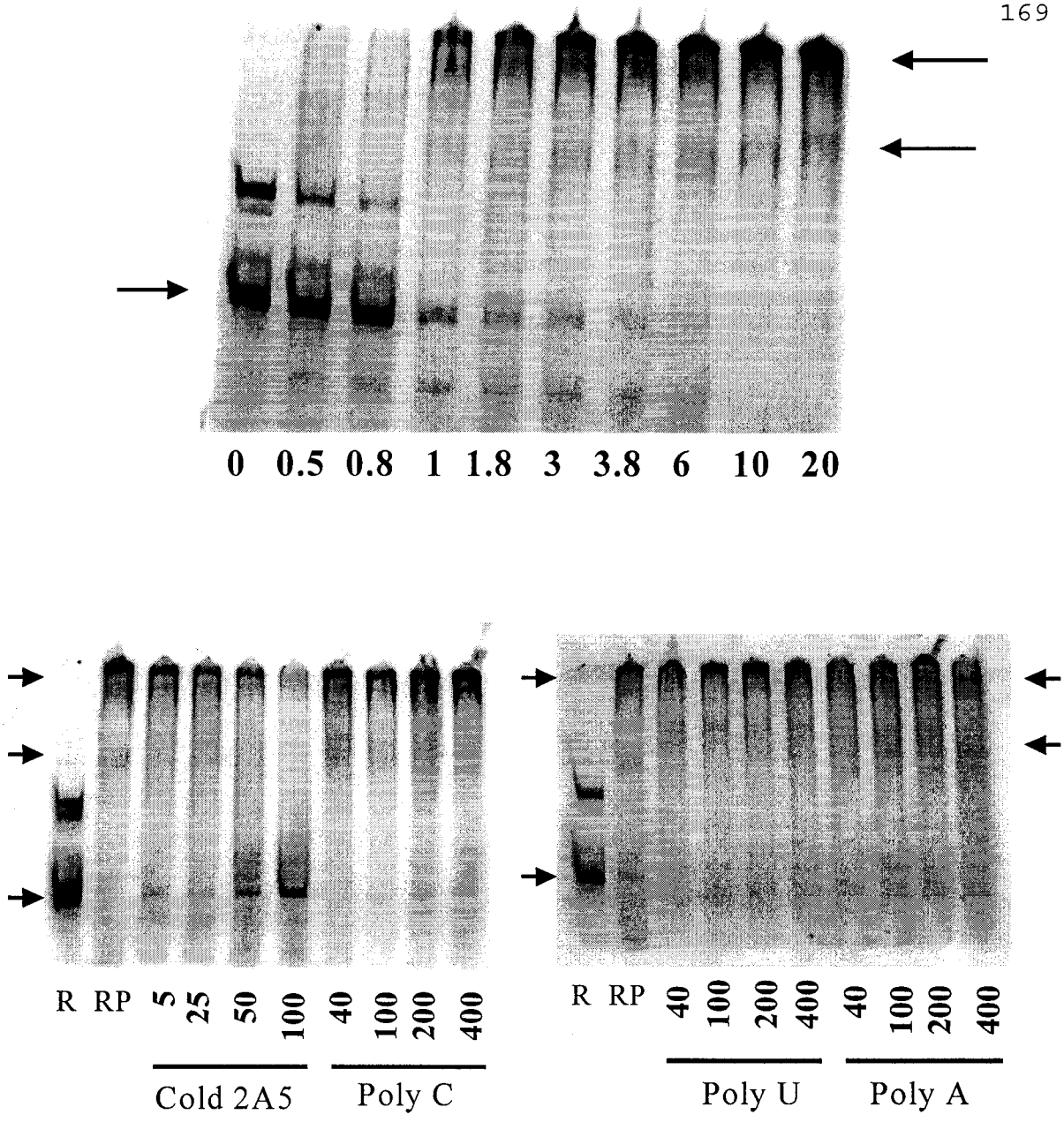

Figure A5. Mobility shift of fragment 2A5.

See Fig.15 for experimental details.

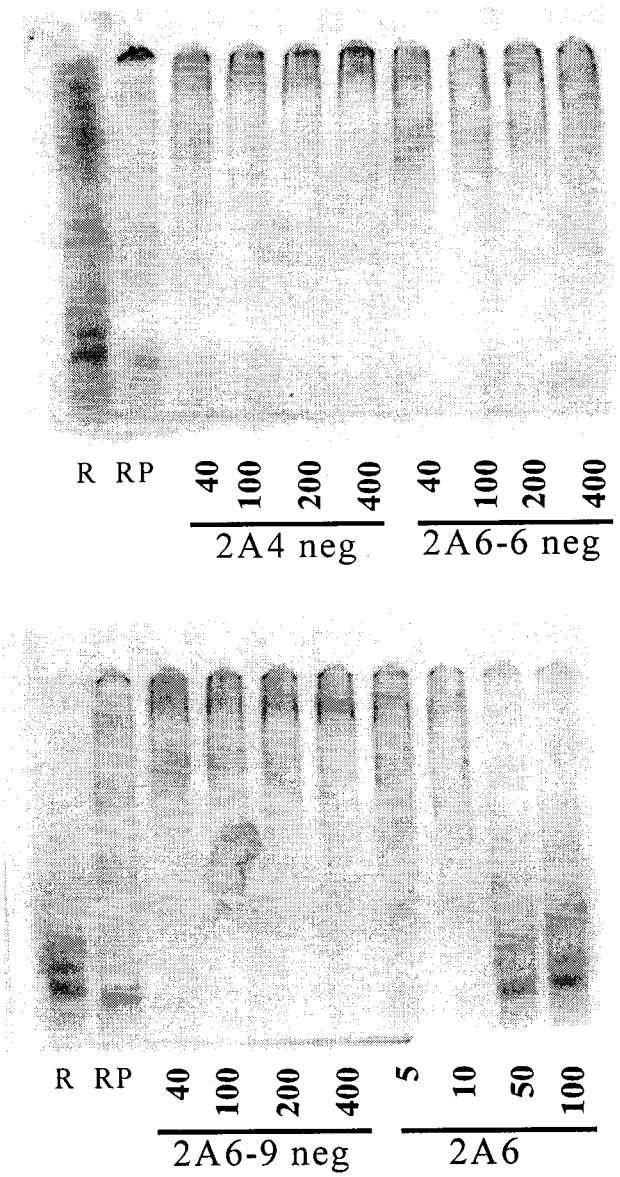

Figure A6. 2A6 competition with negative controls.

See Fig.15 for experimental details.

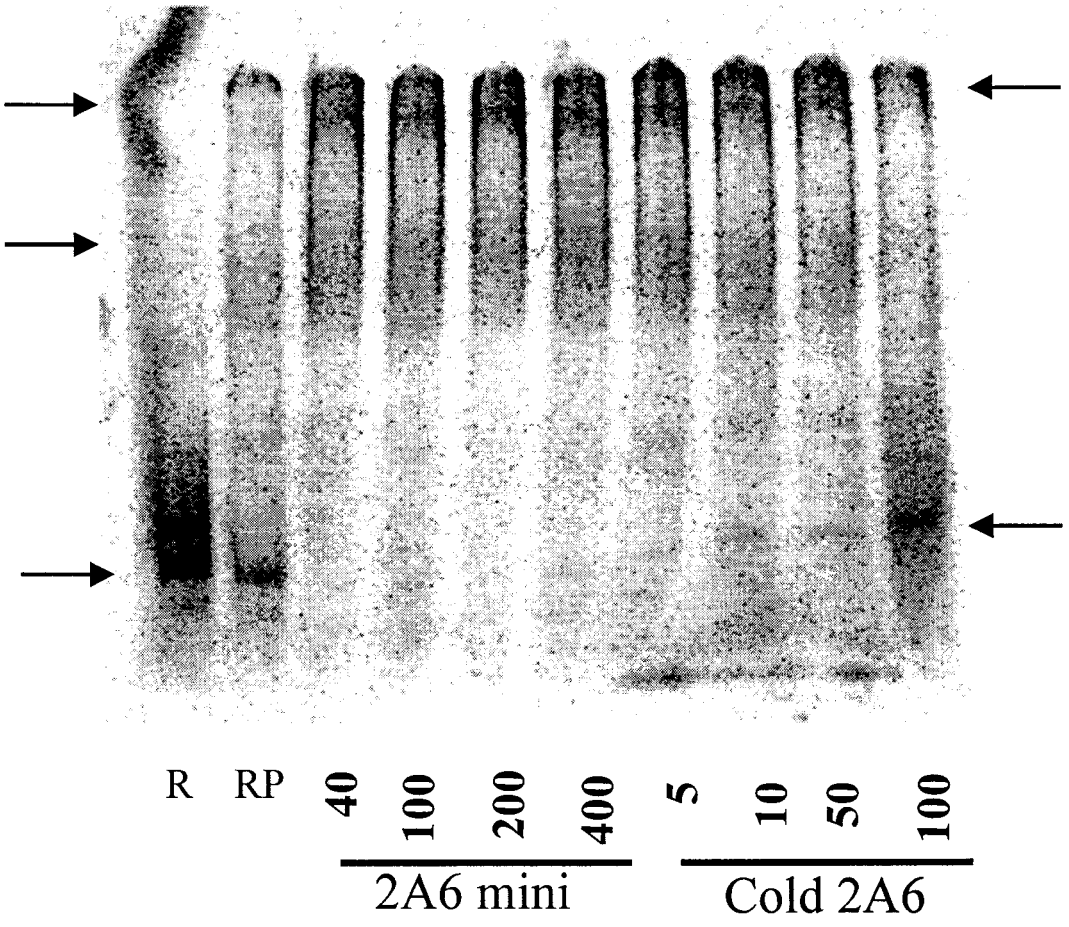

Figure A7. 2A6 competition with mini fragment.

See Fig.15 for experimental details.

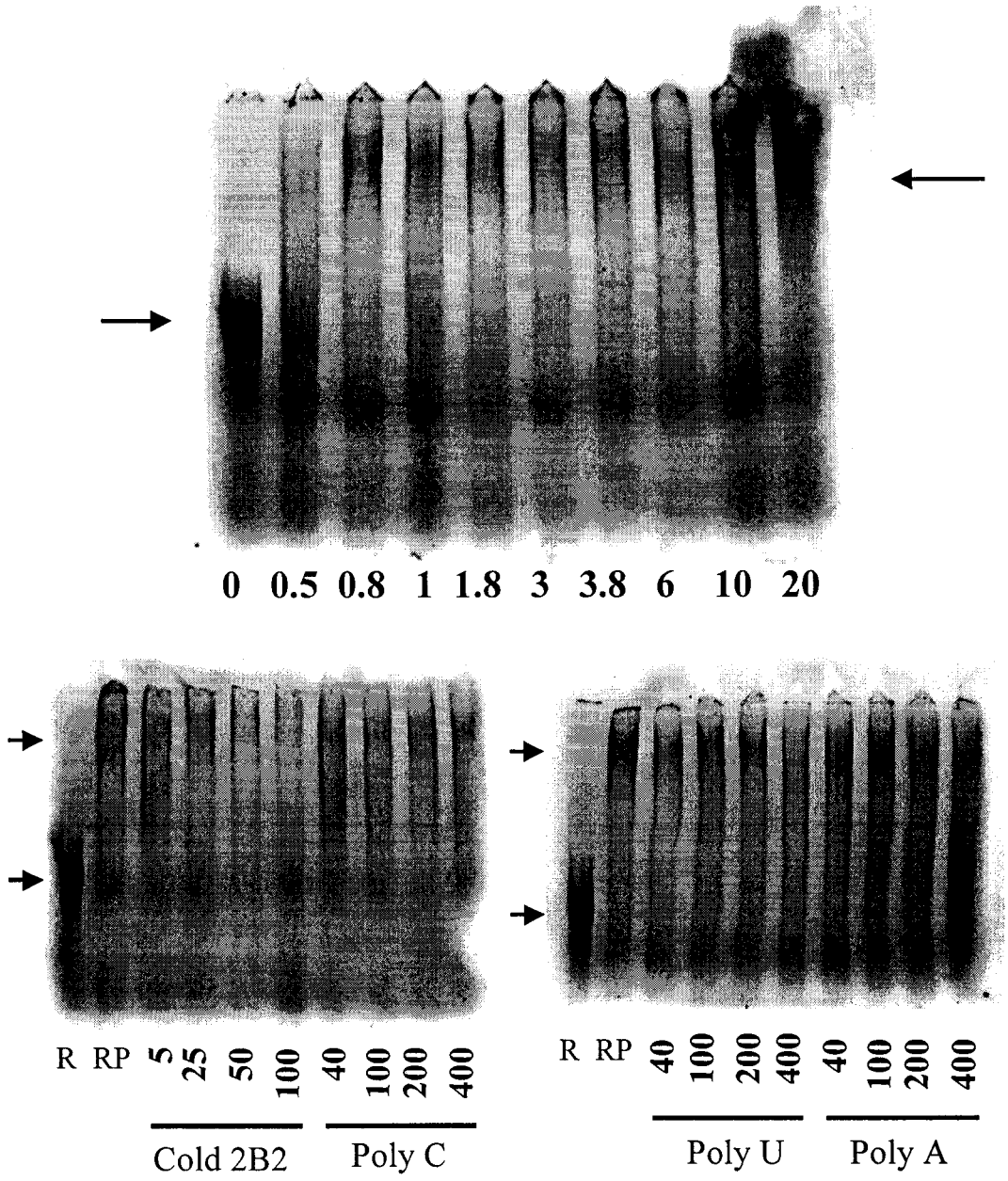

Figure A8. Mobility shift with fragment 2B2.

See Fig.22 for experimental details.

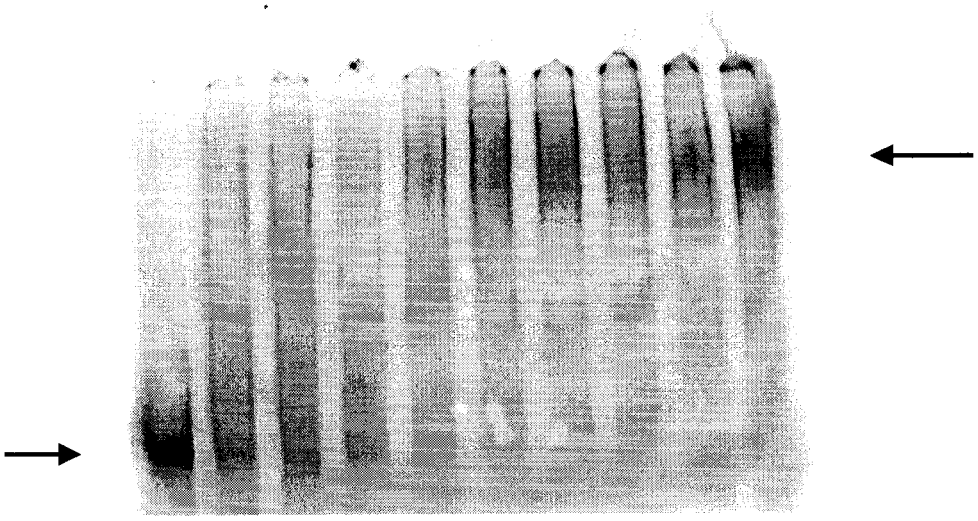

0 0.5 0.8 1 1.8 3 3.8 6 10 20

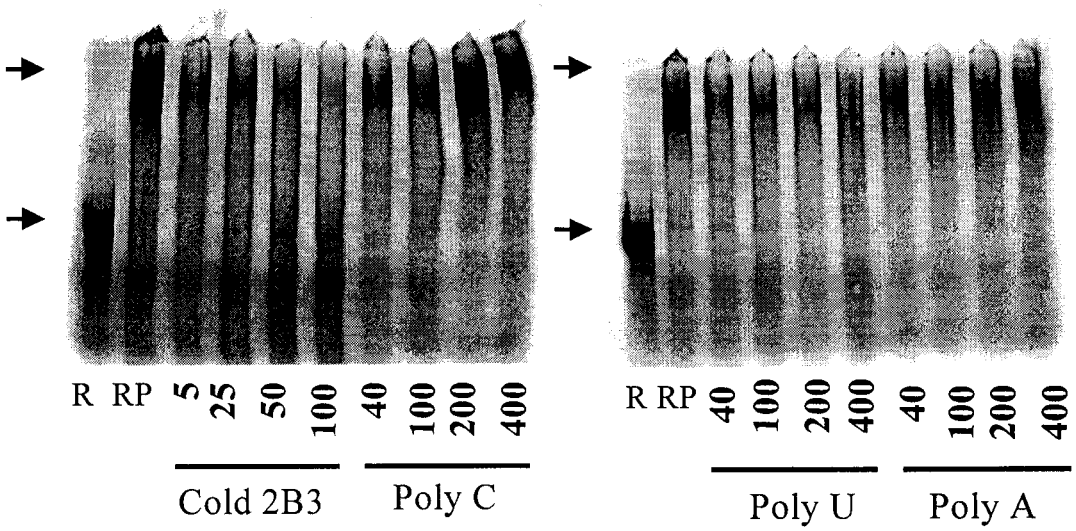

Figure A9. Mobility shift with fragment 2B3.

See Fig.22 for experimental details.

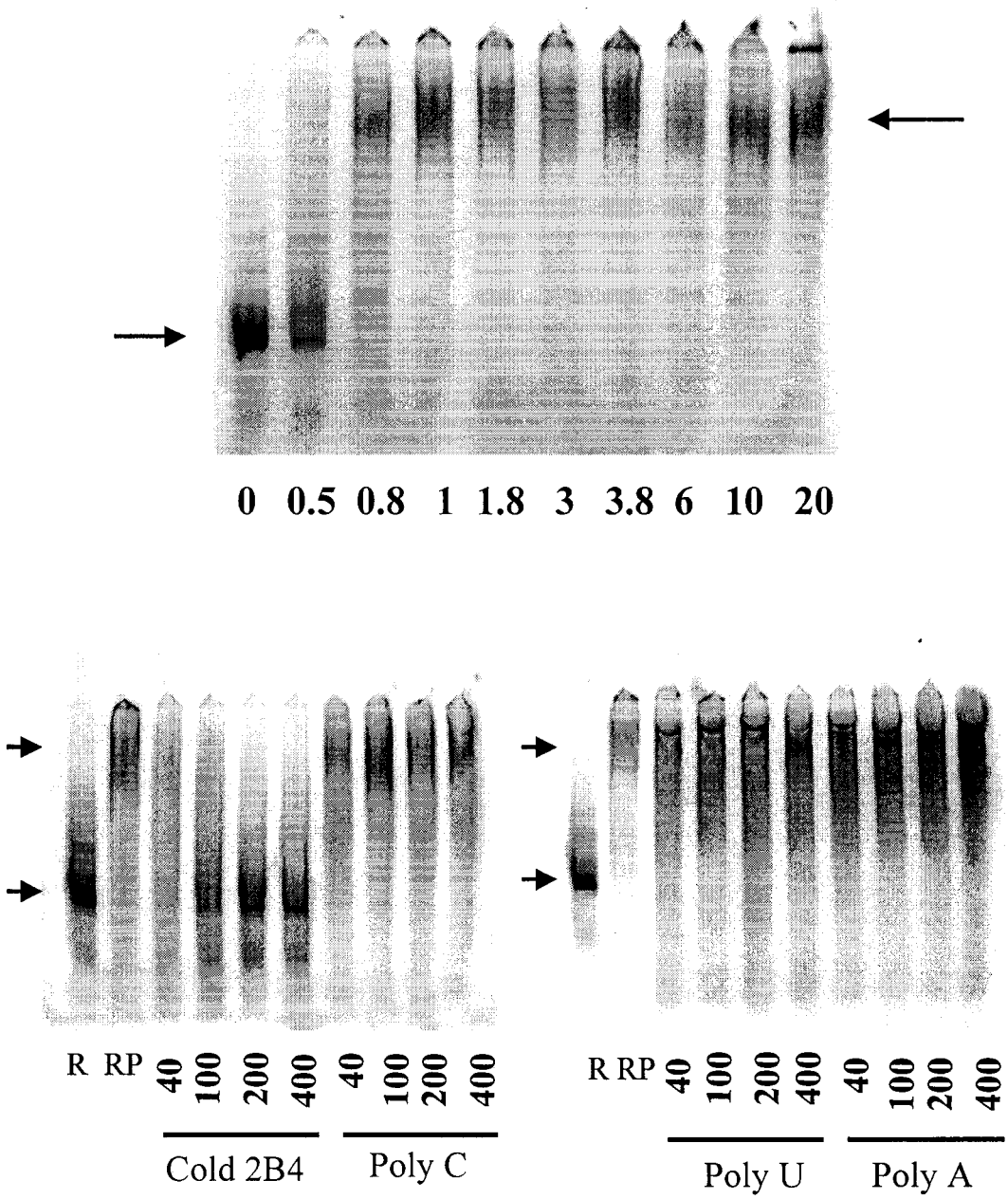

Figure A10. Mobility shift with fragment 2B4.

See Fig.22 for experimental details.

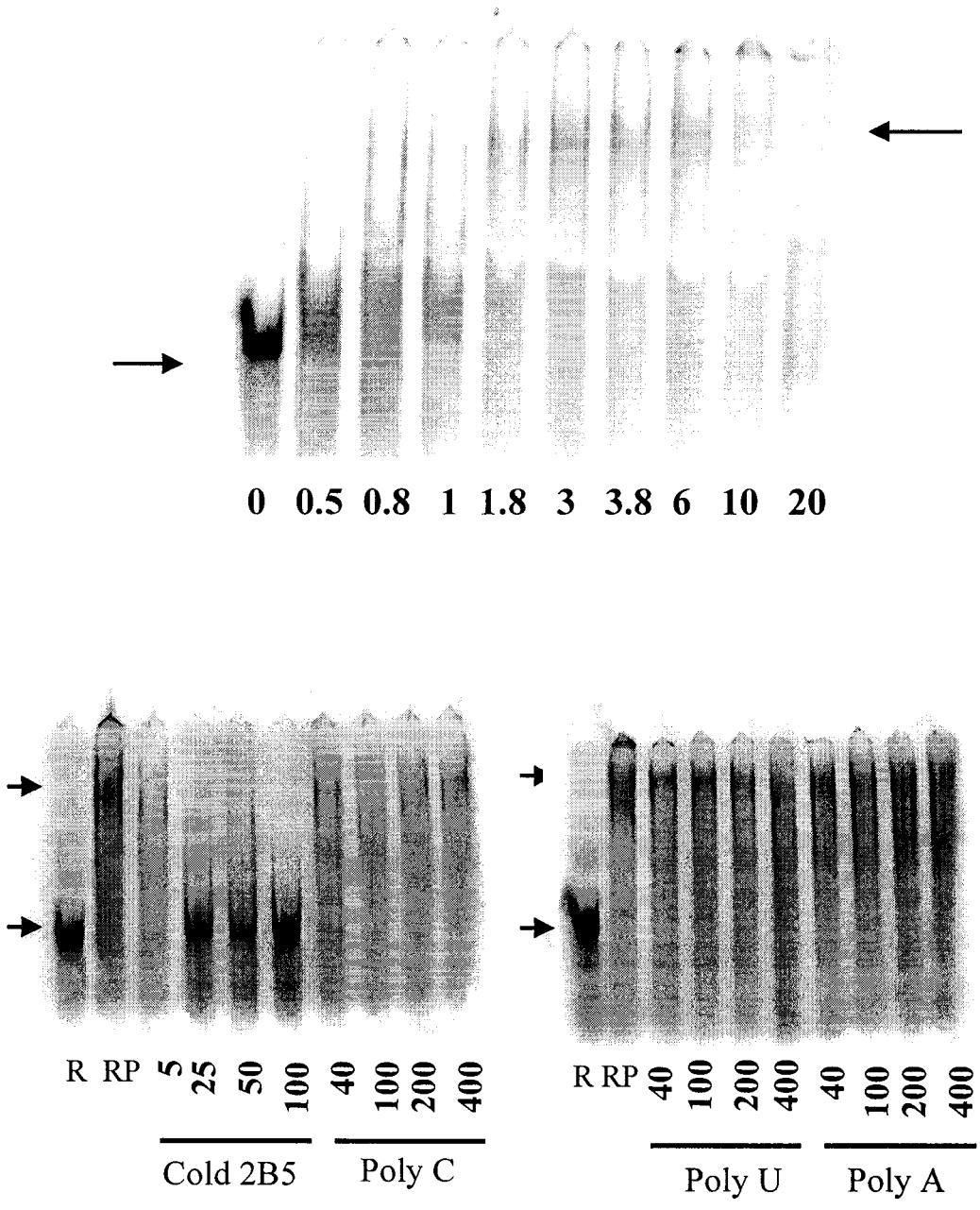

Figure A11. Mobility shift with fragment 2B5.

See Fig.22 for experimental details.

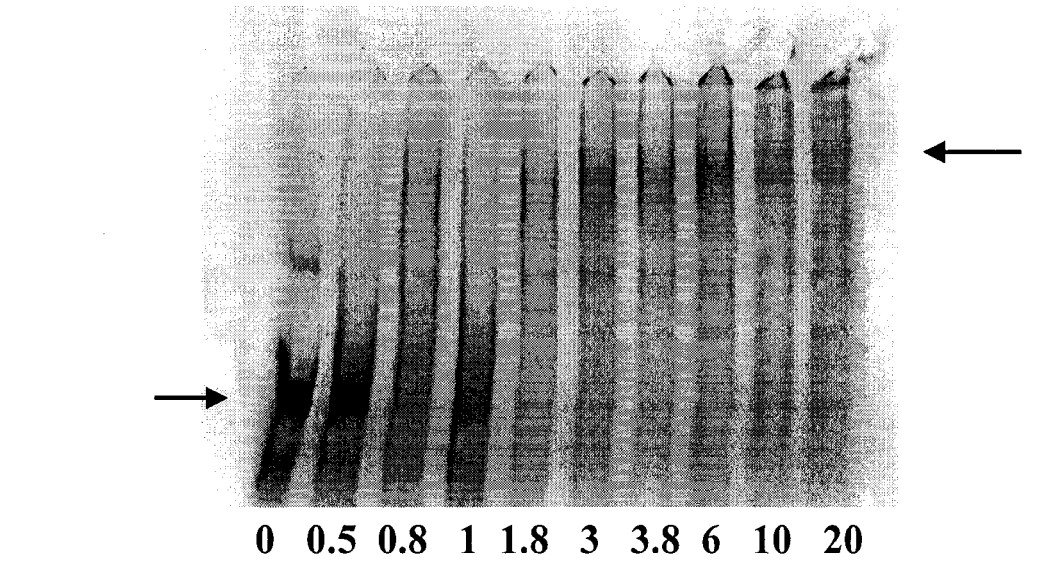

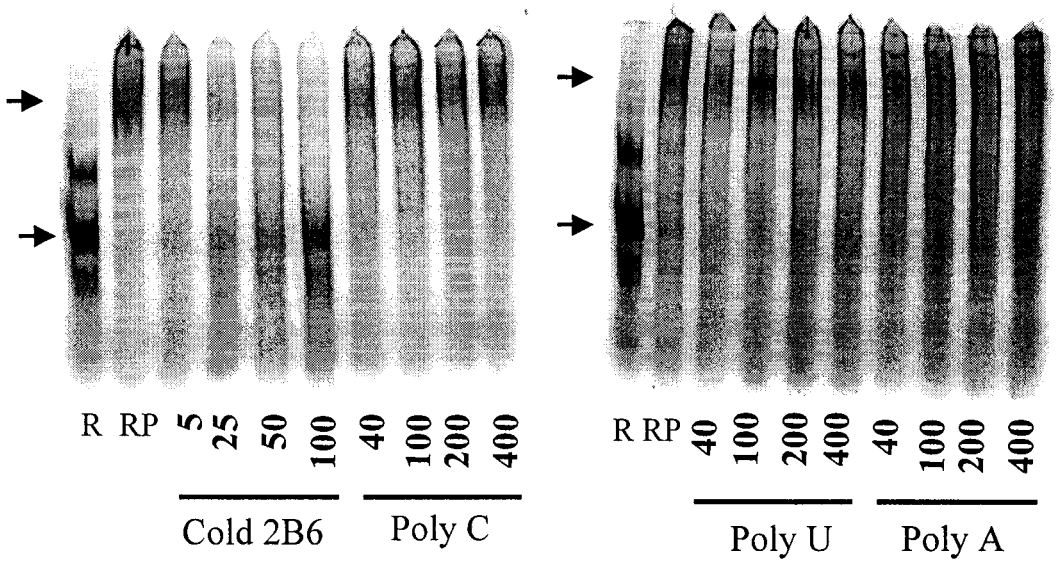

Figure A12. Mobility shift with fragment 2B6.

See Fig.22 for experimental details.

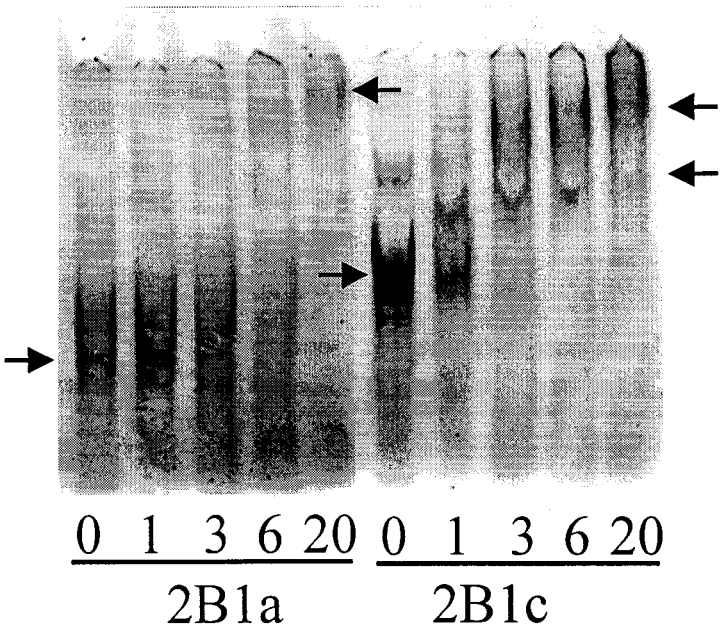

Figure A13. Concentration curves with fragments 2B1a and 2B1c.

See Fig.22 for experimental details.

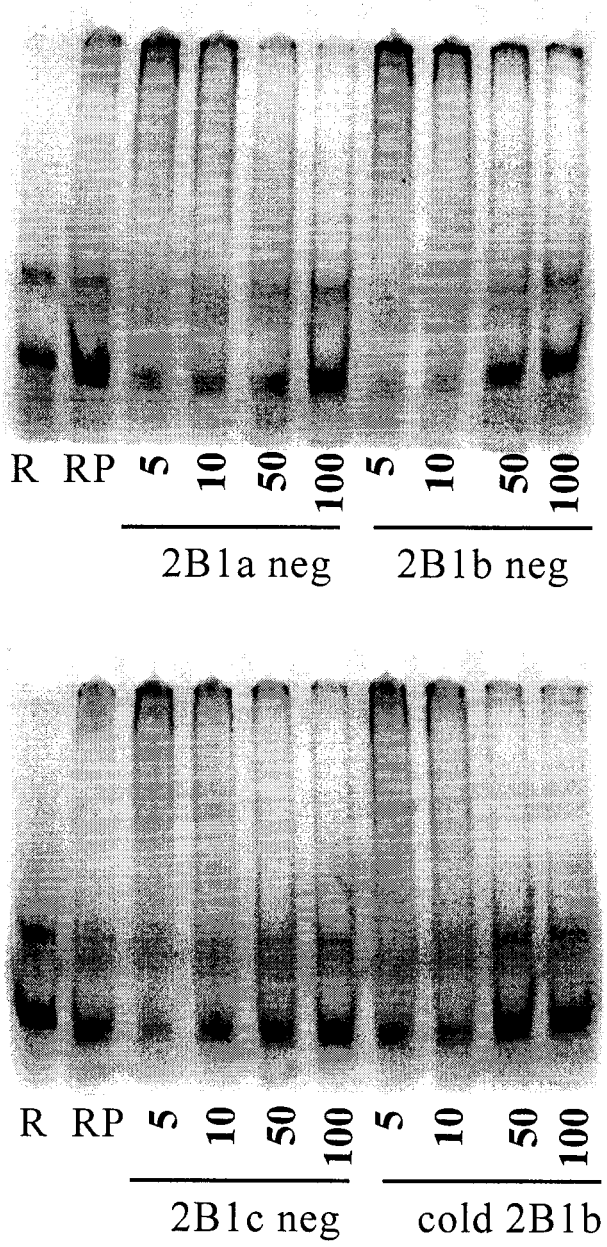

Figure A14. 2B1b Competition with negative controls and self RNA.

See Fig.22 for experimental details.

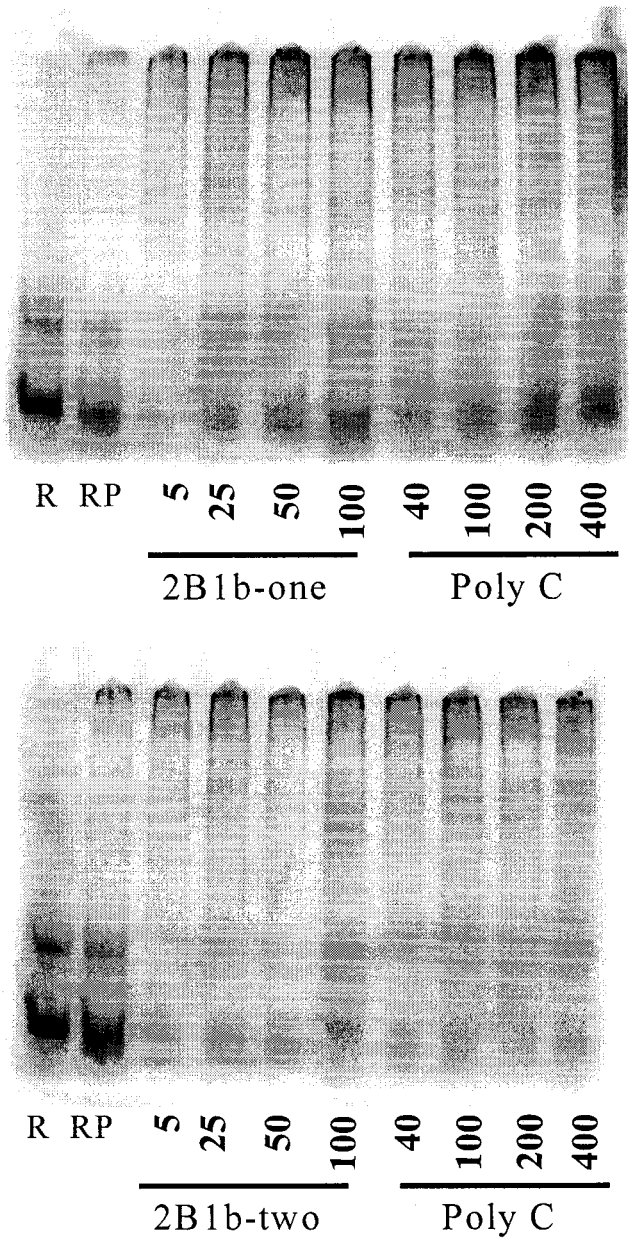

Figure A15. 2B1b Competition with small oligonucleotides, one & two.

See Fig.22 for experimental details.

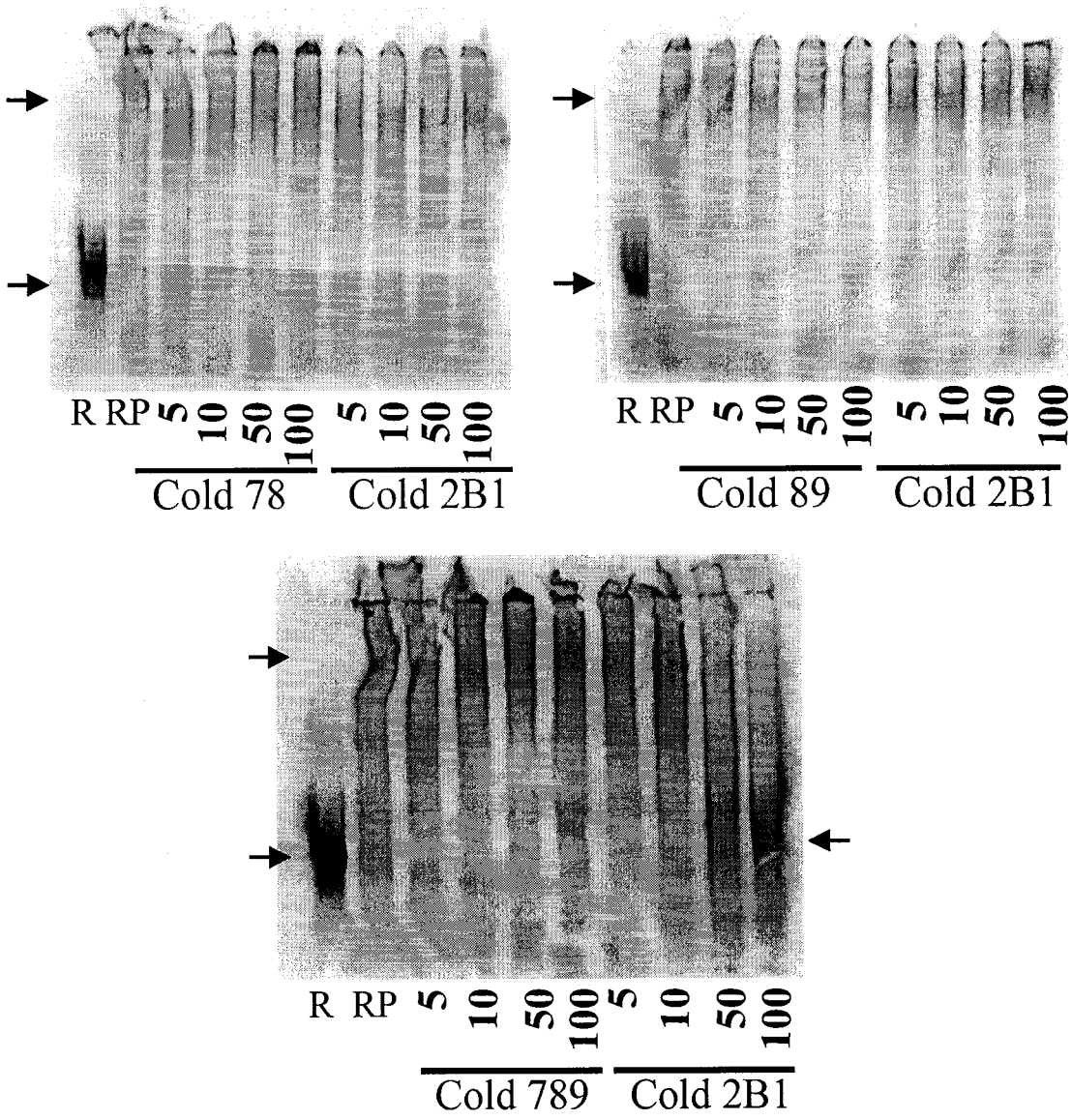

Figure A16. 2B1b Competition with small fragments.

See Fig.22 for experimental details.